Unraveling Intra-Zechstein Structuration and Understanding the Relationship with Geo-Drilling Hazards

By means of detailed seismic mapping in the Dutch Eastern Offshore

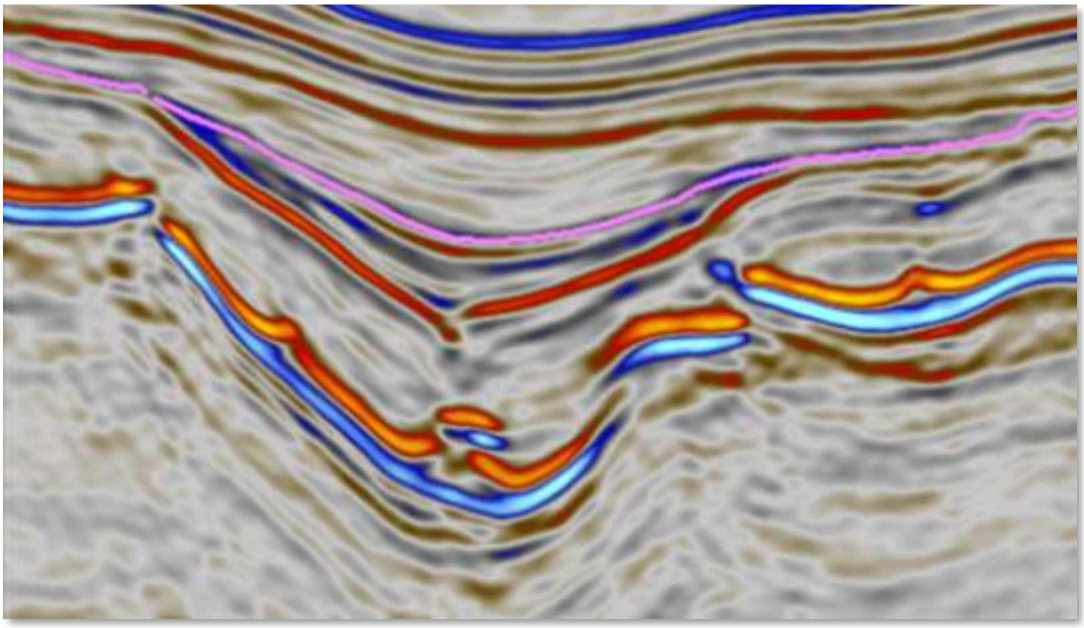

Student	W. Teertstra	**Daily Supervisor (EBN)**	G. Hoetz
Student Number	2529336	**Supervisor (VU)**	Prof. Dr. K. F. Kuiper
Date	July 2019	**Second Assessor (VU)**	Prof. Dr. W. van Westrenen

Front page image: showing anomalous thickened zone features in the stringer of the Zechstein Group, referred to as anhydrite domes by this study. Highlighted in pink is the interpreted Top Zechstein horizon.

Abstract

Carbonates and anhydrites of the Leine formation, the third evaporitic cycle of the Zechstein group, are widely distributed in the Southern Permian basin and these are often drilled through by wells targeting the underlying Rotliegend. The ZEZ3C/A members constitute brittle rocks sandwiched by the ductile halites from the underlying ZEZ2H and the overlying ZEZ3H. The brittle sheet is frequently rifted (boudinage) and the resulting fragments are often referred to as "stringers".

Fully salt encased ZEZ3 Stringers can be heavily overpressured. Drilling through overpressured zones can lead to formation fluids entering the borehole, causing a "kick" situation in the well during the drilling phase. This type of geo drilling incident might lead to delays, increased drilling costs and even safety risks.

Commonly ZEZ3 stringers, also referred to as "Plattendolomite", have a fairly constant thickness of around 50 meters. Deviations from these general observations, in particular anomalously thick stringers, were known from wells but their origin was unclear. This poor understanding was also related to limitations in seismic quality, which generally did not allow detailed stringer mapping. With the arrival of new seismic of the Hansa 4Quad 3D survey (re-processed 2017), the stringer interval could be studied in great detail. Seismic-to-well ties in this area, show that thickened zones consist of a locally thickened Zechstein III anhydrite member.

Isopach mapping of the stringer resulted in new insights of the *thickened zones* distribution which tend to have a characteristic appearance consisting of linear, branching and closing segments. Based on these observations the gypsum dome structure model is proposed in this research, which is largely based on comparable observations described from the Harz mountains. Recently deposited water-rich gypsum behaves very ductile and can create doming features comparable to halite salt domes, albeit on a smaller scale. Subsequent dewatering of gypsum bodies after some burial, causes the transition to anhydrite which has a higher specific density and is more brittle. Also, the associated volumetric shrinkage creates new accommodation space that can be observed in the overlying strata. In addition, the dewatering process might create fluid pathways to the surface and result in the leak-off of over pressures in these zones.
In this study. 154 wells that observed thickened stringers (i.e. > 60-meter of ZEZ3A), were investigated for Zechstein geo-drilling events. Wells with thickened stringers showed significantly lower percentages of kicks in the stringer, compared to kicks encountered in "normal thickness" stringers as described a previous study done by P. Schilder (2019, EBN internship).

By combining the results of seismic mapping and well analyses, a new geological explanation for the thickened stringers is proposed. Planning and drilling new well trajectories might benefit from the improved understanding of stringer thickness variability based on this research.

Acknowledgement

First of all, I would like to thank EBN for creating the opportunity and accommodating me while conducting my Master Thesis project. Thereafter, I would like to thank Guido Hoetz (EBN) for the professional guidance and support he has given me. My gratitude goes to Kees van Ojik (EBN), who helped me with geological interpretations, and to Audrey Roustiau (EBN), who assisted me with the well-to-seismic ties in the area. I am grateful for the conversation with; Nico Holleman (consultant EBN), Marloes Kortekaas (EBN) and John Verbeek who gave me insights in the geological aspects of the study. I would like to thank Gert Lammers (Wellspec), Maarten Middelburg (EBN) and Pieter Slabbekoorn (EBN) for teaching me about drilling and helping to determine and classify Geo-Drilling Events. Also, I am grateful for the excellent seismic data provided by Hansa (ONE). Lastly, I would like to thank my fellow interns; Eline van Malderen, Mohamed Bouchingour, Patrick Reinhard, Vibhuti Wani and Yoël Beaucaire for support and discussion on a daily basis.

Inhoud

1. Introduction

The Dutch subsurface, in many places, includes a thick (50-1200m) sequence of evaporites of the Permian Zechstein Group. Five depositional evaporitic cycles (Z1 to Z5) represent this Group in the Netherlands. The classical evaporitic cycles contain, from base to top; claystone, carbonates, anhydrite, halite, K-Mg- rich salt (‘squeezing salts’), halite and finally anhydrite. Primary controls of this sequence are the glacially induced fluctuations on general sea level and evaporation in the Southern Permian Basin (Van Gent, 2011). This base case cycle is often partially present in the Dutch subsurface and thicknesses (or presence) of members vary subsequently (Ligtenberg, 2007). Figure 1 displays a general overview of the internal stratigraphy of the Zechstein Group and important seismic horizons with corresponding seismic reflection colour. The area used for this research falls in the ‘Main basin’ part section indicated by a red dot in figure 1.

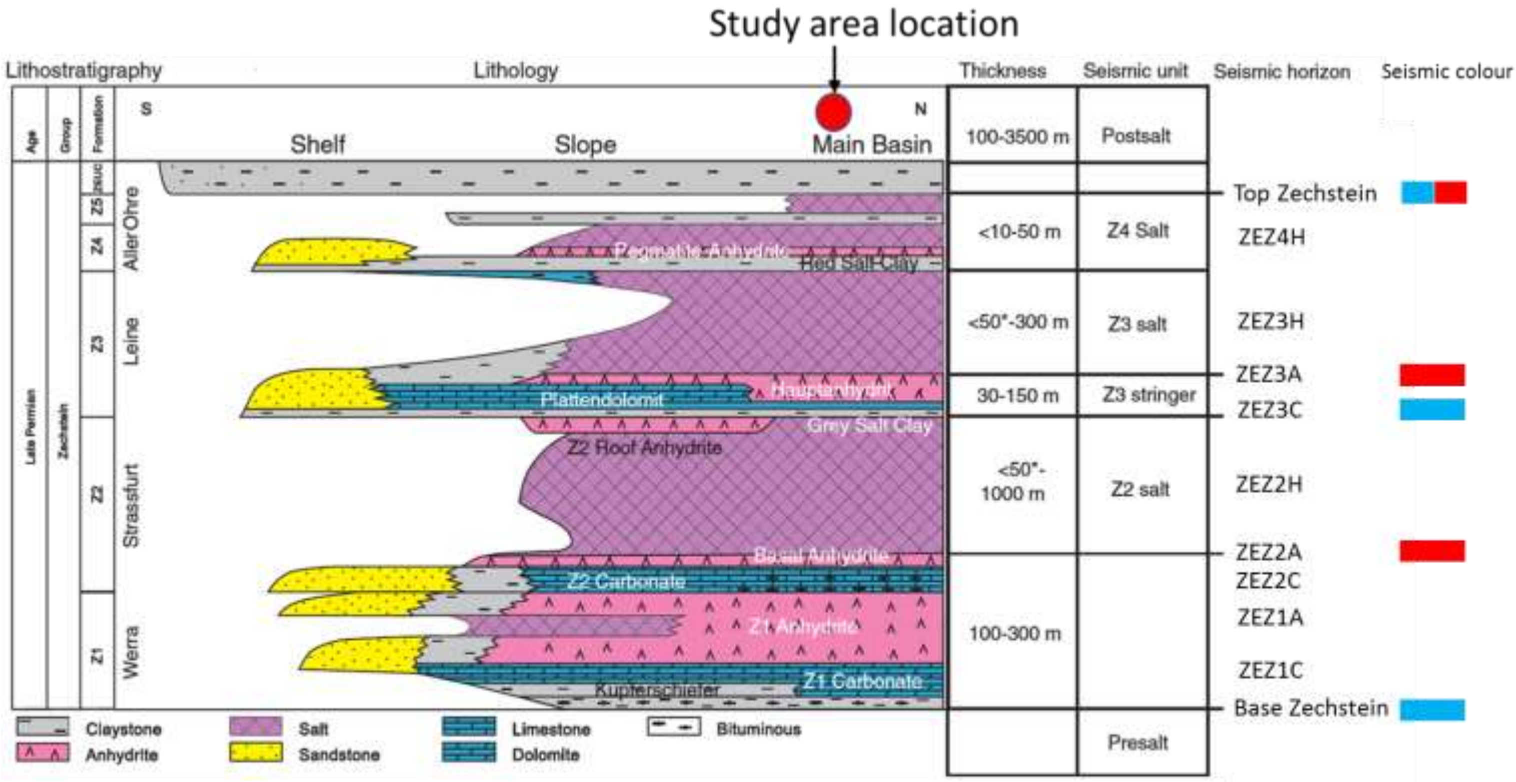

Fig. 1. Stratigraphic diagram of the Zechstein Group after Zijp et al. (2018), modified from Geluk (2007). Research area located under the red dot in the Main Basin region. Important seismic horizons annotated on the right and also the important seismic reflections with the associated colour.

For this research the three members at the base of the Z3 formation will be studied in detail. The relatively competent “Hauptanhydrit” and “Plattendolomit” (figure 1), also referred to as ‘stringer’, ‘floaters’ or ‘rafts’, has an average thickness of 40-50m and is emplaced between two halite members, with a thickness of <50-1000m for the underlying Z2 halite (ZEZ2H) and <50-300m for the overlying Z3 halite (ZEZ3H) (Van Gent et al., 2011). An important feature of the stringer is that several studies, Van Gent (2011), Strozyk et al. (2014, 2017), find branching elongated structures of up to 180m thick anhydrite, which they refer to as ‘thickened zones’ (TZs).

There are three key characteristics of the halite that have a large effect on the stringer. Firstly, the halite has a close to zero percent porosity, thus its sealing capacity is near perfect. Secondly, over geological time the halite behaves ductile in the subsurface. This causes flow under tectonic stresses, which causes the rigid intra-Zechstein layers, especially the stringer to break apart in fragments. The third characteristic is its relatively low density which lead to gravitational instability when heavier sediments are overlying. In particular the latter 2 characteristics are responsible for salt remobilisation (halokinesis) leading to areas with salt withdrawal and areas with salt build up. These tectonic build-ups can be modest (pillows), fair (domes) or mighty to an extend they puncture overlying strata (diapirs)

Fully salt encased stringers might not have a pressure relief path anymore and internal pressures can build up during burial, this mechanism appears mainly active in the Z3 carbonate (ZEZ3C) part of the stringer, because its relatively high porosity. Halokinesis results in extensive deformation of the stringer. Folding, faulting and dislodging (rifting) of the stringer can be seen on seismic sections. This deformation might result in enhanced porosity and permeability in the anhydrite and carbonate parts of the stringer. Both properties can increase the likelihood of (overpressured) formation fluids flowing into the borehole while drilling through the stringer.

- The main aim for this study will be to understand how the present-day geometry of the stringers is created with a focus on the anomalous thickened zones. This includes; understanding the role of; sedimentary, diagenetic and tectonic processes in the geological history.
- Secondary aim will be on drilling hazards related to the Zechstein stringer interval. If there any correlation between geo-drilling events (GDE's) and thickened zones? Can better understanding of stringers help to prevent Zechstein drilling incidents?

This research is conducted as a follow-up of the research by P. Schilder (2019), as an internship with EBN. His study focused on the origin of overpressrued formation fluids observed in the Zechstein Group and he found that the majority (59%) originated from the ZEZ3 stringer interval. He concluded that smaller stringer bodies and highly fractured stringer areas (near ruptured edges and hinge zones), result more often in high overpressures. Schilder (2019) proposed to use the Hansa 4Quad survey to provide a better insight in the stringer geometries and especially the thickened zones.

2. Geological Background of the Zechstein Group

2.1 Depositional Setting and Models

The Zechstein Group is deposited in Late Permian times in an intra-cratonic basin during a hot and dry climate near the equator (Geluk, 2007). Figure 2 displays the extent of this basin, referred to as the Southern Permian Basin (SPB), from east England to Poland and north towards the Bering Sea. In the far north the SPB had a narrow connection to open sea (Ziegler, 1982). This led to occasionally flooding of the entire basin and after restricted outflow of water, evaporation could take over and deposition of the widespread evaporitic sequences followed (Van den Belt, 2007).
The Netherlands is located at the southern edge of the SPB and comprises the three main facies of the Zechstein stratigraphy. With clastics or continental deposits in the south, the platform facies running through the middle from east to west and the basin facies from the middle to the northern part of the Dutch territories.

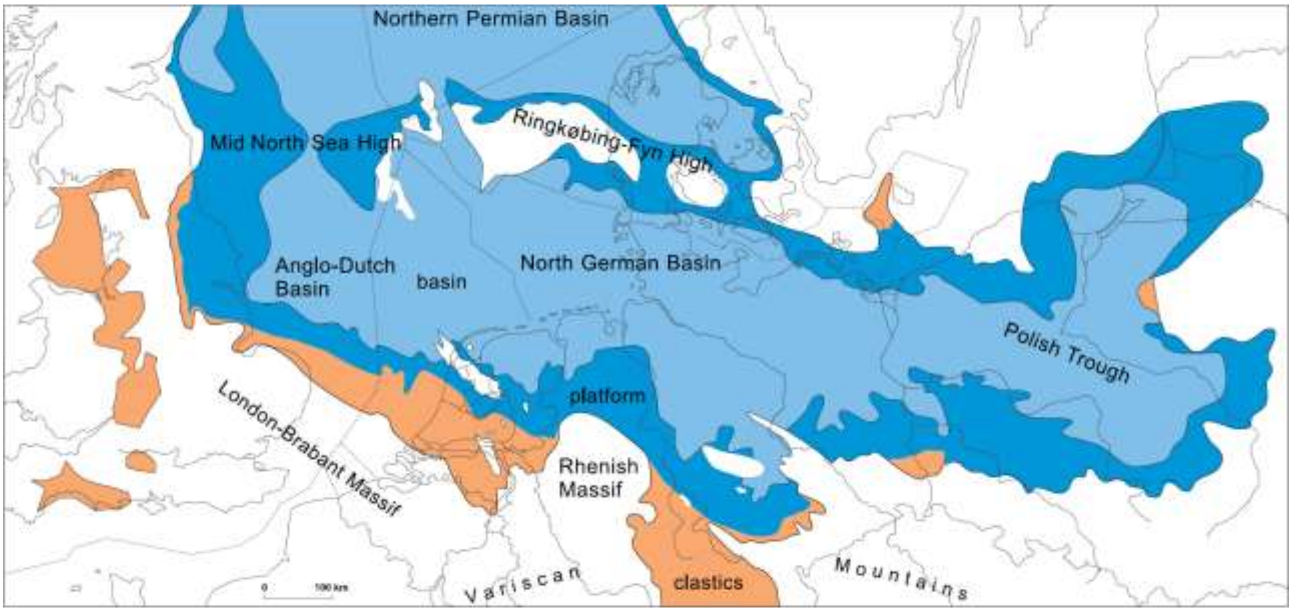

Fig. 2 Present-day distribution and facies map of the Zechstein Group (Z2 Carbonate, Late Permian) in the Southern Permian Basin. Coloured per facies; clastics is orange, platform is dark blue and basinal is light blue. Comparable facies maps of ZEZ3 cycle are not available. From Geluk (2007).

Depositional models for these evaporitic basins have been debated since the discovery of thick carbonate-evaporite successions, often named 'saline giants'. Van den Belt (2007) proposes a shallow-water and shallow-basin model (figure 3) as a response to the deep-basin shallow-water model by Hsü et al. (1973, 1977). To explain the thick halite deposits, the shallow-basin shallow-water model proposes that isostatic compensation is enough to create the accommodation space required. High precipitation rates and a weakened basin crust are the primary contributors to the isostatic compensation. This way thick halite succession can form in a relatively short period of time (~600kyr) and within a water depth of just a few 100 meters (Stanley 1986, Volozh et al. 2003, Van den Belt 2007).

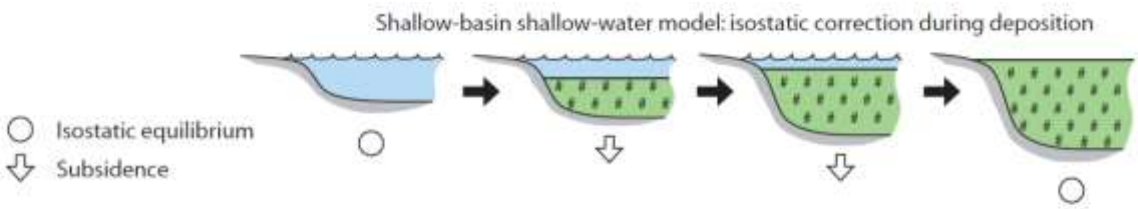

Fig.3. Shallow-basin shallow-water model for saline giants, based on isostatic compensation during deposition. Modified after Van den Belt, 2007.

2.1.1 The Leine Formation

Deposition of the Zechstein II halite filled in the topography of the basin (figure 4), resulting in minor relief in the entire basin area (Geluk, 2007; Van den Belt, 2007). Regional transgression ended the halite precipitation and marks the start of the third evaporitic cycle, also referred to as Leine formation. This transgression floods the entire Southern Permian basin margin (Geluk, 2000).

First to deposit is the 0.5-10-meter-thick Gray Salt Clay member (ZEZ3G), followed by a 0.5-55-meter-thick dolomite/limestone member, also referred to as 'Plattendolomite'. Evaporation takes over and during regression the 15-130-meter-thick 'Hauptanhydrit' is deposited, first as gypsum and with diagenesis it forms anhydrite (Strozyk et al., 2017; Zijp et al., 2018). Both the anhydrite and carbonates are deposited in the platform, slope and basin facies. Geluk (2000, 2005) produced, with publicly available 2D seismic and well data, a paleogeographic map of the Leine formation (figure 5). Visible from this map is the general location and lateral extent of the three facies and areas of non-deposition (highs).

The third cycle ends with precipitation of several salt members. Halite is the most common (>95%), other rare salts are K-Mg rich bischofite, carnallite, kieserite and sylvite (Coelewij et al., 1978). These rare salts, referred to as 'squeezing' salts, are proposed to be precipitated during high temperatures and are only found in the north-eastern onshore and northwestern offshore (Geluk, 2007; Raith et al., 2017).

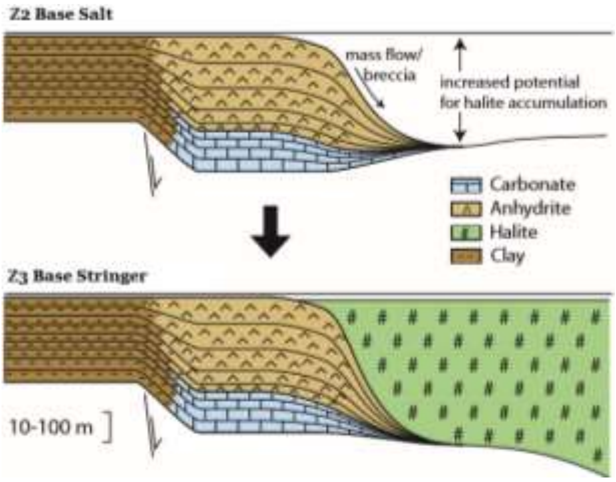

Fig. 4. Schematic visualization of depositional environments of Z2 Base salt and Z3 Base stringer. Modified from Van den Belt, 2007.

Fig.5. Facies and isopach map of the Leine formation. Orange = clastic facies, light pink = platform facies, dark pink = basinal facies and colourless the highs. The UK map has been adopted from Cameron et al. (1992). The German part from Richter-Bernburg (1955). From Geluk, 2007.

2.2 Gypsum to Anhydrite Conversion

The Zechstein III anhydrite, present in the subsurface, has been originally deposited as gypsum. Kosmahl (1969) found swallow-tail pseudomorph crystals of anhydrite, which preserve the typical structure of gypsum, providing evidence for this claim. Conversion of gypsum to anhydrite takes place by equation (1) and is dependent on the following (environmental) geological parameters: temperature, pressure and activity of water (Sonnenfeld, 1984).

$$CaSO_4 \cdot 2H_2O \rightarrow CaSO_4 + 2H_2O \qquad (1)$$

The temperature at which gypsum converts to anhydrite ($T_{gp\text{-}an}$) varies and is primarily controlled by the activity of water (α_{H2O}) in the pore fluid and the pore fluid pressure. If the activity (or availability) of water increases, the gypsum becomes more stable, thus more energy is needed to convert it to anhydrite and vice versa (Jowett et al., 1993). Gypsum precipitates from seawater at a α_{H2O} of 0.93 and halite precipitates at a α_{H2O} of 0.75 from seawater. Corresponding $T_{gp\text{-}an}$ are 52°C and 18°C, respectively (Hardie, 1967). This difference in $T_{gp\text{-}an}$ has a large effect on the depth at which the conversion takes place. When gypsum converts into anhydrite it loses its water and the volume decreases by 39% (Zen, 1965). If this water can escape to the immediate area, e.g. into surrounding porous rocks. The pore fluid-pressure regime will then be hydrostatic. If this is not the case, e.g. when sealed below salt, the overburden pressure will be translated on to both the solid and the fluid and result in the water being lithostatic pressured. The $T_{gp\text{-}an}$ behaves different between both pore-fluid pressure regimes. In the hydrostatic pressure regime $T_{gp\text{-}an}$ decreases with depth, resulting in shallower gypsum to anhydrite conversion. Lithostatic pore-fluid pressure regimes behave the opposite and conversion takes place with more burial (Jowett et al., 1993).

Determining temperature at certain depths is typically done by combining the thermal gradient with the temperature at surface. Estimating these data for the Late Permian is a challenge. Furthermore, the presence of halite as a thermal conductor in the Zechstein Group further complicates temperature reconstructions.
Geological data shows that the dominant calcium sulphate mineral below 450 m depth is anhydrite (Klimchouk, 1996). For the Zechstein III, Marsal (1952) proposes that the gypsum-anhydrite conversion took place at around 100 m of burial depth, while Langbein (1987) assumes 100 m as a minimum depth.

2.3 Geophysical Properties of Zechstein Lithologies

2.3.1 Wireline Log and Seismic properties

Responses of the Zechstein Group, in the Dutch subsurface, on both wireline log data and on seismic are very distinct.
The Zechstein Group has a heterogenous composition, but the bulk of the rock consists of halite lithology. Halite has a lower density of 2000 kg/m^3 compared to average sediments in a basin, but a higher sonic velocity (Urai et al., 2008). With no porosity and the lack of radioactive minerals, the gamma ray response is always zero. Thick deposits, several hundreds to over a thousand meter, of virtually pure halite, create a steady wireline log response in the ZEZ2H and ZEZ3H members. Other common lithologies in the Zechstein are shale, limestone, dolomite and anhydrite. Their densities; ~2500 kg/m^3, 2710 kg/m^3, 2870 kg/m^3 and 2980 kg/m^3 respectively, are significantly higher than that of halite and sonic velocities are also significantly higher for the latter three lithologies (table 1). Together with the density difference this results in very distinct strong, negative and positive, reflectors in the Zechstein interval.

In between the halite bodies, other (K-Mg) salts can be present: bischofite, carnallite, epsomite, kieserite and sylvite (Urai et al. 2008; Raith, 2017). The K-salts can be distinguished on wireline logs by looking at increased gamma ray values. Mg-salts can be distinguished based on their density values. Anhydrite shows a combination of highest sonic velocity and density making it stand out from all other Zechstein lithologies. Carbonates show low readings on gamma ray combined with fairly high sonic and density. Shales show intermediate readings on gamma ray and intermediate sonic and density.

Although this approach of distinguishing the lithologies usually work, caution is required since rock intervals are often mixtures of different lithologies. Thus, careful observation of all the data available (wireline logs, well reports, cutting etc.) is required in this study.

Name	Formula	Density	GR	Neutron "Porosity"	Sonic transit time
		kgm^{-3}	API	%	$msft^{-1}$
Bischofite	$MgCl_2 \cdot 6\,H_2O$	1560	0	> 60	100
Carnallite	$KMgCl_3 \cdot 6\,H_2O$	1570	220	65	78
Epsomite	$MgSO_4 \cdot 7\,H_2O$	1710	0	> 60	
Sylvite	KCl	1860	500	-3	74
Halite	NaCl	2040	0	-3	67
Kainite	$MgSO_4KCl \cdot 3\,H_2O$	2120	245	45	
Gypsum	$CaSO_4 \cdot 2\,H_2O$	2350	0	>60	52
Kieserite	$MgSO_4 \cdot (H_2O)$	2590	0	38	
Calcite	$CaCO_3$	2710	0	-1	49
Polyhalite	$K_2Ca_2Mg(SO_4)_4 \cdot 2\,(H_2O)$	2790	180	15	57
Langbeinite	$K_2Mg_2(SO_4)_3$	2820	275	0	52
Dolomite	$CaCO_3\,MgCO_3$	2870	0	1	44
Anhydrite	$CaSO_4$	2980	0	-2	50

Table 1: The main evaporite minerals and their wireline log properties (after Urai et al., 2008).

2.3.2 Rheology

On a scale of the whole Zechstein Group the rheological behaviour is largely controlled by halite being the dominant Zechstein rock. Important properties of halite are low creep strength, low static porosity, low permeability and low density. These properties make it mobile, by ductile deformation, under tectonic forces and cause trapping of fluids (Urai et al., 2008). The overall rheological behaviour of the Zechstein is more heterogeneous. The anhydrite and carbonate intervals deform brittle, by faulting and folding, discussed in chapter 2.5. Other rheological heterogeneities in the salt are produced by metre-thick K-Mg salt layers. These consists of high soluble and very low viscous minerals, mentioned in chapter 2.3.1. This alteration off K-Mg salts, halite, sulphates and carbonates creates a highly variable mechanical behaviour (Raith et al., 2017).

Figure 6 shows the difference of strain rate per second versus differential stress (MPA) for dry halite, dry gypsum and dry anhydrite. Halite deforms a factor of 10^5 faster than gypsum and gypsum deforms 10^7 faster than anhydrite with increasing differential stress. Note: that water greatly accelerates creep for these rocks, but flow laws for solution-precipitation creep of anhydrite and gypsum are not known. Therefore, comparing wet flow behaviours solely using the relationships given in fig 6 is not reliable (Jackson, 2017).

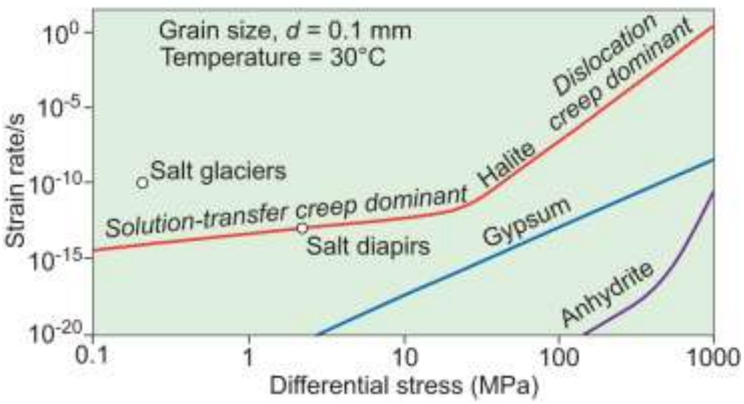

Fig. 6. Strain rate per second versus differential stress of dry halite, dry gypsum and dry anhydrite. Adopted from Jackson, 2017.

2.4 Permian Tectonics

In Early Permian times the Variscan orogeny started to collapse and the Southern Permian Basin started to rift apart. This rifting induced volcanic activity. Several extensional pulses were recorded during the collapse: the Saalian, followed by the Altmark I to III pulses (fig 7, Ziegler, 1986, 1989; Geluk 2000, 2007). After the volcanic intrusions the whole SPB started to thermally subside slowly (van Wees et al., 2000).
In the late Permian, during deposition of the Zechstein Group, two tectonic phases can be distinguished: Tubantian I & II. Tubantian I is an extensional phase and resulted in normal faulting (halfgrabens) and pull-apart basins. These extensional structures are studied in the Netherlands by M. Geluk (1999, 2005) and in Germany by M.A. Ziegler (1989). Geluk (2005) estimates the timing of this extensional event at around 256 Ma.
Tubantian II is described by Geluk (2005) to be a mild compressional event and is estimated to have occurred between 251 and 252 Ma. Based on comparison with dated tectonic events in the UK (Cameron et al., 1992). The structural style of the faults, during this event, suggest that it represents an aftermath of the Variscan orogeny.

Age	Epoch	Marine stage	NE European stages	Lithostratigraphy	Tectonic pulse	Tectonic phase
251		Induan				
		Tatarian		Zechstein Group	~~Tubantian II ~~Tubantian I	
265	Permian	Kazanian	Late Permian	Upper Rotliegend Group	~~Altmark II, III	Late Variscan extension
		Kungurian Artinskian	Early Permian	*hiatus*	~~Altmark I ~~Saalian	
296		Sakmarian Asselian		Lower Rotliegend (locally present)		

Fig.7. Scheme of the several tectonic events during the Permian, grey area is the focus of this research. Scheme is designed for an area nearby the Central North Sea Graben. Modified after Geluk, 1999.

2.5 Zechstein Stringer Deformation

When studying the stringers on seismic, most notable is the large amount of visible deformation. Van Gent (2010) noticed a large, 10 km-scale fold structuration following the top Zechstein and in the salt domes a smaller, km-scaled, fold structuration. He also found that the Z3 stringer is broken, faulted and boudinaged regionally. Even smaller scale fold structures are present in the mechanically layered ZEZ3H member, observed in core logs by Raith et al. (2017).
Strozyk et al. (2014) provide a classification for the stringer deformation into three structural styles (figure 8). Boundaries of these structural styles match with the boundaries of structural elements, or blocks, in northeast Netherlands (Kombrink et al., 2012). Structural configuration and reactivation of the underburden faults result in different styles of salt movement, which lead to different styles of stringer deformation (see Strozyk et al. 2014; figure 8). Strozyk et al. (2014) proposes that initial extension during the Early Triassic lead to lateral movement in the salt, causing rupturing of the stringer into fragments. Continued extension in the Late Triassic and until the Cretaceous, resulted in more vertical movement of the salt, leading to constructional folding in the stringer (figure 9).
The stringer fragments are proposed to have experienced little to no lateral movement during deformation, because of the much higher viscosity of the stringer compared with the surrounding salt. The deformation of the stringer is through brittle and ductile deformation (Van Gent, 2011; Li et al., 2012).
Strozyk et al. (2014) identified minor changes in stringer thickness along folds. This indicates that folding in the stringer is by means of bed length shortening, referred to as “buckle folding” (Ramsay, 1967; Ramsay and Huber, 1987).

Fig.8. *Sketches showing the three structural styles (not to scale). a) Thin Z3 halite above the stringer and gaps between stringer fragments. b) Stringer mirrors the top Zechstein and shows boudinages on the flanks of large scale folds (F1). Also, a smaller scale fold type is present as F2. c) Highly folded stringers (F3), with parts of thick Z3 halite above it. TZs are located in the synclines of these folds. From Strozyk et al. (2014).*

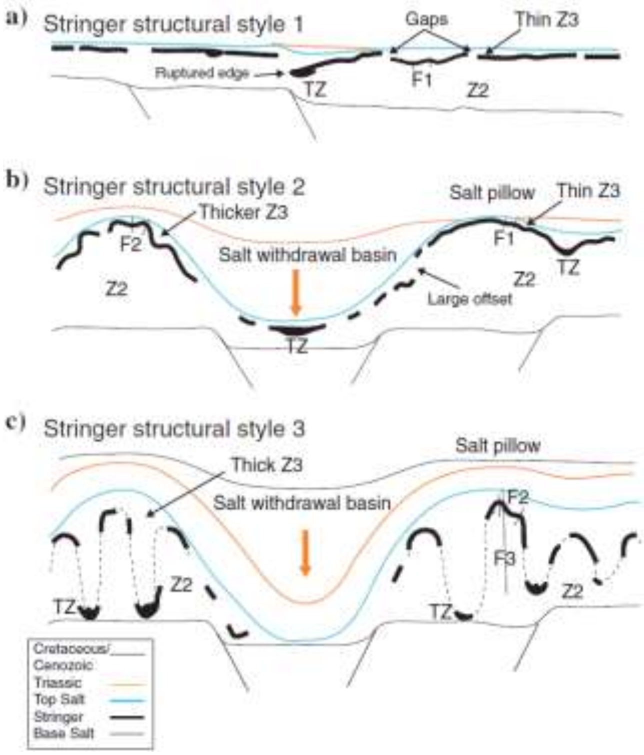

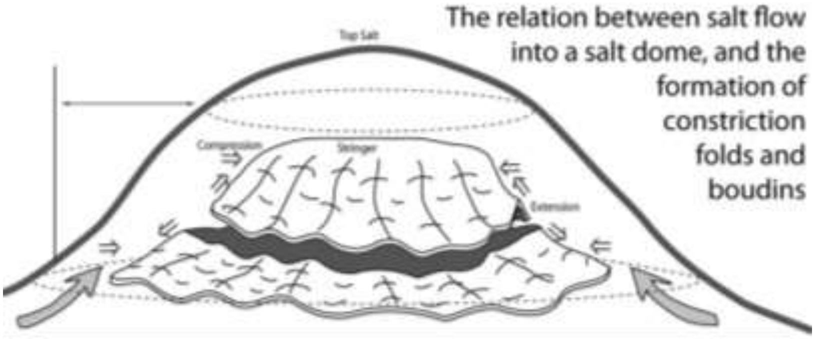

Fig. 9. Schematic drawing of the formation of constriction folds and concentric boudins due to flow into a salt dome. Combination of tensile forces due to vertical extension and coeval horizontal compression due to the decrease in salt dome diameter results in contradicting structural styles. From Van Gent. 2010.

2.6 Borehole Data and Geo-Drilling Events

Information provided in this paragraph mostly obtained from the EBN internship report of P. Schilder (2019).
In the Netherlands, by 2018, a total of 6489 boreholes have been drilled and 6011 of these have stratigraphy data available for analyses. Close to one third (2031) have been drilled deep enough to penetrate the Zechstein III stringer and are referred to as “conclusive” (In this analyses conclusive means heaving reached the ZEZ2H or older strata). From the conclusive 2031 boreholes, 1321 registered the Zechstein III stringer (figure 10b).
During the process of drilling a borehole, drilling incidents might occur that result in either loss of time, money, safety or a combination of these. Analysing those incidents show that they are typically caused by one or more of the following three factors; organisational mishaps, engineering (e.g. tool failure) and geological hazards. EBN has created a database with (classified) cases of Geo-Drilling Incidents (Geo-Drilling Events or GDE’s) where unexpected or hazardous geology played a key role. For this study, this database has been used and expanded in order to understand what drilling experience was gathered during drilling Zechstein stringer. In figure 12 (Chapter 3.2) classification and guideline scheme is provided for any Geo-drilling Event (GDE). For the Zechstein Group and especially the Zechstein stringer, gains are the most problematic GDE’s (figure 10a). The Zechstein halite members are perfect seals, this can lead to very high, up to lithostatic, overpressures in members where porosity is present. Brine is the most common formation fluid that is present during a gain event in the Zechstein Group (figure 10c).

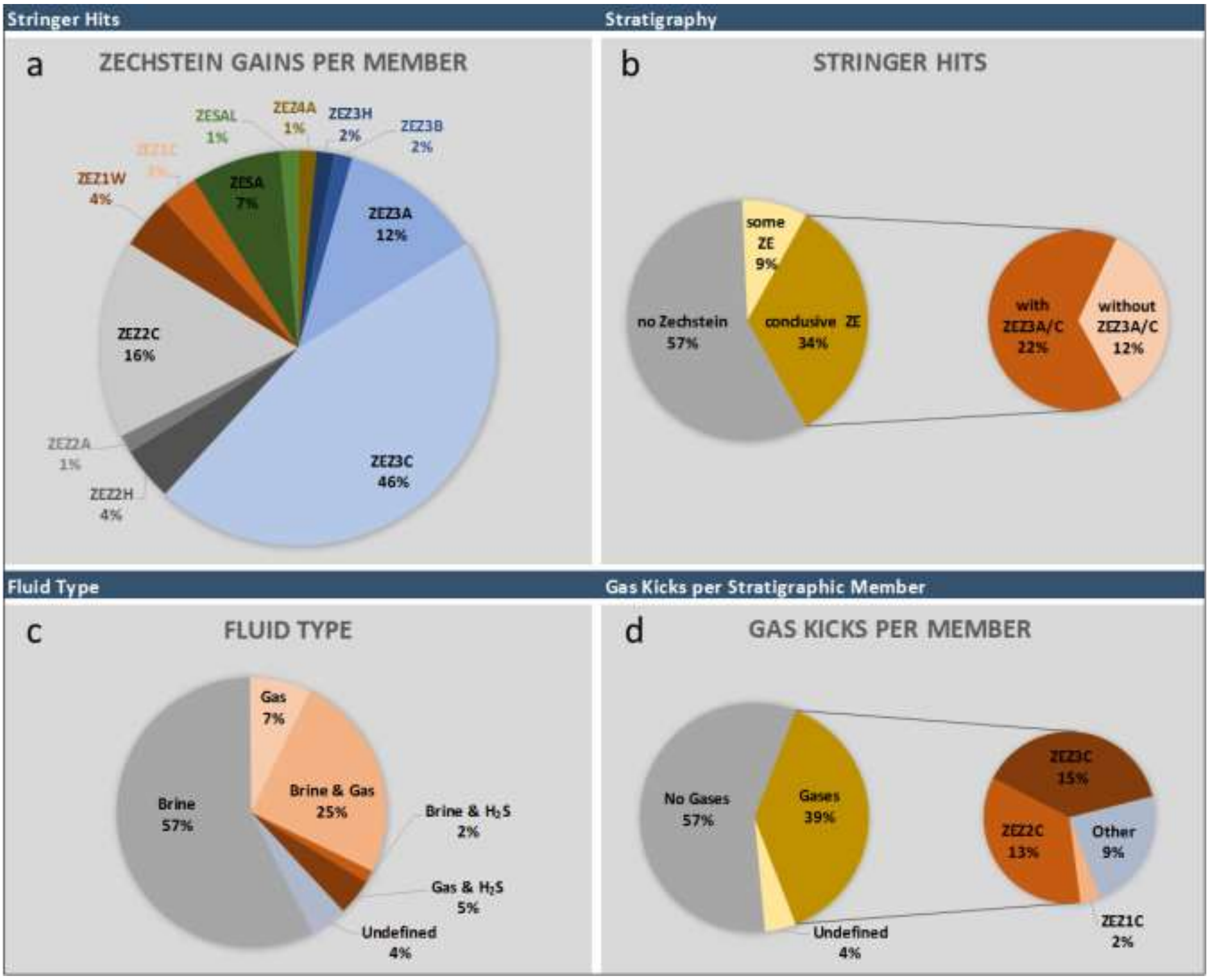

Fig. 10. a) Pie chart showing the relative amount of ZE gains per stratigraphic member, total of 68 gains within 174 wells. (b) Pie of pie chart showing the relative number of boreholes, from all boreholes in The Netherlands, that were conclusive and encountered ZEZ3A/C. (c) Pie chart illustrating the fluid type of kicks from the 68 gains. (d) Pie of pie chart illustrating the relative amount of gas kicks that originated from ZE carbonate members. From EBN internship report by P. Schilder (2019).

3. Data and Methods

3.1 Seismic Survey Data

Two recent seismic data sets were analysed for this research. Survey locations are indicated on the map in figure 11. The Hansa 4Quad re-processing of 2017 pre-stacked time SEG-Y cube is used for most of this study, due to its exceptionally high quality, in particular for the intra-Zechstein details. The Hansa Gems re-processing 2015 pre-stacked time SEG-Y cube is of lesser quality and is therefore used as a reference to check results from the Hansa 4Quad survey. Both surveys extent to 4500-5000ms two-way traveltime and processing focus has been on the Rotliegendes at 4 seconds. Horizontal resolution for both surveys is 25 meters for the In-line's and 12,5 meters for the X-line's. Vertical resolution at the zone of interest is in the range of 10-15 meter. General European seismic polarity convention will be used for this research, unless stated otherwise (appendix A). This means that an increase in acoustic impedance results in a signal *trough* and is displayed on seismic as a red loop, the opposite results in a blue loop.
The top stringer response is a profound impedance contrast increase because of the salt to anhydrite transition. The base of the stringers is marked by transition from anhydrite/carbonate to halite and hence an impedance decrease (the intermediate ZEZ3 clay is too thin to resolve seismically). This results in a typical stringer response of high-amplitude red loop followed by a high-amplitude blue loop. Synthetics and seismic-to-well ties were made to verify this response.
To interpret well logs and seismic, the data was loaded into the Petrel software version 2018. Horizon interpretation was done by manually picking seedlines every 10-50 In- and X-lines. To fill the horizon completely, the 3D auto-tracking tool in Petrel was used. The horizon created, is quality checked for any mis-picks and thereafter corrected manually. From the horizons, surfaces were created with the use of minimum curvature interpolation. This workflow was used for the top and the base of the stringer separately. Other horizons have also been manually picked, but with an 25-250 In- and X-line interval, dependent on reflection strength and continuity. The same method of surface interpolation has been used.

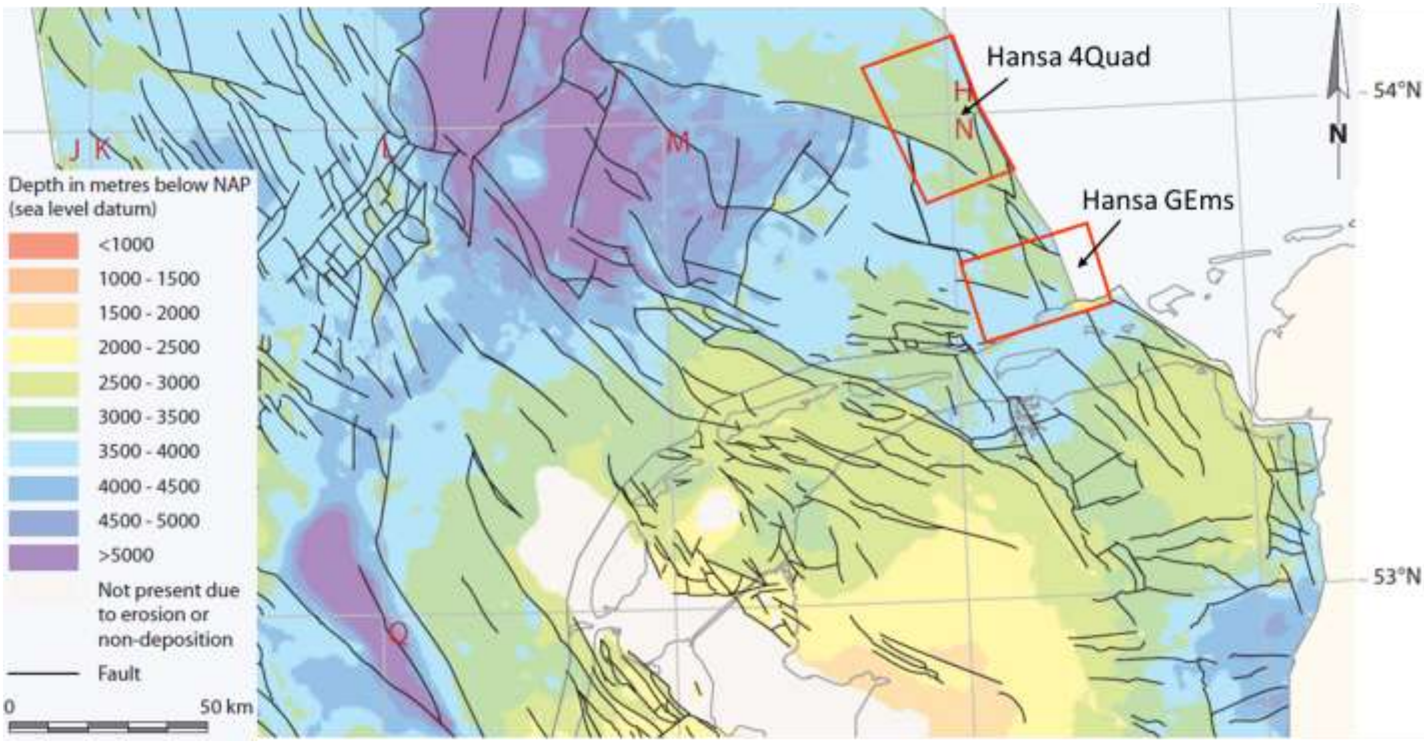

Fig. 11. Depth map of base Zechstein with faults in black. On top of a territorial map of the Netherlands, red numbers (H,J,K,L,M,N,Q) indicate block names. Study areas indicated by the red squares. Modified from Kombrink et al., 2012.

Subsequently a 3D stringer time-isochore grid has been produced by subtracting the stringer top (time) map from the stringer base (time) map. This was done using the simple grid modelling feature in Petrel and the geometrical stratigraphic cell height tool. The time difference map can be converted to a depth thicknessmap using the applicable velocity of 5500 m/s as dictated by the sonic logs.

Well-to-seismic ties in this research are produced with the seismic-to-well tie feature in Petrel. Wire-line sonic and density log data from NLOG were used to make the tie. Checkshot data from velocity reports, also available on the NLOG website, were used to create a time-depth relation for the wells. From this data a sonic calibration for selected wells was made and quality checked. Subsequently, the final seismic-to-well tie was made by linking seismic responses manually to the synthetic signal, with the use of the Petrel tool palette, to produce a sound correlation between well and seismic.

3.2 Well Data and Geo-Drilling Event Classification

The well database available on the NLOG website, provided by TNO, was used to evaluate stringer thicknesses and in particular the variation in thickness from well to well. From this data, 154 wells where selected based on their anomalously thickly developed stringer. These cases have been cross validated in the GDE database for possible drilling events. Selected wells and relevant auxiliary data are recorded in appendix B.

To assist operators in the Netherlands with well planning and assessing subsurface risks, EBN created a 'Geo-Drilling Event database' containing GDE data from wells drilled in the Dutch subsurface. The GDE database of EBN is developed and described by Kuiper (2017) and extended by Baud (2018).
Geo Drilling Event recorded in the database are described by four types of data:
1) general well data (e.g. coordinates, year of spud, operator),
2) Geo-Drilling Event (describing observations, type following classification rules and incident severity),
3) Geo-Drilling Hazard (based on geological interpretation of the facts),
4) audit trail documentation.
Figure 12 displays the EBN classification scheme and guideline used to define GDE's. As per December 2018, 960 wells are incorporated into the GDE database and 1171 events are recorded. Examining wells for GDE's, the NLOG database and the internal EBN database were used to gather final well reports and weekly- or monthly drilling reports. Normal procedure would be to study wells from spud to TD and integrate all events in the GDE database making use of the Mendix environment of EBN. For this study it was decided to investigate wells for GDE's, only in the Zechstein Group. To avoid a Zechstein bias in the GDE database, events found in the selected wells were not incorporated into the database straight away. An Excel sheet was produced with the same input markers as the Mendix environment and these wells will later, when completely checked, be added to the GDE database. Twenty-two wells, out of the selected 154 in this study, were already fully investigated and incorporated into the EBN GDE database.
For this study the well trajectories have been investigated at the locations where it drilled through the Zechstein stringer. At these well locations the seismic has been studied in detail in order to understand lateral extend of the (anomalous) stringer response. Seismic surveys were taken from the EBN database. Most locations have been studied with the use of the combined seismic surveys, called Terracubes, produced by Fugro in 2007 and reprocessed in 2011. This analysis was carried out using Petrel 2018 software.

Geo-Drilling Event Classification			Severity Guidelines		
GDE_CODE	GDE_Type	GDE Description	High examples	Medium examples	Low examples
		Hole Geometry			
1	**Stuck Tubular/Tool**	Stuck pipe and/or excessive overpull and/or torque of the drill string or casing. Incidents may include: - Stuck pipe occurence during the drilling phase - Casing stuck and/or prematurely set due to no further progress while running in - Hole pack-off - Excessive reaming and/or hole cleaning required in combination with excessive overpull/torque - Differential sticking - Obstruction running liner or casing in the hole - Stuck logging tool (with the exception of a washout)	Lost drilling assembly in hole Prematurely set casing string in different than planned formation with effect on shoe strength Prematurely set casing string	Excessive jarring, reaming and/or circulation required Differential sticking requiring to spot a light fluid (e.g. base oil) pill to reduce overbalance Hole obstruction during casing running requiring an additional BHA check trip or opening up the hole	Excessive torque and/or overpull, but manageable
2	**Clay Balling**	Swelling and sticking clay causing - a packed off drilling assembly - blocked flowline/flowriser - inability to continue drilling (no ROP)	Lost tophole and/or sidetracked due to pack off and subsequent stuck pipe	Significant time delay due to clay balling Multiple trips required High-volumes swabbing occurence due to clay balling	Clay balling occurence but manageable
3	**ROP**	Excessive wear of the drill bit resulting in reduced rate of penetration and/or excessive number of bit trips Unexpected reduction in ROP resulting in significant delay	Excessive number of bit trips required due to extreme bit wear	Multiple bit trips required due to excessive bit wear	Reduced ROP and significant bit wear observed
11	**Steering**	Difficulties while steering the drilling assembly during drilling, either in rotary or sliding mode. For example due to formation change or formation dip angle	Failed to reach objective	Steering difficulties, multiple BHA's required. Trajectory outside targetbox (at objective)	Steering difficulties, more time required to steer BHA
10	**Washout**	Unconsolidated formation, collapsing into the hole. Washed out formations as a result of mud type or excessive local circulation, possibly in combination with (anomalous) geology.	Washout resulting in accidental sidetrack Washouts resulting in insufficient cement around casing or liner	Washout resulting in significant quality loss of logging results	Washout requiring additional reaming or working of pipe/tools
9	**Deformed Tubular**	Deformed or collapsed casing/liner/tubing during well contruction or re-entry of an existing well, possibly in combination with (anomalous) geology	Deformed casing/liner/tubing resulting in - significant operational delay (> 5 days NPT) - Complete loss of functionality of well	Deformed casing/liner/tubing resulting in - moderate operational delay (1-5 days NPT) - partial loss of functionality of well	Deformed casing/liner/tubing resulting in - minimum operational delay (< 1 day NPT) - no loss of functionality of well
		Pressures			
4	**Gain**	Flow of formation fluid into the borehole during well construction	Influx exceeding kick tolerance Kick-loss situation Well Control situation resulting in >5 days regaining well control Kick resulting in prematurely setting casing	Well control situation requiring well to be circulated to heavier fluid in controlled manner (over the choke) High pressures requiring a contingency liner to be set to allow drilling ahead	Able to control influx whilst drilling ahead Increased mud weight to overbalance formation pressure
5	**Losses**	Lost drilling fluids and/or cement into the formation during well construction	Total losses, unable to keep the hole full Total losses leading to a kick/loss situation Losses during cement job resulting in lower TOC than planned Losses compromising section target Losses resulting in prematurely setting casing	Numerous LCM pills required to cure losses Gunk and/or cement pills required to cure losses	Losses curable whilst drilling (eg. By adding LCM material)
		Geology and Fluids			
7	**HC**	The unpredicted occurance of hydrocarbons while drilling	Mitigating the unpredicted occurance of HCs giving rise to: - significant operational delay (> 5 days NPT) - Complete loss of functionality of well - Prematurely setting casing	Mitigating the unpredicted occurance of HCs giving rise to moderate operational delay (1-5 days NPT)	Mitigating the unpredicted occurance of HCs giving rise to minimum operational delay (< 1 day NPT)
8	**H2S**	The unpredicted occurance of H2S while drilling	Mitigating the unpredicted occurance of H2S giving rise to: - significant operational delay (> 5 days NPT) - Complete loss of functionality of well - Prematurely setting casing	Mitigating the unpredicted occurance of H2S giving rise to moderate operational delay (1-5 days NPT)	Mitigating the unpredicted occurance of H2S giving rise to minimum operational delay (< 1 day NPT)
6	**Lithology**	Unexpected and/or unpredicted formation encountered while drilling. Actual formation depth significantly different than prognosed.	Missed final drilling target Failed to find objective	Found objective but after significant delay e.g. after sidetrack	E.g. Formation coming in significantly deeper or shallower than prognosed (>100m) but no compromises on well design and/or target missed
12	**Other**	Other geological-related incidents that cannot be categorized by any other code in this table **Note: Non-geological drilling incidents are not recorded in this database**			

Geo-Drilling Hazard Classification		
HAZ CODE	HAZ Type	Description
	Rocks	
F	**Fault** (Faults/fractures in the borehole)	Destabilised rocks due to (natural) faulting/ fracturing. Resulting in anomalously high permeability (losses) and/or excessive cuttings/ cavings. Note that karstification might show up similarly as faults but is strictly spoken a different geological phenomena (see R)
C	**Swelling Clay** (Chemically unstable sediments)	Reactive formations (eg. swelling clays)
S	**Squeezing Salt** (Unstable evaporites)	Borehole formation deforming caused by high (litho) pressures mobilising evaporites
W	**Unstable Sediment** (Mechanically unstable sediments)	Unconsolidated formation (eg. washouts) Cavings due to high pressure Weak zones in formation
B	**Boulders**	Large detached rocks in borehole, typically originating from conglomerate
R	**Rock Properties** (Unexpected hard/soft or unexpected permeable)	Unexpected hard or soft formations Abrasive formation causing excessive bit wear Steering difficulties due to soft/hard alternation Dip angle
	Fluids	
D	**Depleted Reservoir**	Low reservoir pressure (e.g. due to nearby production)
E	**Shallow Gas**	Unexpected gas shows at shallow depths
G	**Anomalous Pressures**	Unexpected or unpredicted high or low geopressures: High pressures exceeding expected formation pressures (e.g. unexpected brine flows, brine pockets) Formation fluid pressures lower than expected (e.g. unexpected depletion due to nearby production)
H	**H2S**	Unexpected occurrence of hydrogensulfide gas in borehole
	Other	
M	**Mapping Uncertainty**	Unexpected formations Subsurface mapping is generally based on well and/or seismic data. Results are based on interpretation and can contain errors or has large uncertainty. Structural complexity, T2D conversion, flanks, unexpected fault/offset
Z	**Other / Unknown** (Other/Unknown Geo Hazard)	Other geological hazard (e.g. unconformities) or unknown geological hazard.

Fig. 12. Classification scheme of 12 types of GDE's, with per type the severity guidelines. Supplemented with 12 different Geo-Drilling Hazards, with description of a probable geological cause. Produced by EBN B.V.

4. Results of 3D Seismic Interpretations

4.1 Interpreted Zechstein Horizons in the Hansa 4Quad Survey

Seismic reflections of different tops and bases in the Zechstein can be traced relatively well through the research area, due to the high quality of the data set. Figure 13 shows time depth maps of; Basal Anhydrite (ZEZ2A), Top Zechstein, Base Stringer (ZEZ3C) and Base Cretaceous Unconformity (BCU). The time depth Basal Anhydrite map (figure 13a) shows the shallowest extent of the pre-salt faults and two different fault sets can be distinguished; NNW - SSE and WNW – ESE. Roughly through the middle of the area the Rifgronden Fault Zone (RFZ) can be seen, running WNW – ESE and dividing the Ameland Platform and the Schill Grund Platform (Kombrink et al. 2012).

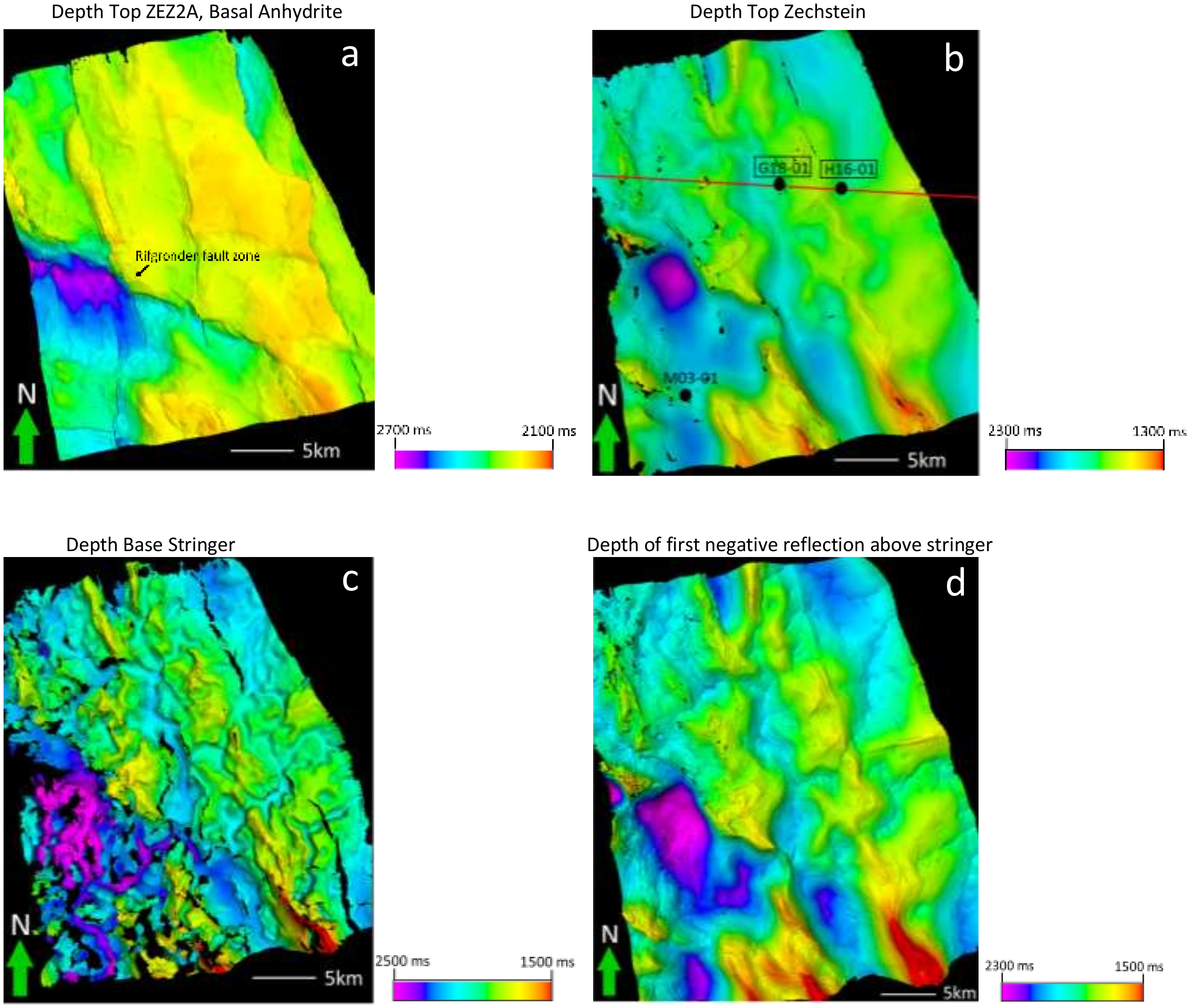

Fig. 13. a) Time depth map of the top Basal Anhydrite, ZEZ2A. Visible in this horizon are the two fault sets, WNW - ESE and NWN - SES, running through the research area. b) Time depth map of Top Zechstein, salt pillows in the south and the structures running mainly NWN - SES. Location of the three wells drilled in the area shown as black dots. Red line shows the cross section further discussed in chapter 4.5. c) Time depth of Base Stringer map, heavy folding visible and the strong correlation to the top Zechstein. Note: the black "gaps" in the map are considered real gaps. d) Time depth of first negative reflection above stringer, correlating to different lithologies. Note: the branching depressions in the salt lows.

Salt structure orientation and geometries are clearly visible in the depth map of the Top Zechstein (figure 13b). The main orientation of the salt pillows is NWN -SES, although south of the RFZ salt structures also orientate in a WNW -ESE direction. Furthermore, salt structures south of the RFZ are more profound and penetrate higher into the overburden. Figure 13b depicts the locations of the three drilled wells; M03-01, G18-01 and H16-01, all deep enough to penetrate through the entire Zechstein sequence.

The time depth map of the Base Stringer or 'Plattendolomite' (figure 13c) visualizes the large amount of (concentric) folding present and the vertical position of the stringer which follows the Top Zechstein closely. Black areas, zones where no stringer could be picked, are visible throughout areas. This can either be a real 'gap' in the Stringer, caused by tectonic extension, or the result of a (steep) stringer not visible on seismic (figure 14). Well M03-01 penetrates a black zone present on seismic, and log data records no stringer present and therefore, this is proposed to be a real 'stringer gap'.

Figure 13d represents the first negative reflection (red) above the stringer. This reflection does not correlate to the same lithology throughout the study area. Seismic to well ties in chapter 4.4 show that in well H16-01 the reflection originates from a K-Mg salt in the middle of Zechstein III halite member and in well G18-01 from an anhydrite interval at the top of the Zechstein III halite (chapter 4.4). In the north western and southern part of the study area the first negative reflection is derived from the top Zechstein. Important to note here are the narrow branching depressions in the lower parts of the horizon and in between the salt structures.

To get a complete image of the stringer the Top Stringer or 'Hauptanhydrite' reflection was also interpreted. This horizon has a similar appearance as the Base Stringer horizon. The top often differs in the deeper or synclinal parts of the stringer. Here the Two-Way Time (TWT) difference is larger than the average of 15 milliseconds. Figure 14 shows some of these zones where the Base and Top of the stringer divert in deeper and synclinal areas of the stringer. These features can be found throughout the study area and are referred to as "Thickened Zones" (van Gent, 2011).

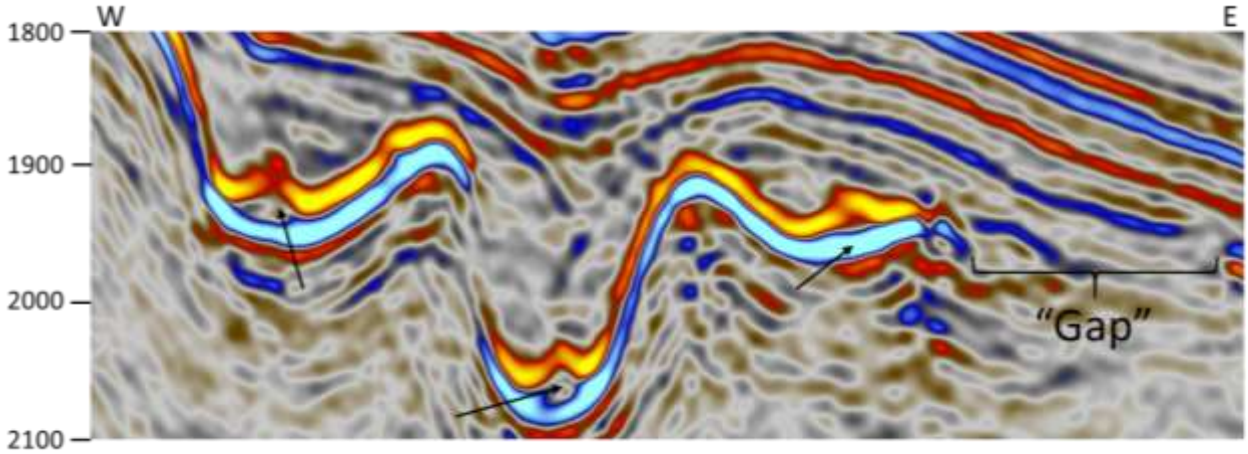

Fig. 14. W-E cross section in TWT, black arrows point to features in the deeper and synclinal parts of the stringer, referred to as "Thickened Zones" (van Gent, 2011). In the right part of the image a "gap" can be seen, resulted by the rupturing of the stringer.

4.2 Isopach Maps

4.2.1 Stringer Thickness Map

Geometries and distribution of thickened zones (TZs) can best be assessed with a stringer thickness map. Figure 15 shows a top view of a 3D model for the stringer in the Hansa 4Quad survey. This map is colour coded to the stratigraphic height of the cells representing the stringer time thickness. To produce thickness in meters multiplication with the interval velocity of the stringer is required. Checkshot and sonic data from the wells in the Hansa 4Quad survey resulted in a stringer velocity of 5500 m/s for this area. Black zones in the map have a 0-meter thickness which corresponds mostly to real stringer gaps but can also be data gaps (e.g. poor data or steeply dipping stringers). The western part of the map, marked by a pink polygon, is an area of lower seismic quality, resulting in many black zones.

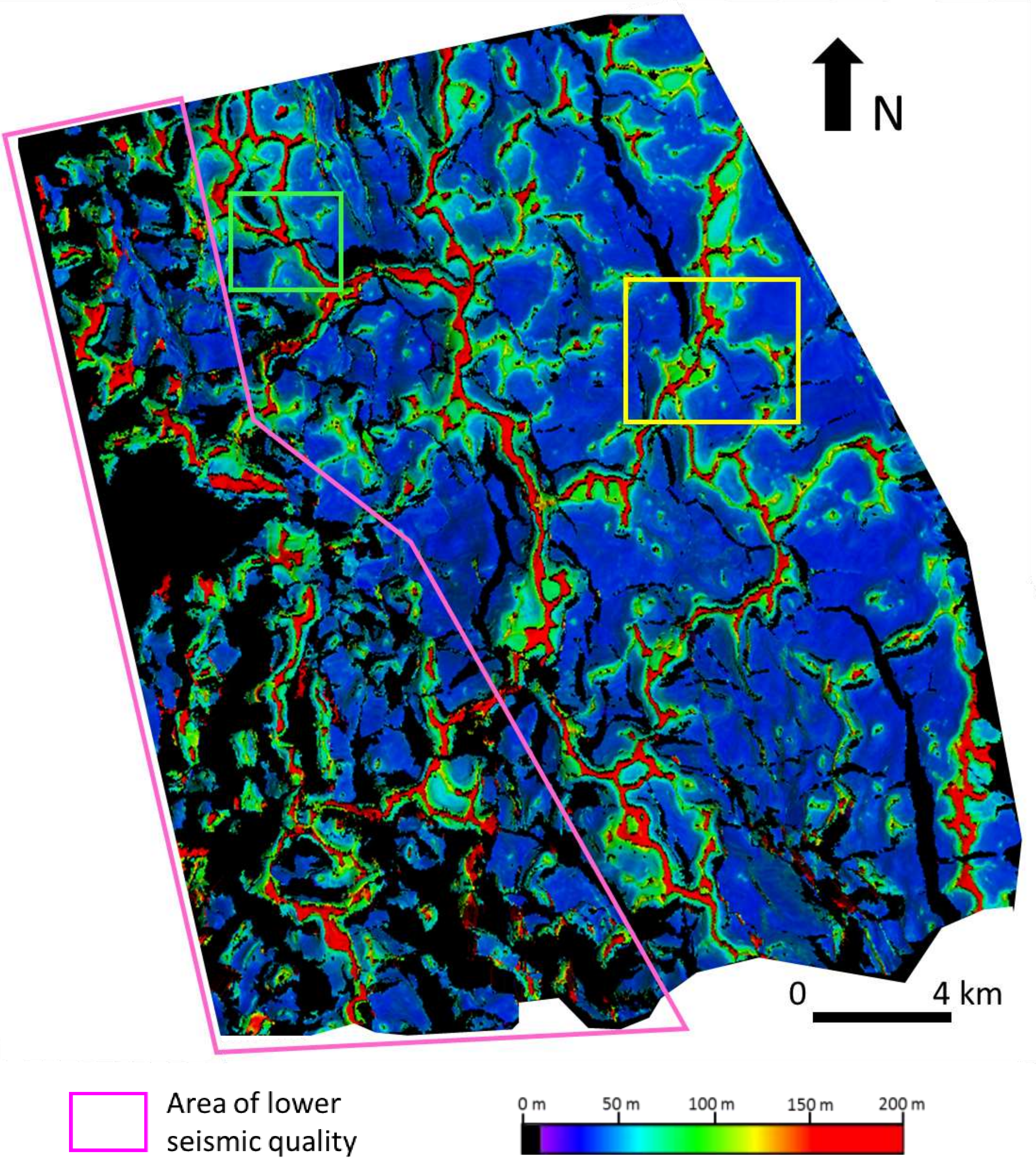

Fig. 15. Map view of the 3D stratigraphic cell height model of the stringer interval. Black parts of the map are stringer gaps, in the lower quality these gaps are mostly due to seismic and picking inaccuracy. Outside the pink polygon, the black stringer parts are predominantly considered to be real gaps, or ruptured stringer segments. Green to red, respectively 70 to 200 m, are referred to as thickened zones. Blue parts are shallower areas and follow the outline of salt structures. The green square shows a TZ offset by a fault, further enlarged in figure 16. In the yellow square clear polygonal geometries can be seen in a concentric synclinal part of the stringer (enlarged and discussed in chapter 5.1.1).

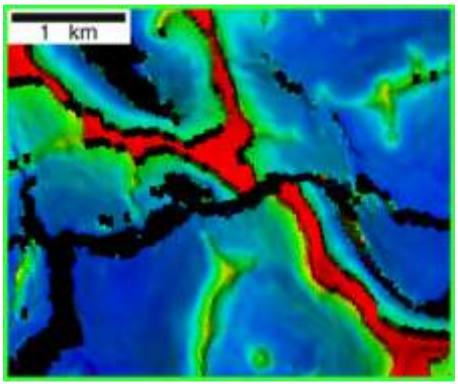

Fig. 16. Fault off setting a TZ (in red), for location see Figure 15.

The TZs in figure 15 are coloured from green to red and are present predominantly in between the salt highs (figure 13b). Regionally the TZs appear as narrow, elongated features with some (superficial) resemblance to a drainage pattern.

Thickened zones are strongly correlated to synclinal structures in the stringer (correlations also found by van Gent (2011) and Strozyk et al. (2014)). Furthermore, a strong correlation can also be found with the local depressions visible in figure 13d. Cross sections in chapter 4.5, figure 22 and 23, show nice examples of these depressions located directly above TZs throughout the study area.

In figure 16 the green square of the stringer thickness map (figure 15) is shown enlarged. This is a clear example of a fault off setting the TZ, an observation that can also be seen in different parts of the Hansa 4Quad survey.

4.2.2 Isopach Map of Top Zechstein to Base Rijnland Interval

In figure 17 a visualization is made from the (time) stratigraphic thickness (TST) Top Zechstein to the Base Rijnland or the Base Cretaceous unconformity (BCU). The red and green areas represent a TST of 125 to 300 ms, corresponding to a thickness of 230 to 555 meter. To convert ms to meters, an average velocity for this interval of 3700 m/s was used. Blue, purple and black areas exhibit lesser thicknesses from 0 to 125 ms. The black parts, mostly present at the tops of the northwest salt structures (figure 13a), are areas where the BCU eroded all the way to the top Zechstein and perhaps even partly into the upper Zechstein formations.

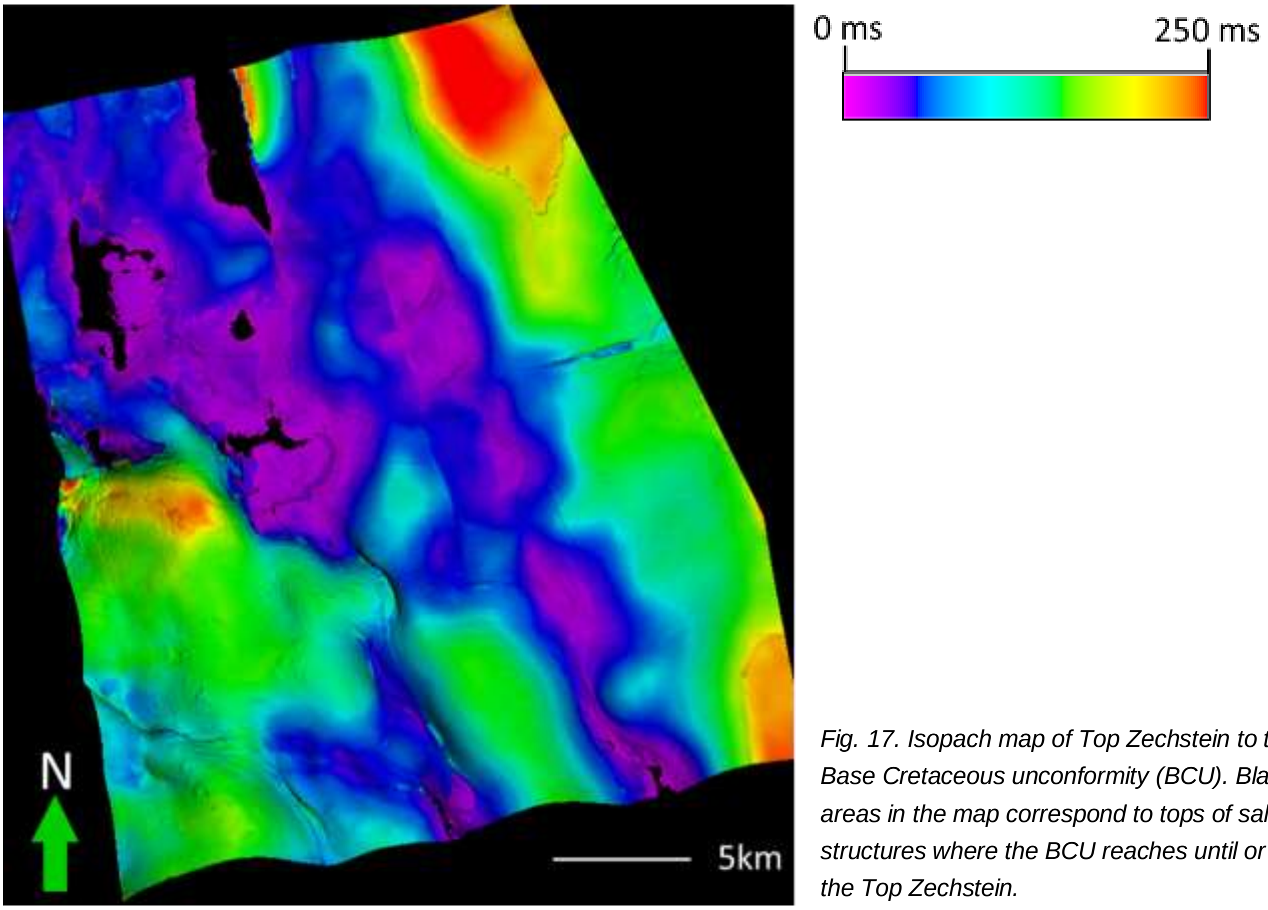

Fig. 17. Isopach map of Top Zechstein to the Base Cretaceous unconformity (BCU). Black areas in the map correspond to tops of salt structures where the BCU reaches until or into the Top Zechstein.

4.3 Thickened Zone Distribution

To get a better insight on the geometries of TZs and surrounding structures, measurements of the TZ top width and the associated syncline width have been taken from seismic sections. Cross sections of 64 different TZs perpendicular to the synclinal hinge, were examined (figure 18A) and results displayed in a scatter plot (figure 18B). Appendix C shows the locations of all cross sections taken from the study area (images of all cross sections on request). Note: some cross sections capture several TZs.

A linear regression trendline drawn through the data in figure 18B, has a R^2 of 0.69. There seems to be a moderately strong, positive correlation between the width of the stringer syncline and the width of the TZ top. Seismic appearances of these TZs are divided in to three different groups or types based on the most common appearances. Figure 18A shows representative 'type-sections' for the three different types. Type 1 TZs have a broad upper red reflection and below it upward curved red reflections with a blue reflection in between. Furthermore, they have the steepest (or broken) syncline flanks. Type 2 TZs have a small red reflection with below a small blue reflection, on top of two curved red reflections that show a very small gap in between. Type 3 TZs appear as continuous, flexed and not broken-up, red reflections in the stringer. From the 64 TZs examined, 9 are categorized as type one, 34 as type two and 21 as type three. Type 2 & 3 have some overlapping data points (visualized by the colored circles), while type 1 does not overlap the others and the ellipse axis is tilted more to 45°.

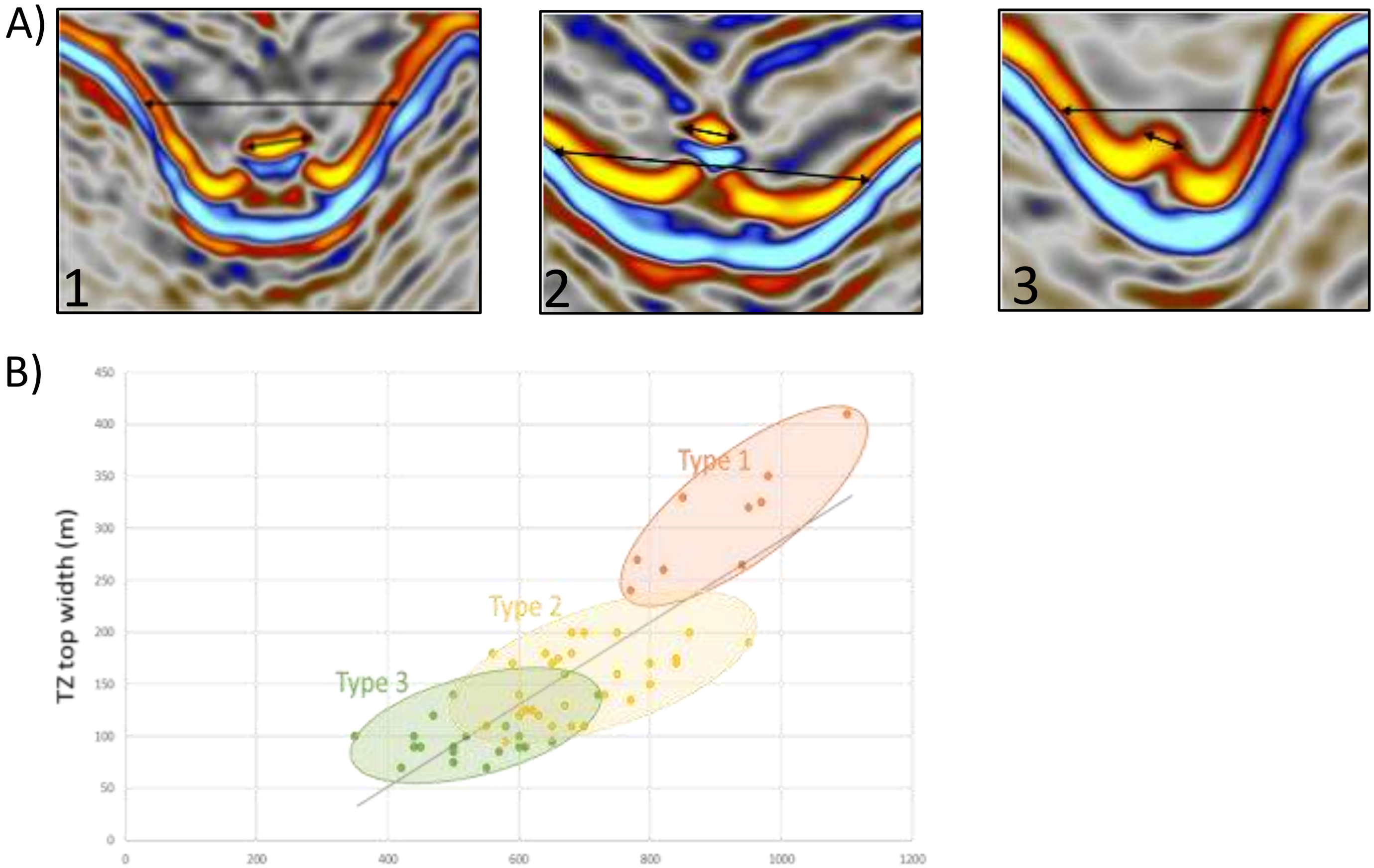

Fig. 18. A) The three 'type-sections' for each type of TZ, chosen in this research. Longer black arrows represent the synclinal width and shorter black arrows represent the TZ top width. B) Cross plot representation of the TZ top width against the synclinal width, measured perpendicular to the syncline hinge. Drawn through it a linear trendline with an R^2 of 0.69.

4.4 Seismic-to-Well Ties in the Hansa 4Quad Survey

For the three wells in the area, two succesful seismic-to-well ties could be made. Well M03-01 had insufficient log data to produce a robust tie with the seismic. The results of the seismic-to-well ties of well H16-01 and G18-01 will be discussed separatly. Note: to facilitate the seismic and synthetic comparison, the reversed colour convention (compared to the EBN convention) had to be used.

4.4.1 Well H16-01

Figure 13b shows the location of where well H16-01 penetrated the stringer (1982). Most interesting about this well is that is it one of the few wells that penetrates the stringer in a TZ location as seen on seismic. This allows for a good understanding of lithological well log responses and the representing seismic response of the TZ feature.

In figure 19 the seismic-to-well tie from Lower Triassic to the upper part of the Zechstein II halite is shown. The bottom part of the well tie, until the first strong reflector, is part of the Zechstein II halite. Most of the reponse is a classic halite response (low density and low GR). At the top density and sonic show light changes, but especially the GR response increases significantly. This is the response of the K-Mg salts present at the top part of the Zechstein II formation. A sharp transition can be seen at the interval between the Zechstein II & III, present in the form of a red reflection (generally shown as a blue reflection). Density values increase greatly and together with the sonic and GR log stay stable for ~180m. This interval is the "Thickened Zone" of the stringer and consists for more than 95% of anhydrite, with below the base a carbonate layer (ZEZ3C) and a shale (ZEZ3G).

Another sharp transition marks the boundary between the TZ and the overlying Zechstein III halite member (ZEZ3H), resulting in a strong blue reflection with strong side lobe loops. These side lobes are also visisble on seismic, but do not represent a lithological change.

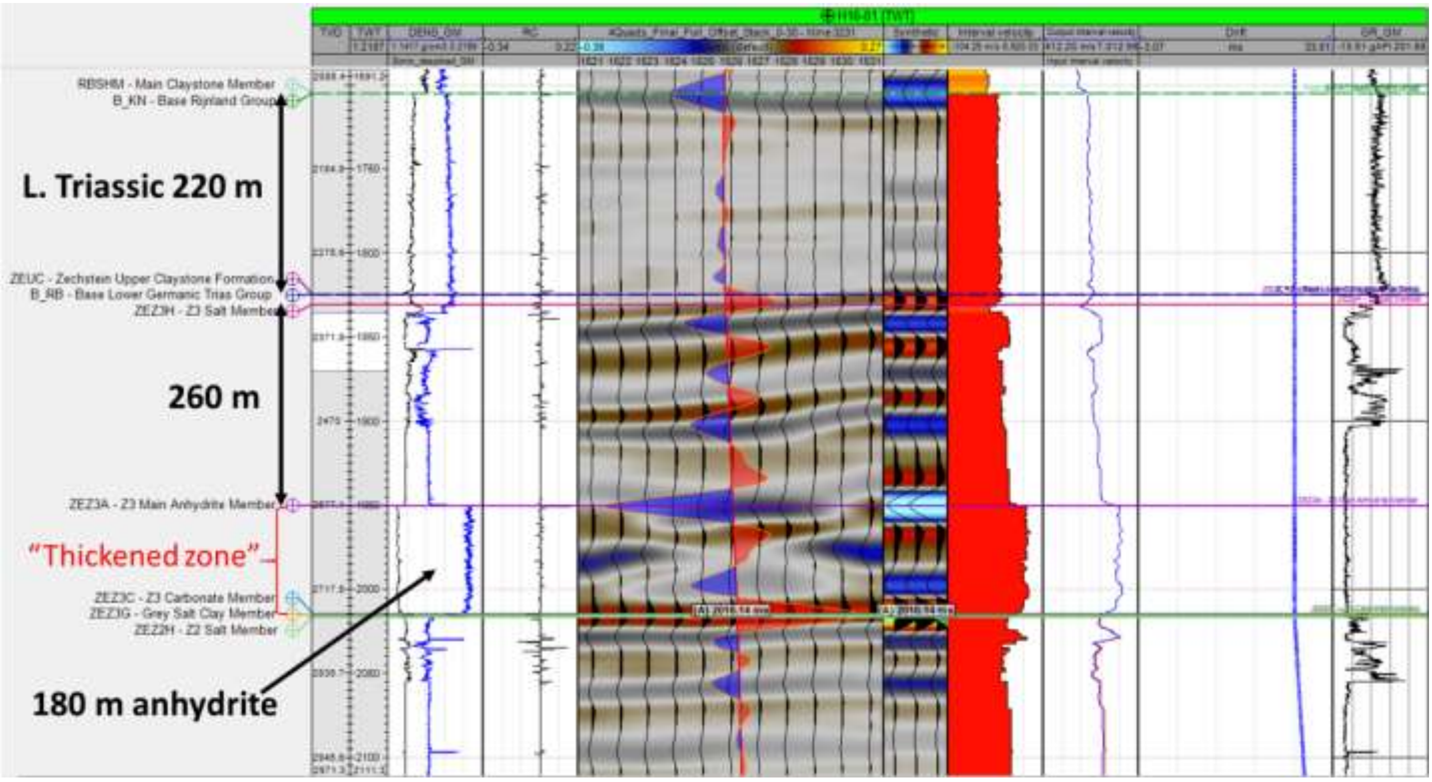

Fig. 19. Seismic-to-well tie of H16-01 well in the Hansa 4Quad 3D seismic survey, with density, sonic and GR log data. The 180 m anhydrite interval, depicted by the black arrow, is referred to as a "Thickened Zone" (TZ). Above the TZ a 260 m ZEZ3H and a 220 m Lower Triassic is recorded. Note: reversed colour convention, compared to the standard EBN convention, is used.

At the lower part of the 260 meter ZEZ3H another classic clean halite response can be seen which results in no reflections on seismic. From this interval to the Top Zechstein three blue and three red reflections are recorded on seismic. Density and GR data show that there are indeed changes in the salt member here. No specific information can be found in the well reports about what the type of salts are. Since there are numerous high peaks in the GR, these are most likely intervals of several different K-Mg salts like; carnallite, sylvite, kieserit, bischofite, tachyhydrite and polyhalites (Raith, 2017).
Above the ZEZ3H a small interval is recorded, which is correlated to the Zechstein Upper Claystone Foramation (ZEUC). This formation has a steady log response and due to its thickness it is, for this study, incorperated into the Top ZEZ3H and Top Zechstein. This means that the Top Zechstein is represented by a red reflection (with EBN convention shown as a blue reflection). The upper part of the well tie consists of the Lower Triassic, the Main Claystone Member (RBSHM). No significant reflections are imaged over the 220 meter formation. The top of the Lower Triassic, or the Base Rijnland Group, corresponds to a moderately strong blue reflection.

4.4.2 Well G18-01

Exploration well G18-01, drilled in 1983, penetrated the stringer at the location of a salt pillow (figure 13b). Well data and the seismic-to-well tie in figure 20 shows that it drilled through 48 meters of ZEZ3A and a couple of meters of ZEZ3C. This thickness is referred to as a normal or an average stringer for this study.
Below the stringer the ZEZ2H interval shows roughly the same response as well H16-01, with mainly a classic halite response and several K-Mg salt intervals. The stringer interval is responsible for two bright reflections, red base and blue top, stacked on top of each other. This well tie does not produce any significant side lobes from these strong reflections, with respect to well H16-01. Above the stringer the ZEZ3H interval shows mainly no reflections and core log data suggest halite to be present here. Just below the Top Zechstein one red and one blue reflection are recorded on seismic. The red reflection is produced by a high-density interval, correlated to anhydrite. The blue reflection seems to be produced by a medium density and sonic interval between two anhydrite layers, which likely correlates to a carbonate or shale layer. In this well the Top Zechstein has no separate reflection of its own, as this marker falls inside the upper part of the last blue reflection.
Only 30 meter of Lower Triassic is recorded by well G18-01. Inside the member no significant reflection is recorded, and the Top of the Lower Triassic is recorded with a blue reflection.

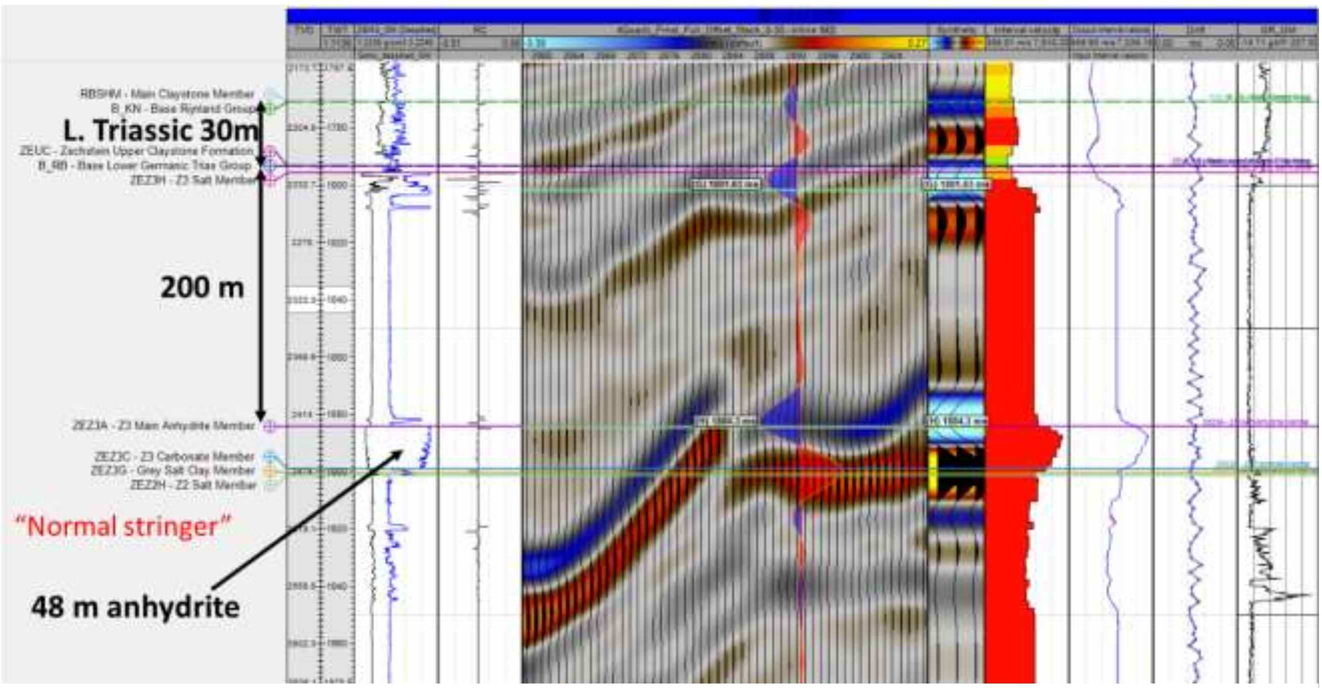

Fig. 20. Seismic-to-well tie of G18-01 well in the Hansa 4Quad 3D seismic survey, with density, sonic and GR log data. The 48 m anhydrite interval, depicted with a black arrow, is referred to as an average stringer thickness for this study. Above the stringer 200 m ZEZ3H and a 30 m Lower Triassic is recorded. Note the reversed colour convention, compared to the standard EBN convention is used.

4.5 Hansa 4 Quad Cross Sections

Well ties as described in chapter 4.4 provide a good base from which to understand the seismic response in the area. Differences between the two wells are significant and are discussed here on a more regional scale by investigating seismic cross sections. Figure 21 displays a W-E cross sections through the location of well G18-01 and H16-01. In this cross section the Top Zechstein is displayed in pink and locations of the wells are highlighted.
Lithological responses observed in both seismic-to-well ties (chapter 4.4), can also be seen regionally in the study area. The ZEZ2H seismic response shows no significant differences throughout the cross section, except the thickness of it. Similar seismic responses of the TZ from well H16-01 can be seen throughout the cross section. Above these TZs a similar seismic response of the ZEZ3H is also present. When tracking this response from H16-01 towards the west, the reflections seem to truncate to the Top Zechstein. From here west, towards G18-01, the seismic response is similar to the response seen in the G18-01 well tie and no TZs are present in the stringer here. Following the ZEZ3H further to the west a slight response difference is visible and below in the stringer, two minor thickenings can be observed. Slightly to the west from here a 2 km wide, fault bounded, synclinal part of the stringer can be observed. In the deepest part a TZ seismic response is present and above the syncline the same, depression shaped, ZEZ3H response as observed in well H16-01. Furthermore, directly above the TZ here a small depression or pull down of the reflections can be seen. This feature is also observed directly above the TZ in the far east and above many other TZs in the area.

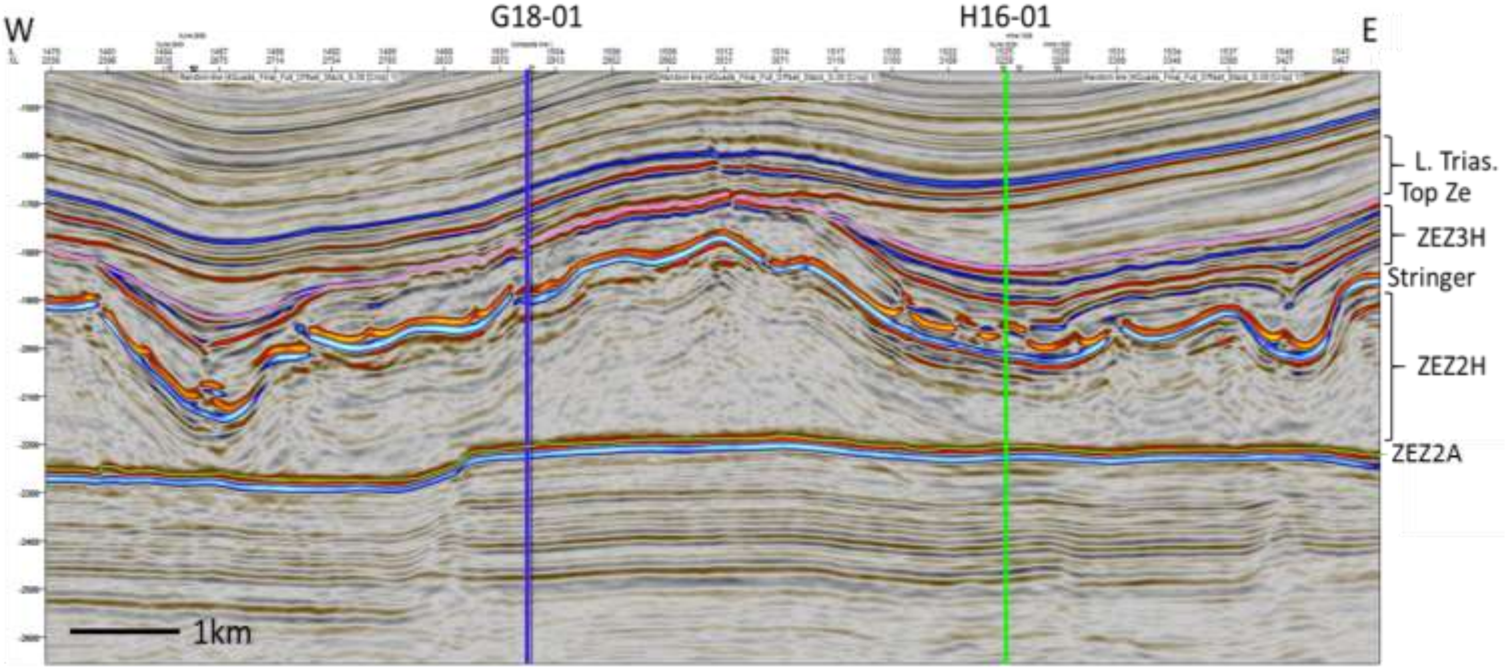

Fig 21. Hansa 4Quad W-E seismic cross section through well G18-01 (blue) & H16-01 (green). Indicated on the right with top and ZEZ2A, the two halite members, the stringer response and the Lower Triassic sediments (L. Trias.).

A better view of the geological features around the Top Zechstein can be created by flattening this horizon. Figure 22 shows the same cross section as figure 21 but flattened on the Top Zechstein horizon. The mini-basin like features in the ZEZ3H above the TZs are better visible with this flattening. Furthermore, this flattening shows that the Lower Triassic sediments, reflection less package (figure 19), follow the outline of the accommodation spaces (or-mini) basins of the ZEZ3H.

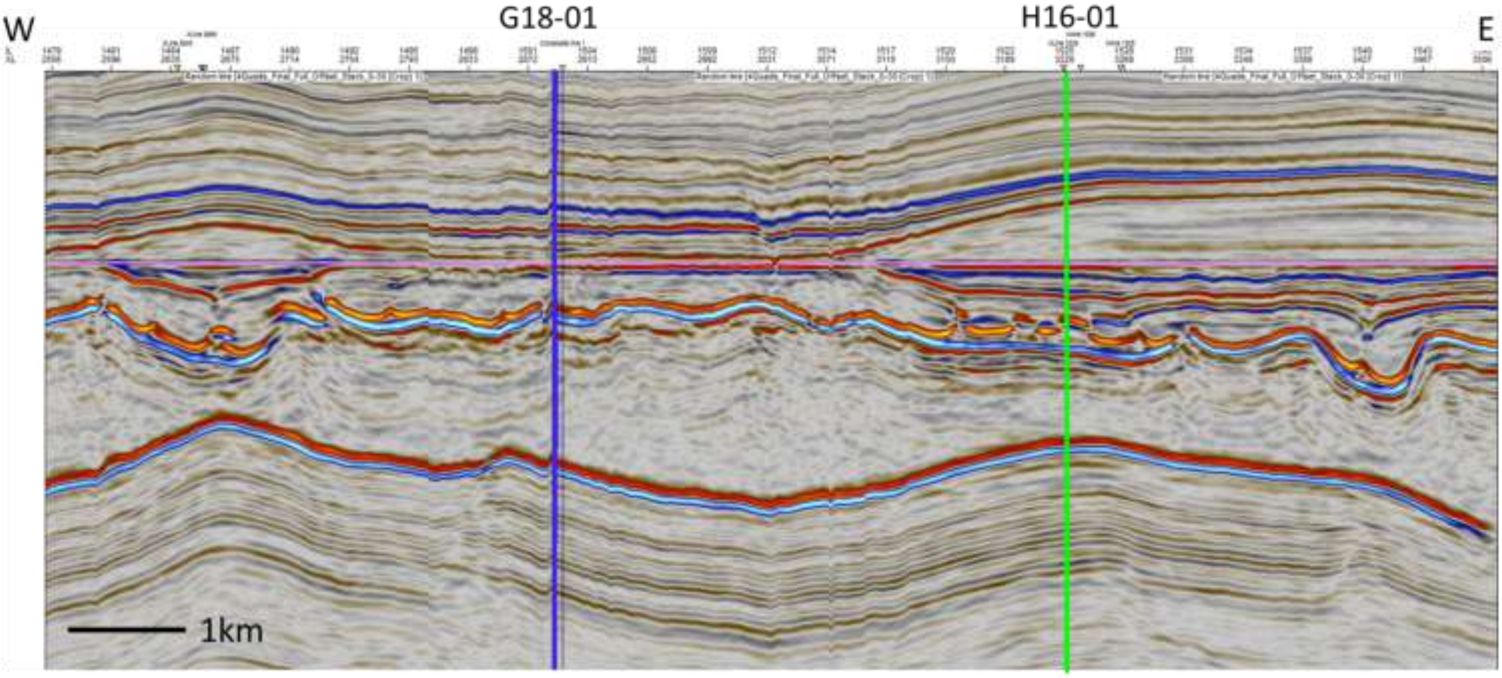

Fig. 22. Hansa 4Quad W-E seismic cross section through well G18-01 (blue) & H16-01 (green), flattened on the Top Zechstein (pink). Note the basin features of the ZEZ3H member and the mirroring of Lower Triassic basins.

Similar correlations can be seen on the, Top Zechstein flattened, NWN-SES seismic cross section through well H16-01 (Figure 23). Basin features from this view can been seen almost entirely from NWN to SES. Different in this cross section is the thickness distribution of the Lower Triassic member compared to the ZEZ3H member. Whereas the ZEZ3H is mostly uniformly thick, the Lower Triassic and the deepest part can be found in the north.
Stringer parts with no TZs are also present here underneath the basins, so here there is no straightforward correlation between the TZ and basins.

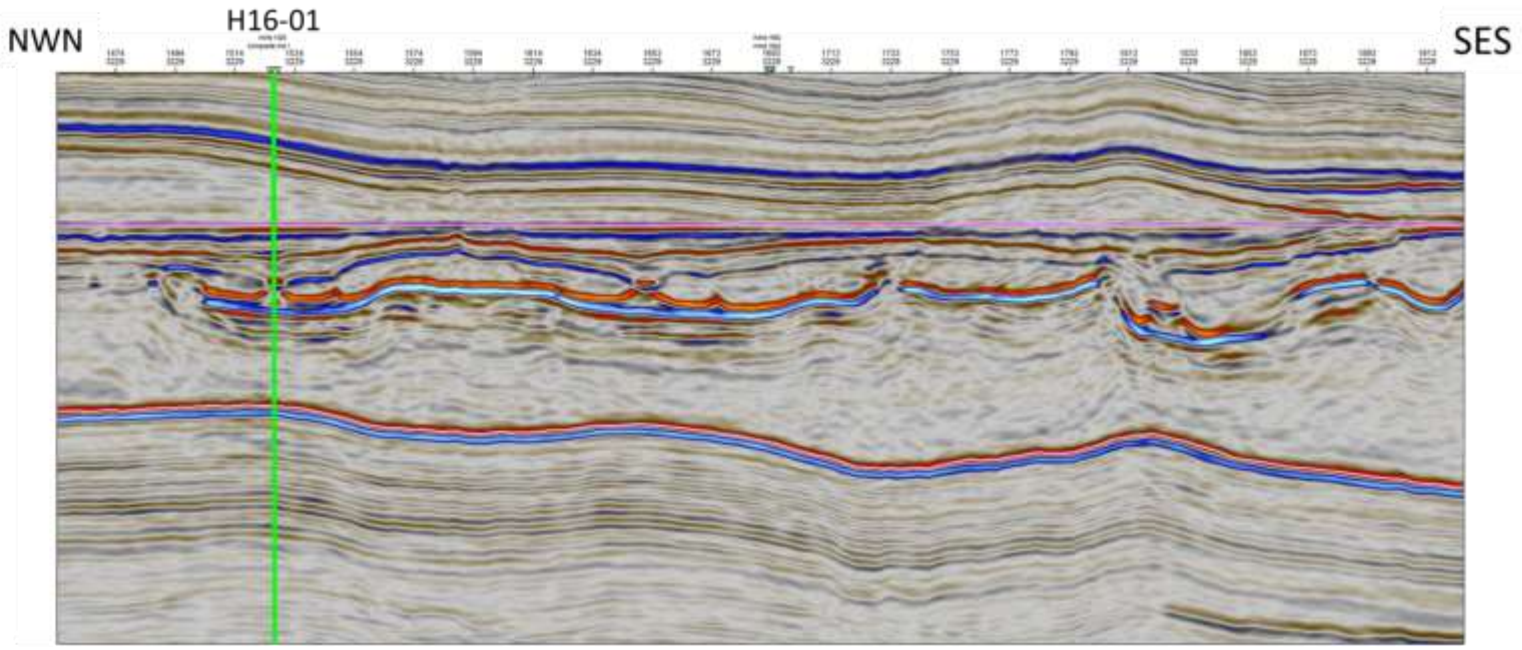

Fig. 23. Hansa 4Quad N-S seismic cross section through H16-01. Flattened on the Top Zechstein, lower horizon represents the ZEZ2A reflection.

4.6 Borehole Data for the Zechstein Stringer

Visualizing thicknesses of the stringer members, over the whole of Th Netherlands, has been done to get an overview of the overall and internal variablity of the stringer. Figure 25 displays these visualizations in true vertical thickness (TVT). The TVT of a member is not the initial bed thickness or true stratigraphic thickness (TST), TVT is dependent on the dip of the bed (figure 24).

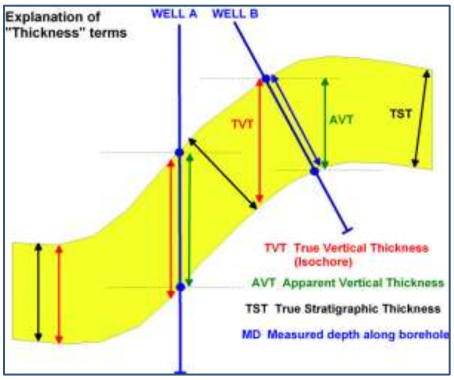

Fig. 24. Explanation of "Thickness" terms used when drilling through formation beds in the subsurface.

The grey salt clay is the thinnest member of the stringer, with an average thickness between 1 and 2 m. Outliers (up to 3 m) in this data set can be explained by rounding off to real numbers, by drillers when recording this member.

In the carbonate member TVT histogram an interesting distribution can be seen. Roughly a third of the wells record a thickness of ~5 m, while the rest of the wells record thicknesses up to 75 m, with a slight peak in the data between 20 to 25 m.

For the anhydrite member the vast majority of the data falls between 0 and 35 m. From 40 to 55 m the counts are roughly equal, whereafter 60 m the counts drop

The last histogram in figure 25 shows the TVT of the ZEZ3B, which represents the thickness from the top of ZEZ3G to the top ZEZ3A. For this thickness less wells (~1000) could be used, since all three members had to be recorded and drilled. Roughly 88% of the data points form a normal distribution from 0 to 80 m. Just under 8% of the data points fall between 80 and 110 m and the last ~6% of the points are scattered over 110 m.

Thickened zones are, by definition, stringer areas with anomalously thick development. In this study, stringers areas thicker than 80 m are referred to as thickened zones. From well H16-01 (and others), it can be observed that these zones are the result of thickened Zechstein III anhydrite. G18-01 well-to-seismic tie (figure 20) and ZEZ3B TVT histogram (figure 25), show that an average stringer is between 40 and 50 meters thick. Therefore, it was decided to investigate GDE's in all the wellls that registered more than 60 meters of anhydrite. As it is possible that from this thickness, wells drilled through a TZ.

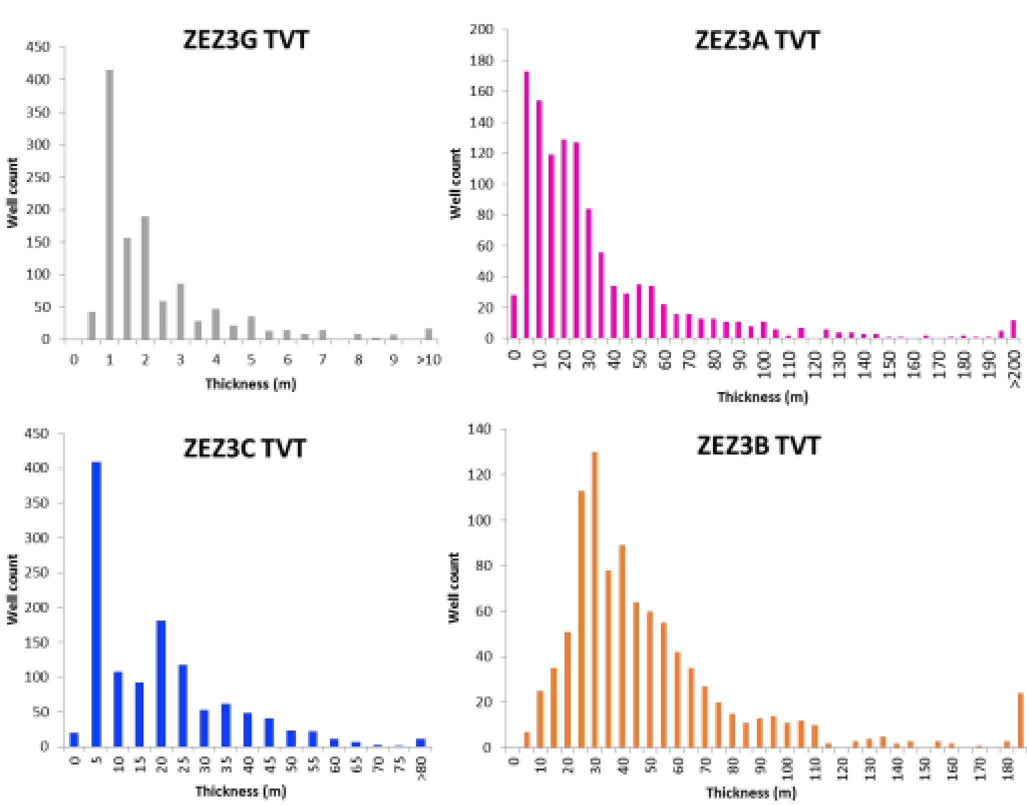

Fig. 25. True vertical thickness (TVT) histograms, from NLOG well data, of the stringer members; gray salt clay (ZEZ3G), Plattendolomit (ZEZ3C) and Hauptanhydrit (ZEZ3A). ZEZ3B represents the combined thicknesses of ZEZ3C and ZEZ3A.

4.6.1 Uncertainties with Selected Wells

As mentioned above wells have been selected that showed anomalously thick stringer development (using cut-off of 60 m ZEZ3A) according to NLOG thicknesses based on TNO stratigraphy. Not all these wells might have recorded the true anomalously thick zones (or TZs).
Proper stratigraphic thickness calculations from well data requires, in addition to the well deviation data, knowledge of the structural dip. Steeply dipping layers requires large correction factors and those factors are often poorly constrained.
This is exacerbated by the often large amount of deformation in the stringer: folding, faulting, rupturing and boudinaging. When this effect is likely playing a role and the apparent thickness is erroneous, the case is referred to as a “pseudo TZ”. To validate whether a well has penetrated a genuine TZ instead of a “pseudo TZ”, well trajectories, composite logs and seismic have to be examined. Despite the fact that these data might be incomplete, or non-conclusive, an interpretion is made for some wells regarding the case is a “true” TZ or a “pseudo TZ” (appendix A).

4.7 Geo-Drilling Events Data Results

For this study 154 wells, that penetrated the stringer, were selected and reviewed for geo-drilling events in the Zechstein Group. Geo-drilling events were present in 74 wells, 70 wells had no events and 10 wells had not enough data. From the 74 wells, 109 geo-drilling events were found and registered (figure 26). 54 (49,5 %) events were due to a stuck tubular/tool, 20 (18,3 %) gains, 19 losses (17,4 %), 11 ROP events (10,1 %), 3 lithology events (2,8 %) and both steering and H2S had 1 event (0,9 %). From the 154 wells, 22 were already incorporated into the EBN GDE database and the available data was used for this study. All selected wells are located in the northern half of the Dutch territories, in the basin or slope area of the ZEZ3C paleogeogrpahic map (figure 27). Figure 27 displays these locations, on a map from The Netherlands, and are coloured based on; the occurrence of a GDE in the Zechstein Group or not, or *no data availability*.
The summarized GDE data, for all 154 wells, is provided in appendix A.

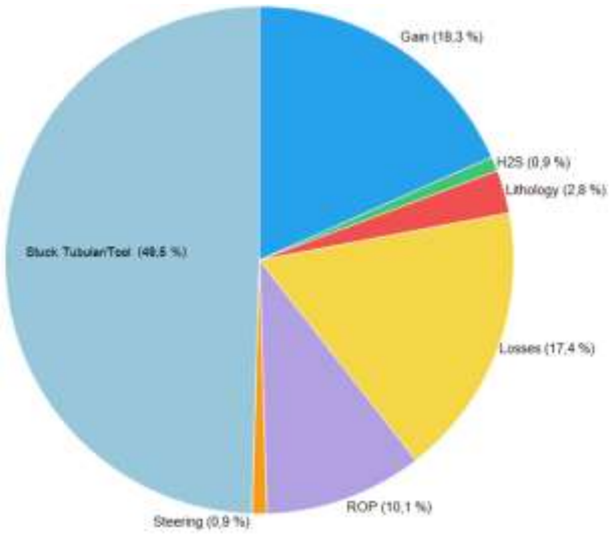

Fig. 26. Pie chart displaying the distribution of the different types of Geo-drilling events (total 109 GDE’s) found in the 154 selected wells.

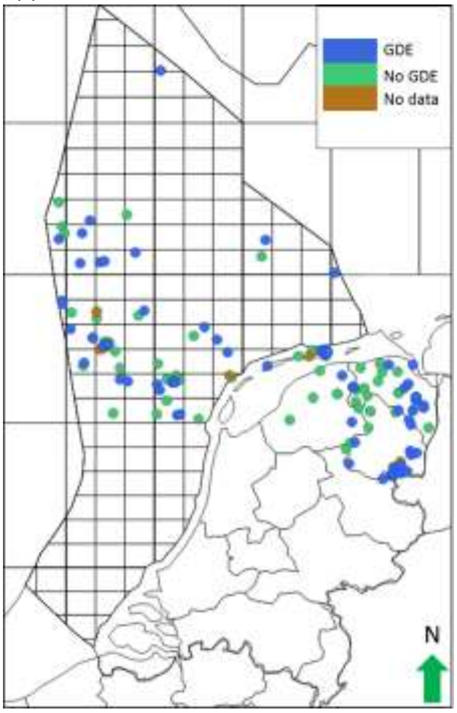

Fig. 27. Map of The Netherlands showing all the 154 selected well locations for this study with the provinces, Blocks and sublocks added. Blue dots represent a GDE in the Zechstein Group, green no GDE in the Zechstein Group and brown wells had no available data.

4.7.1 Zechstein Flow Events

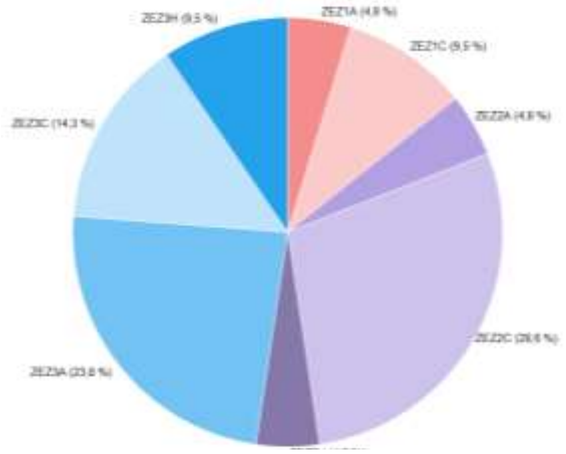

Fig. 28. Pie chart showing the distribution of 21 flow events registered in the different Zechstein members. Colour-coded per Zechstein formation; blue shades correspond to the Leine formation, shades of purple to the Strassfurt formation and red shades to the Werra formation.

While drilling the selected 154 wells, 21 (13,6%) flow events (gains due to high pressure porefluids) occurred in the Zechstein Group. Figure 28 shows the distribution, in precentages, of these gains among the Zechstein members. Almost half of the flowing wells happened in the Leine formation members; 5 in the ZEZ3A (23,8 %), 3 in the ZEZ3C (14,3 %) and 2 in the ZEZ3H (9,5%). Also a significant amount of flows happened in the Strassfurt formation members; 6 in the ZEZ2C (28,6 %),1 in the ZEZ2A (4,8 %) and 1 in the ZEZ2H (4,8 %). The remainder of flows happened in the Werra formation members; 2 in the ZEZ1C (9,5 %) and 1 in the ZEZ1A (4,8%). No flow events were registered in the Aller (Zechstein IV) and Ohre (Zechstein V) formation.

Locations of where the GDE's were registered are shown in map view in figure 29. In map A, the locations are coloured based on the Zechstein member in which the GDE happened and shades of colours represent the same formation. Note the difference between the colours in the eastern and western part of the Netherlands. The west is predominantly coloured by shades of blue (Leine formation), with exception for the ZEZ2H GDE in well E17-01. The GDE's in the middle to east belong to either the Strassfurt or Werra formation, no events recorded in the Leine formation here.

Map B depicts the same GDE's, but here coloured by the severity of the event. For the severity there seems to be no spatial correlation, rather a random distribution. Although, what can be concluded is that the events in the ZEZ3C (western part of figure 29A) are all high severity level. The other high severity event also happened in a carbonate member, but of the Strassfurt formation (ZEZ2C).

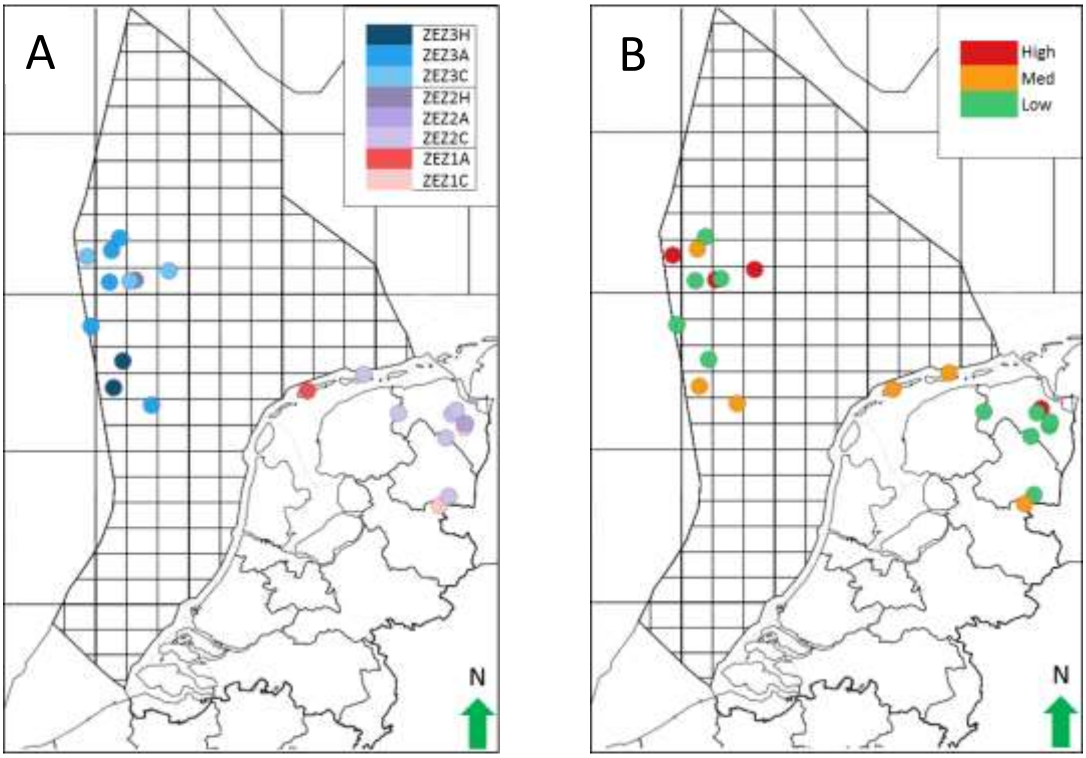

Fig. 29. A) Map view showing the locations of the 21 flow events per stratigraphic member. B) Map view illustrating the geo-drilling event severity of the same 21 flow events.

4.7.2 Seismic Expressions of Gain Events in the Stringer

The 8 wells with gain events in the stringer interval (blue and light blue dots in figure 29), have been further investigated with the use of 3D seismic. Appendix B contains S-N and W-E cross sections for all 8 wells, at the location where it penetrated the stringer. Discussed here are the main observations made per specific stringer member

Figure 30 displays two cross sections through the wells E10-03-S2 and E13-02, where GDE's took place in the ZEZ3A. These cross sections are indicative of the two types of seismic expressions that can be seen between the five gains in the stringer anhydrite member. Well E10-03-S2 (figure 30A), E16-02-S2 and J06-01-S1 registered low severity brine kicks in the top part of the thickened zone. Wells E13-02 (figure 30B) and K14-05 both registered a medium severity brine kick at the base of the ZEZ3A, just before drilling into the ZEZ3C. Composite log for well K14-05 mentions an inverted doubling of the stringer, thus it is assumed that this borehole did not penetrate a TZ, rather a folded or faulted zone.

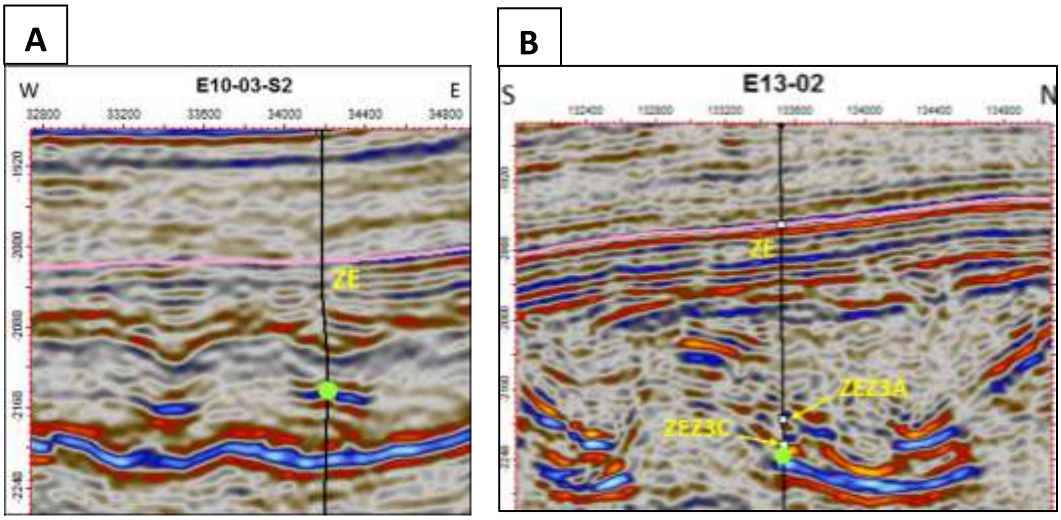

Fig. 30. A) West-East cross section through well E10-03-S2. Pink horizon is the Top Zechstein and the green dot the location of the brine kick. B) South-North cross section through well E13-02. Pink horizon shows the Top Zechstein and the green dot the location of the brine kick. Note: for this well the NLOG well tops are shown, with in yellow the member notations. The well tops do not correspond perfectly to the seismic.

In the Zechstein III carbonate, three brine kicks were registered. Figure 31 shows two cross sections, which represent the two types of seismic expressions that can be seen between the three gains in the carbonate member of the stringer. Well D15-04 (figure 31A) penetrates the side of a thickened zone, here the blue reflection of the ZEZ3C is irregular and seems broken or boudinaged. Furthermore, no distinct depression in the ZEZ3H reflections can be seen directly above the TZ. Wells E17-02 (figure 31B) and E18-02 hit the edge of a broken thickened zone. All three brine kicks in the ZEZ3C were high severity.

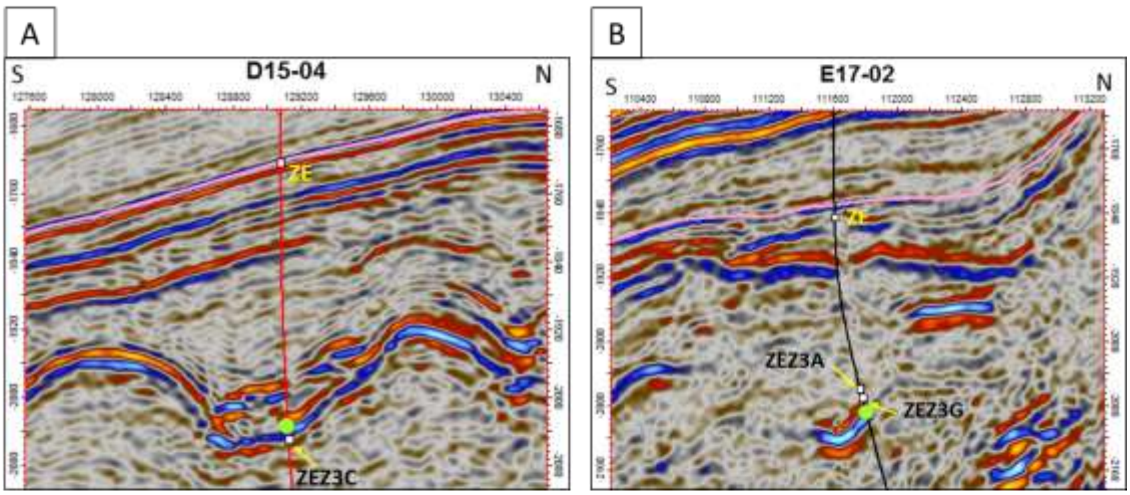

Fig. 31. A) South-North cross section through well D15-04. B) South-North cross section through well E13-02. For both wells the pink horizon shows the Top Zechstein and the green dot the location of the brine kick. Note: that also the NLOG well tops are shown (indicated with yellow arrows) and that these do not correspond perfectly to the seismic.

5. Discussion

5.1 Interpretation of the Thickened Zones

As Van Gent et al. (2011) stated; "The Pattern of TZ and the peculiar internal structure cannot be explained by salt tectonics and basement-related faulting alone." These authors suggest the TZs to be the product of sedimentary and diagenetic processes, modified by deformation in the flowing salt. They propose that karst systems evolved in the Z2 halite, after deposition of the Z3 anhydrite, resulted in collapse structures along Z2 dissolution channels, which lead to slides of the Z3 stringer that collected at the base of synclines. Thereby adding that other interpretations are certainly possible.
Although I disagree with their TZ evolution scenario (discussed in chapter 5.2), the above statement by Van Gent et al. (2011) is well-founded and different processes must be considered to explain the TZs features. Therefore, in the following chapters an alternative explanation of the origin of TZs is proposed based on the results from the Hansa 4Quad 3D seismic survey.

5.1.1 Thickened Zone Geometries

To understand the geological processes behind the TZ seismic features, their regional geometries are first considered. The excellent quality of the stringer's seismic response in the Hansa 4Quad is shown in figure 15. Regionally the TZs are lineaments in the stringer and can be found throughout the study area. On a smaller scale faults and gaps in the stringer offset the TZ lineaments. This shows that TZ features are of earlier origin than these faults. Other observations are, in addition to the lineaments, the branching and polygonal features (figure 16), which can be seen throughout the study area. The geometries observed have some semblance with drainage patterns and/or rock dehydration (mud crack) patterns.
A possible explanation for occurrence of TZ can be found when looking at salt structures analogues around the world. Rowan and Vendeville (2006) produced a map of present-day salt architecture in the northern Gulf of Mexico. Figure 32 displays a comparison between their map and figure 16 from this report. Geometries of the salt walls in the Gulf of Mexico (in grey) are strikingly like the geometries found in the TZs (in yellow and red). Important to note are the different scales between the two examples by more than 1 order of magnitude. Furthermore, the stringer TZs consists mainly of anhydrite whereas the salt walls are predominantly halite: rocks with very different rheological behaviour. Regarding this rheological behaviour, it is important to consider the rheology at the early stage of the TZ formation and diagenetic processes involved. The anhydrite present today is assumed to be deposited as gypsum (Kosmahl, 1969). Gypsum has a flow behaviour much closer to halite than anhydrite (Williams-Stroud and Paul ,1997).

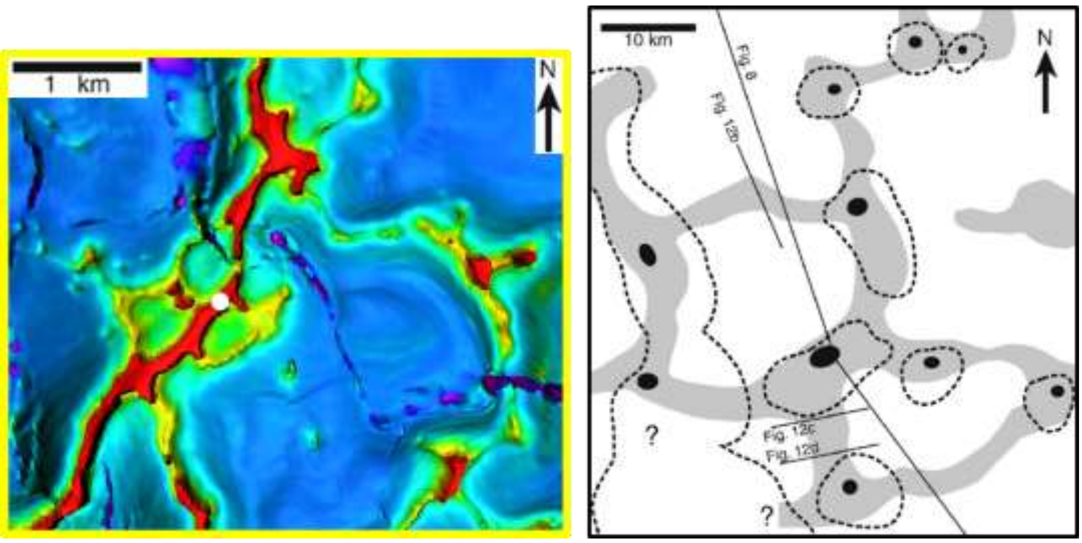

Fig. 32. Comparison of geometries in the stringer, left (figure 16), with geometries of salt walls (in grey) in northern Gulf of Mexico, right. Right image modified from Rowan and Vendeville (2006).

Another example of comparing the stringer TZ geometries with salt dome patterns can be done closer to the study area. Figure 33 shows a comparison between Zechstein salt structures (mainly produced by halokinesis) in the M-block (Dutch offshore) and an area in the northeast of the stringer thickness map (figure 15). Both images show similar geometries consisting of elongations, branches and closed polygonal structures. Also, the orientation is fairly comparable with a NNE-SWS strike direction. For this example, the same order scale difference as in the previous example is evident.
This triggered the idea that flow of the ZEZ3A gypsum, similar to halokinesis, can be the cause of the structural geometries that are observed in the Hansa 4Quad survey.

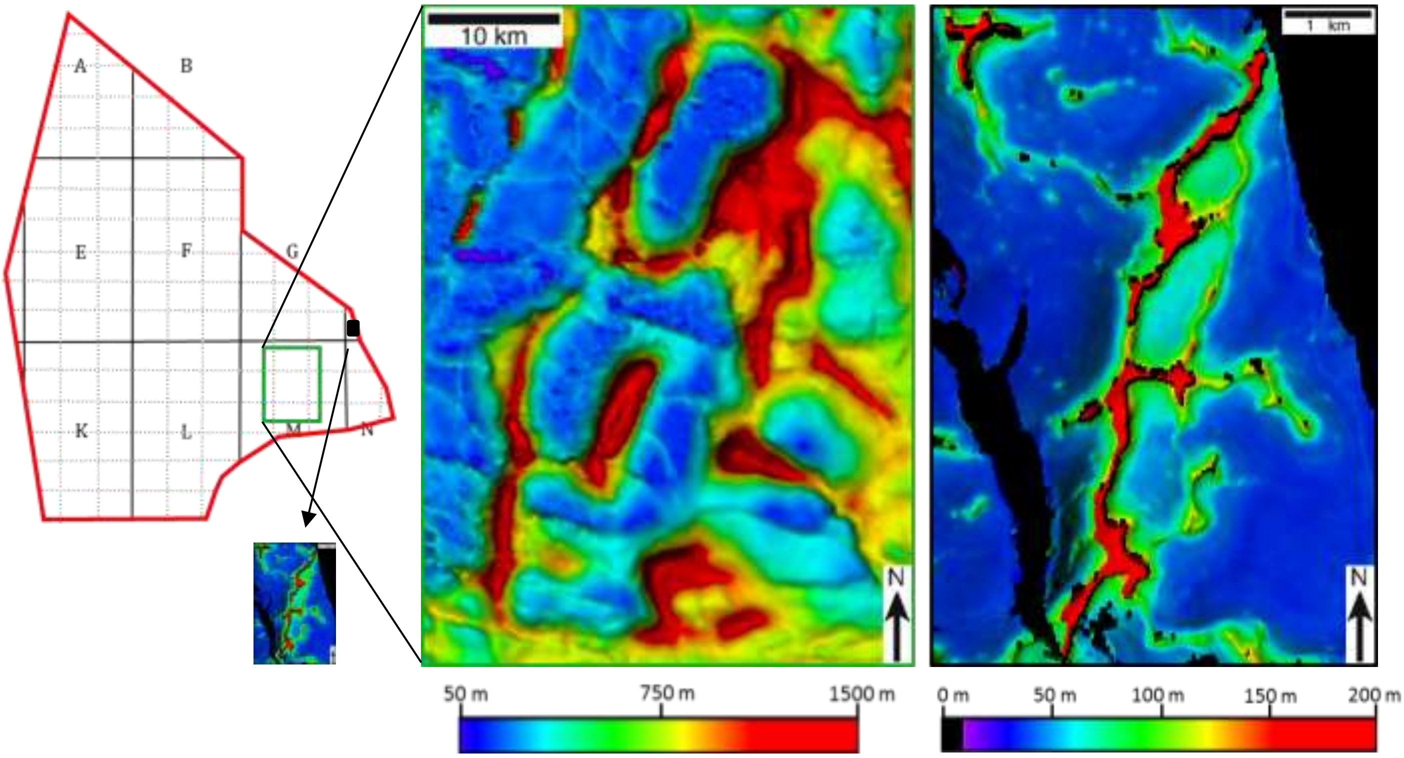

Fig. 33. Comparison of geometries in the stringer (right image), with geometries of Zechstein salt walls in the Dutch offshore M-block (middle image). Locations shown in map of northern part of the Dutch offshore. Similar scale size shown in with the small image of the stringer geometries. Used Top Zechstein horizon from NLOG.

5.1.2 Thickened Zone Analogue

In the first part of the 20th century salt miners around the city of Strassfurt (Germany), found irregular thicknesses of the Leine Anhydrite (ZEZ3A) and referred to them as “anhydrite klippe” (anhydrite cliffs). Hemmann (1986, 1972) first described these features in detail, concluding that these “klippe”, or rather domes, have a pear-like shape with steep flanks. He also indicated that these domes are up to 50 m high, 15 to 120 m across and can be traced horizontally over several hundred metres. This is in the same order of scale as the TZs found in the stringer (figure 15). These anhydrite domes found around the Harz area in Germany are suggested to be formed before gypsum to anhydrite conversion at a depth of at least 100 m burial (Langbein, 1987; Paul, 2014).
Furthermore, it is proposed that the gypsum doming is independent of salt doming in the area and although the size of the gypsum domes is relatively small, if more gypsum was initially present they could become larger (Paul, 2014). An idealized cross section of anhydrite domes found around the Harz mountains, Germany, is shown in figure 34 (Hemmann, 1972).

Observations made by the authors mentioned above, demonstrate that gypsum can flow comparable to halite after sufficient burial and can form domal ridges, orientated predominantly parallel and normal to the strike of the salt ridges. During flow of the gypsum into the salt above, the contact zones (e.g. edges of the dome) tend to mingle and clasts of gypsum can be encapsulated into the salt.

In the case of figure 34, the growth of the dome is vertically confined by an intercalation of anhydrite and salt or when such a layer is not present, the doming halts when an equilibrium has been reached between the hydrostatic pressure and the overburden lithostatic pressure.

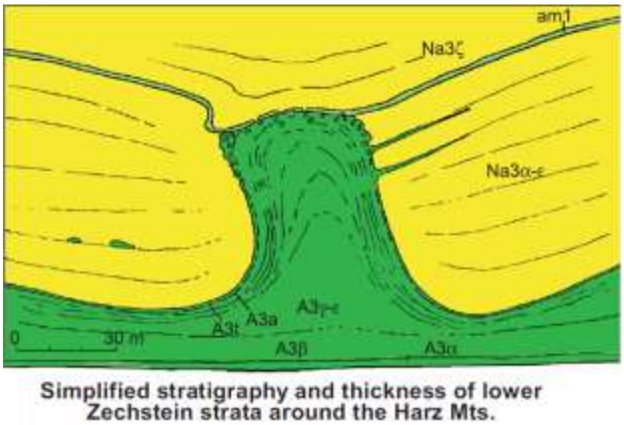

Stratigraphy	Thickness [m]	Characteristics
Na3 zeta-eta	30	with anhydrite layers
am1		intercalation of anhydrite in the salt
Na3 alpha-epsilon	50	rock salt
A3a Anhydritschale	>0.5	thin anhydrite layer
A3t black clay layer	0.0–0.1	residue of dissolved evaporites
A3 epsilon	0–30	very few carbonates and clay
A3 delta	1–9	middle grey, bedded
A3 gamma	2–8	chicken wire anhydrite
A3 beta	7–12	light grey, less carbonate content
A3 alpha	1–3	dark grey, high carbonate content

Fig. 34. Idealized cross section of a Zechstein III gypsum dome (green) into Zechstein III halite (yellow), with added an abbreviation table. Taken from Paul (2014), modified after Hemmann (1972).

The growth of the gypsum dome is proposed to be only happening in the upper part of the gypsum, because the lower part tends to be more crystal grown gypsum, while the upper part was deposited as gypsum mud with greater water content. Conversion from gypsum to anhydrite released the water and aided in the uplift of the dome (Paul, 2014).
Released water could have escaped to nearby porous rock, e.g. the Zechstein III carbonate, or find a pathway to the surface. Another possibility, when escaping is not possible, is that water will form isolated brine pockets in the anhydrite.

5.1.3 Seismic Responses of Gypsum Domes

From the information presented above, it is suggested that gypsum doming is responsible for the salt-like geometries found in the stringer thickness map (chapter 5.1.1). Here I would like to compare this proposal with cross sections of seismic responses from 3D lines in the Hansa 4Quad area. Important to note is that salt movement or doming is observed in many forms (figure 35). This would argue that the same principle plays a role for mobile gypsum doming. Salt structures in figure 35, annotated with numbers, are compared to seismic responses of TZs in figure 36. Important to note is that in the Hansa 4Quad area the TZs form branches or look more like linear salt structures (1,2 &3) and circular structures (4,5 & 6) are rarely observed. Furthermore, salt welds are not recognized in between the TZ structures, suggested that this is due to bottom part of the gypsum not being part of the doming (Paul, 2014).
The purpose of comparing the variability of salt structures with seismic expressions, is to show that thickened zones, while having very different seismic responses, can still be correlated to the same geological process. A process that can be observed in outcrops on surface, which will increase the knowledge of detailed features in the subsurface.

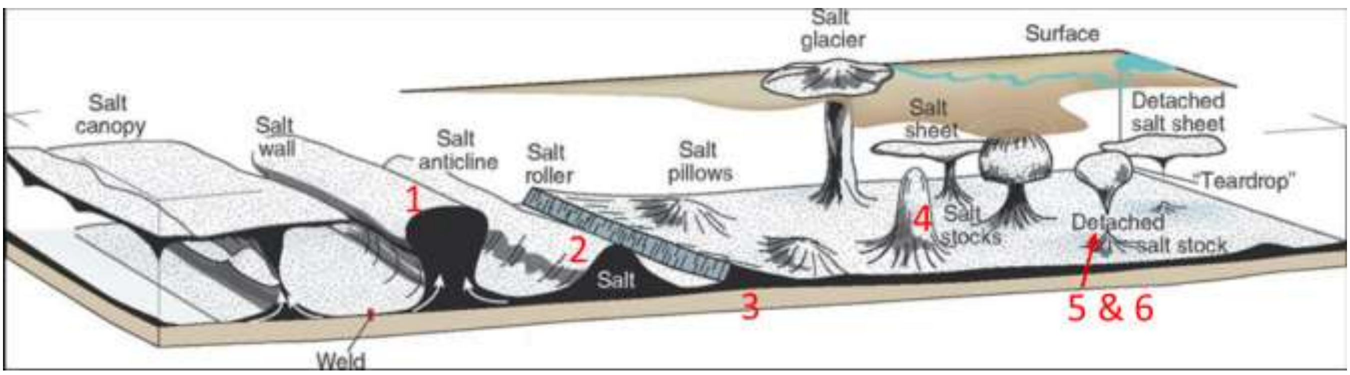

Fig. 35. Variety of salt structures; linear structures to the left side and circular structures to the right. Numbered structures are correlated to cross sections of seismic features in figure 36. From Fossen (2010).

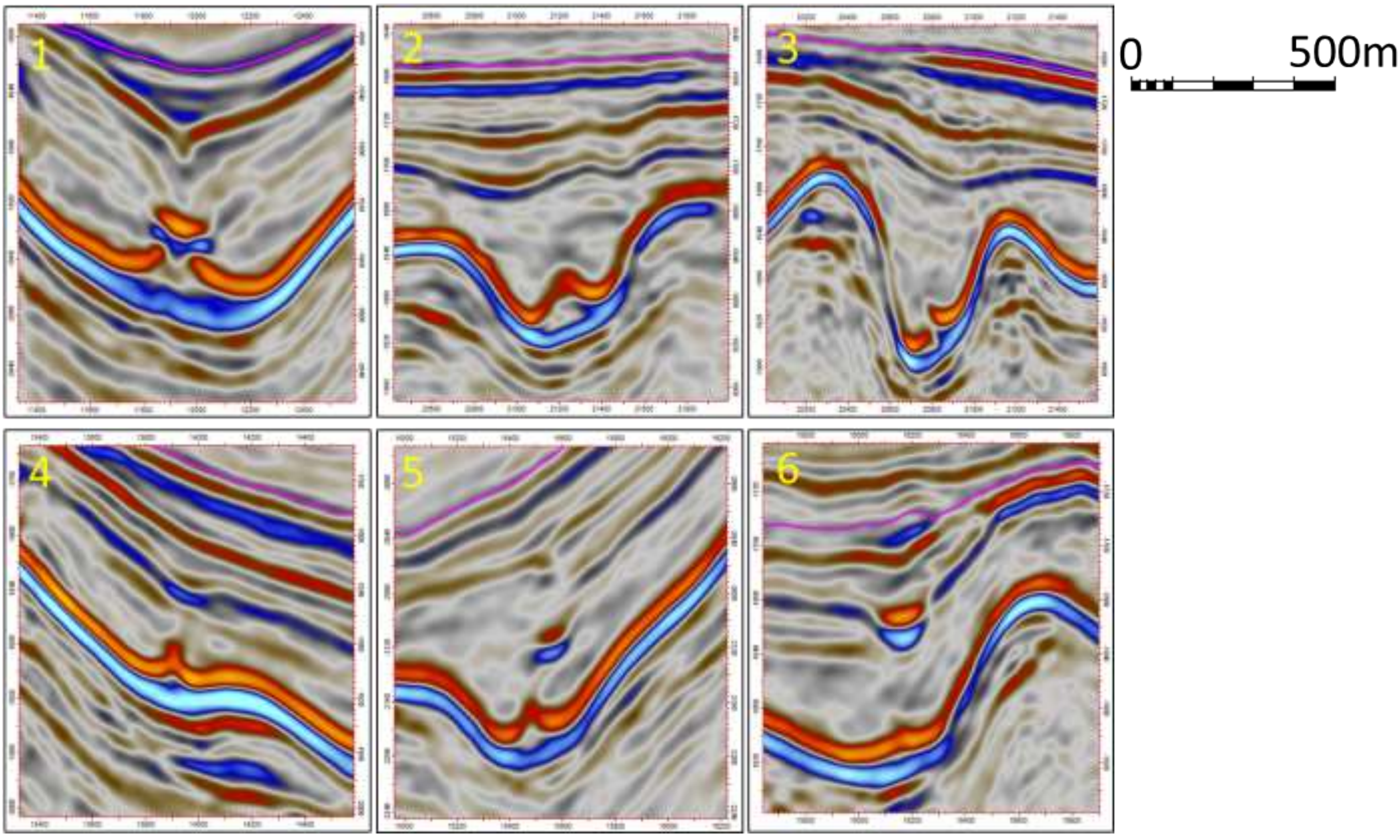

Fig. 36. Cross sections through thickened zones in the Hansa 4Quad seismic survey. Numbers correlate to salt structures in figure 35.

5.2 Proposed Geological History of the Stringer

Here I would like to propose an early geological history for the Zechstein stringer that can explain its seismic expression and local variation of lithologies and thicknesses thereof, seen in the Hansa 4Quad 3D survey, as well as for other locations in the Zechstein III basinal facies.

Deposition of the stringer started with the grey shale (ZEZ3G) on a flat Zechstein II surface. The Southern Permian Basin filled with water and the basinal facies turned into a shallow marine environment and a rather thin (~5 meter), through pelagic rain, carbonate layer was deposited. Evaporation in the basin resulted in a lower water activity and gypsum started to crystalize first, followed by deposition of gypsum mud resulting in a uniform thick stringer interval. Thereafter, when the activity of water lowered even more, halite started to precipitate from the shallow waters.
After roughly 100 meter of halite deposition a compressional tectonic pulse (Tubantian II), resulting from the Ural mountain range formation, initiated movement of the Zechstein II halite by reactivation of subsalt faults (Geluk, 1999; Biehl et al., 2014; Strozyk et al., 2014). This produced an undulated surface, where on the highs halite continued to precipitate and lower areas left with hot brine ponds, that lead to the precipitation of K-Mg rich salts (Raith et al. 2016, 2017).
Simultaneously the Zechstein II halite movement resulted in the movement, i.e. doming, of the Zechstein III gypsum parallel and normal to the highs, thus predominantly in the lower areas. With increased burial, gypsum of the Zechstein stringer started to convert to anhydrite. Directly above (most) gypsum domes, water escape paths resulted in the creation of mini basins by dissolution and collapsing of the overburden. These two processes could be ongoing, locally dependent on amount of deposition, until the end of Zechstein Group.
Figure 37 displays a thickness map of the first negative reflection to the top Zechstein (chapter 4.1), next to the stringer thickness map (figure 15). Red to green zones in the left map are interpreted to be the lows or basins where, in brine ponds, K-Mg salts precipitated and the blue to purple zones correspond to the highs. Specifically, the red zones in the left map are the mini or dissolution basins that can be found directly above almost all the thickened zones in the right map.

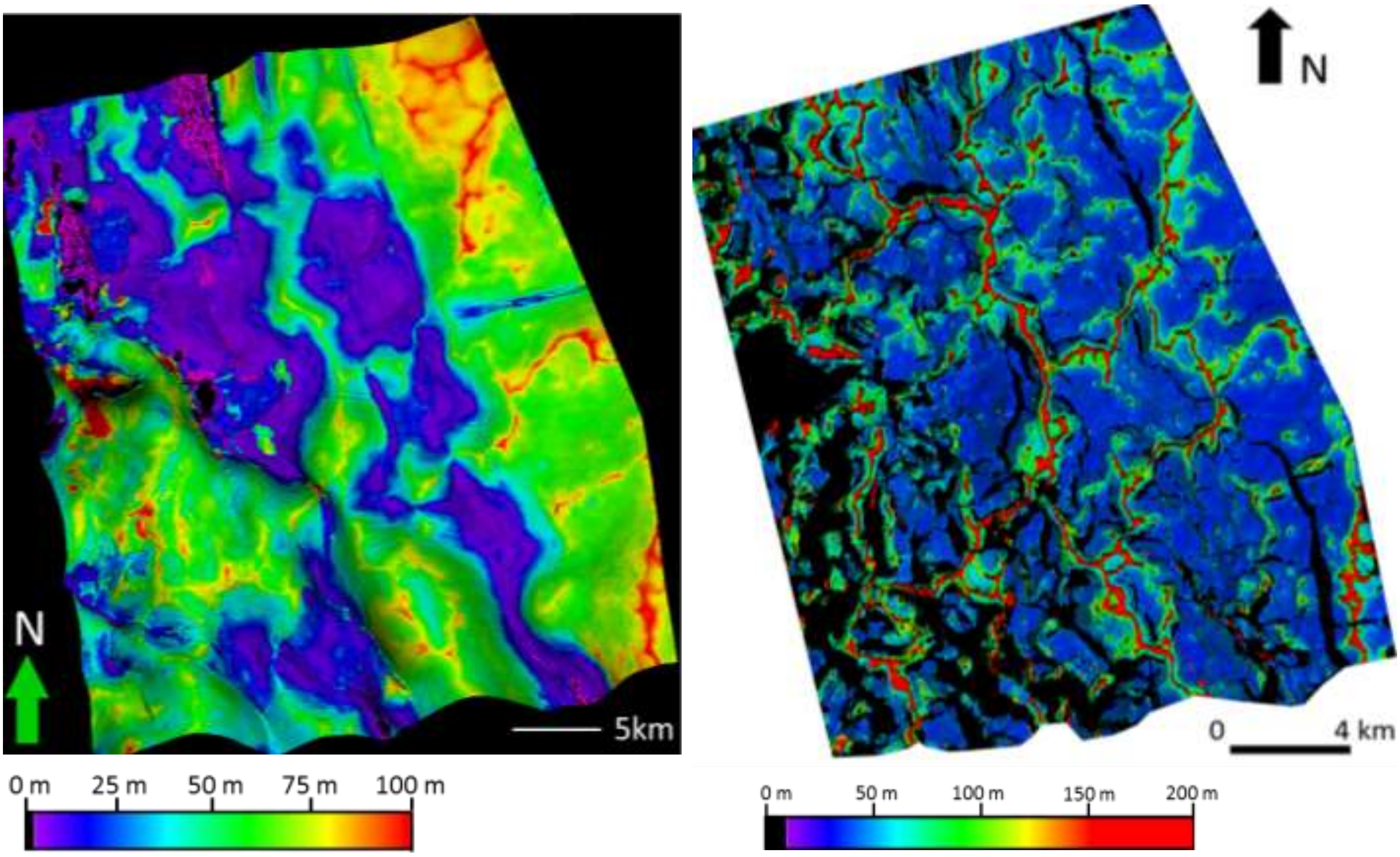

Fig. 37. Left: thickness map of first negative reflections to top Zechstein. Right: stringer thickness map from figure 15. Note: the correlation of the thicker areas (red and yellow) between both maps.

From the start of the Triassic until the present day, tectonically induced movement in the Zechstein Group is almost entirely transposed onto the Zechstein II halite as described by many authors. Suggested is that the salt movement, initiated by the Tubantian II, continued with later tectonic pulses in the same way. Thickness map from chapter 4.2.2 show, that the same regional distribution of highs and lows, as in figure 37, still exists in the Early Cretaceous.

Generally, it is thought that although large amount of movement happened in the Zechstein II halite, the stringer remained roughly at the same position as deposited (Van Gent, 2011; Strozyk et al., 2014, 2017). Here it is suggested that the anhydrite domes did sink slightly into the underlaying salt over geological times, by differential loading. This effect is illustrated in cross plot in figure 18B. This is best observed at the "broken" TZs (type 1 TZ), where the stringer broke on both sides of the anhydrite dome and sunk deeper into the Zechstein II halite, sometimes onto the top of the Zechstein II anhydrite.

The thickened zone geological origin proposed by van Gent (2011) several seismic features that have been observed in this study. It can not explain the many different seismic responses of thickened zones as well as the strong correlation with the overburden depressions and K-Mg salts. Furthermore, the proposed breaking and sliding of the stringer, that would result in thickened zones in synclines, can be rejected based on observed well logs. These wells register and log a thickened ZEZ3A only and the mechanism proposed by van Gent (2011) would result in multiple stringer responses, but neither the ZEZ3G or ZEZ3C can be found in these wells.

This study proposed geological history can explain all the seismic features surrounding the stringer and the well log data present in thickened zone wells.

5.2.1 Gypsum Domes Around the Southern Permian Basin

Paul (2014) states in his research that it is highly probably that gypsum domes occur in many areas of the Zechstein basin. This research states that thickened zones visible in the Dutch subsurface are similar to these gypsum domes features observed in the Harz mountains. Van Gent (2011) and Strozyk et al. (2014) observed TZs in the Groningen and Friesland area as well as a small part of the western Dutch offshore. This study observed TZs in many parts of the D, E, K, L, G, H, M and N-blocks of the Dutch subsurface. Furthermore, a cross section from the PhD Thesis report of Al-Habsi (2016) in the Silverpit Basin (UK) shows two seismic features, present in synclinal structures of the stringer, that show the same characteristics of TZs observed in the above-mentioned areas (figure 38).

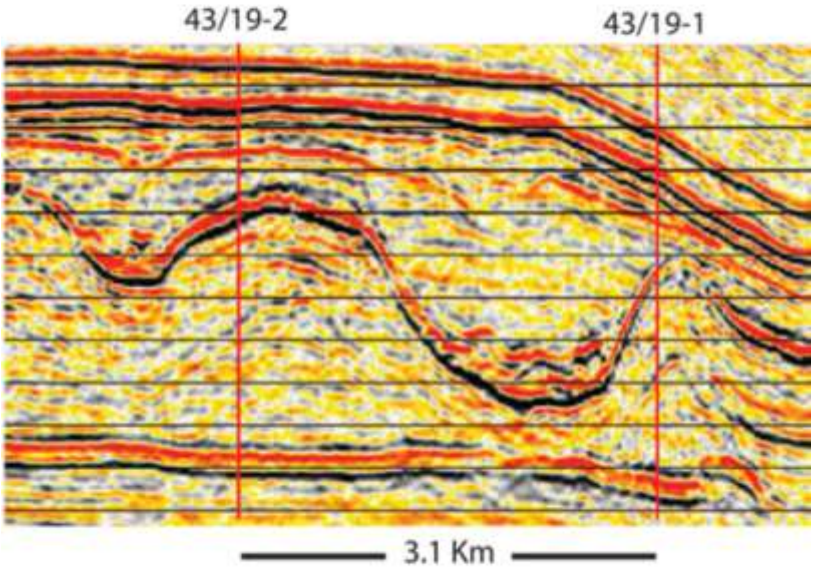

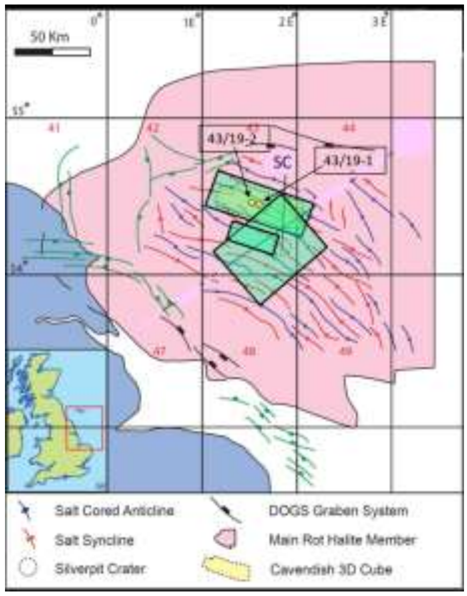

Fig. 38. NW-SE cross section through well 43/19-2 and 43/19-1 of the Zechstein Group in the Silverpit basin (UK), map of location on the right. Note the two Thickened zones in the synclinal parts of the stringer. Modified after Al-Habsi (2016).

Figure 39 displays a similar Zechstein configuration in the D-block (Netherlands) to the cross section from the Silverpit Basin (figure 38). Furthermore, similar configurations have been observed in the Hansa 4Quad survey and the Groningen area. This suggests that the statement of Paul (2014) might be valid. Adding to that statement, I propose that anhydrite and gypsum domes are highly probable to be present in the basinal and slope facies of the Zechstein III formation throughout the Southern Permian basin.

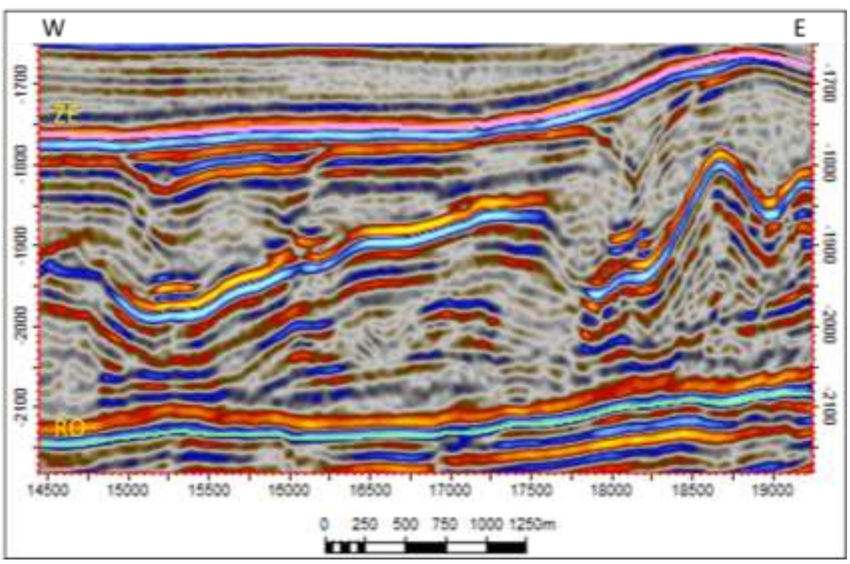

Fig. 39. W-E cross section in the D-block, northern Dutch offshore. Showing a similar configuration of the Zechstein Group with TZs, as seen in the Silverpit Basin (figure 38).

5.3 Quantifying Geo-Drilling Gain Events in the Zechstein Stringer

To validate the reliability of the geological processes proposed above, reports from the selected 154 wells were checked for GDE's in the Zechstein (chapter 4.7). The results of the brine kicks observed in the stringer interval will be discussed and interpreted her, as well as compared with the results from EBN report by P. Schilder.

A total of 21 flow events were discovered in the 154 selected wells in this study. Schilder (2019) found 68 gains in the Zechstein Group, from a total of 174 investigated wells. Figure 40 shows pie charts of gains per Zechstein member from both studies. When comparing the gains in the stringer interval (ZEZ3C and ZEZ3A), three differences can be observed. First, in the report by Schilder (2019) the stringer produces 58% of all gains and this study it produces 38% of all gains. Secondly the distribution between the members off the stringer is different. P. Schilder found that more than three quarters of the gains happen in the Zechstein III carbonate and this study found it only comprising a third of the total gains. Finally, this study found a total of 8 brine kicks in the stringer, an occurrence of 5,2% and Schilder (2019) found 40 brine kicks in the stringer, occurrence of 23%. Although this latter percentage is an overestimation due to the biased nature of the EBN GDE database (Schilder, 2019).

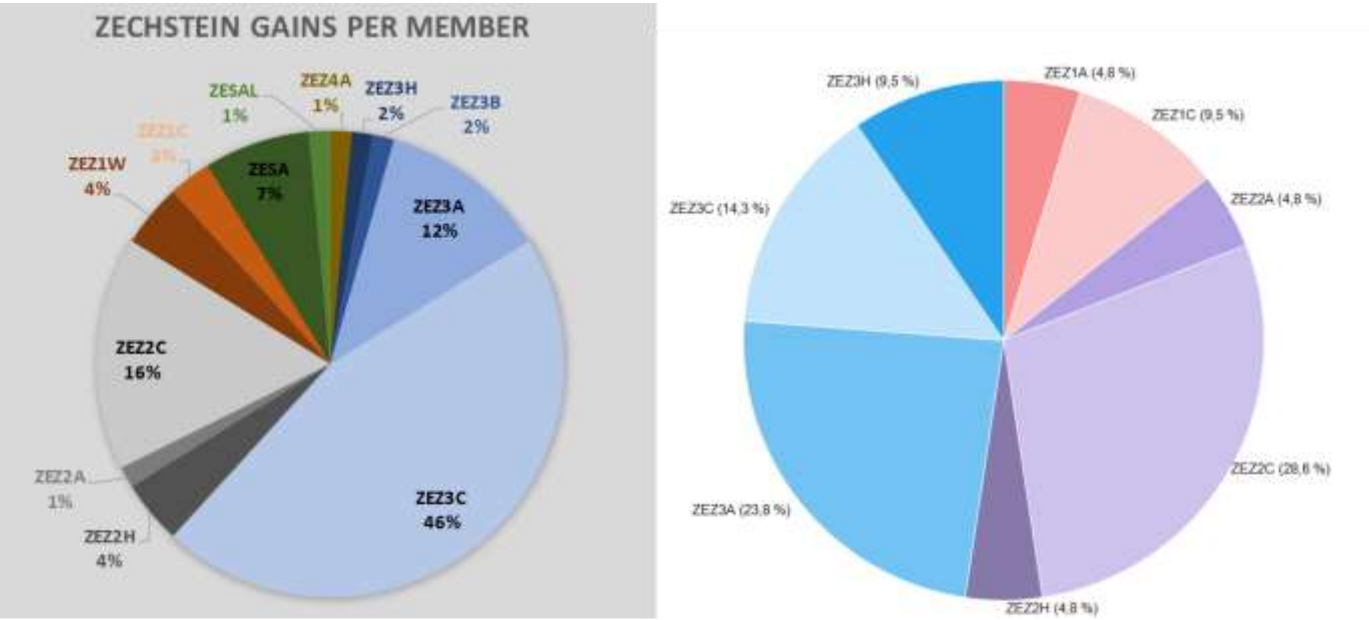

Fig. 40. Pie charts of Zechstein gains per member. Left taken from EBN report by Peter Schilder and Right chart from this study.

Even with the percentage being overestimated, the difference between the two studies is large. Especially when looking at the total number of medium- to high severity events in the stringer and the extra costs involved. Schilder (2019) found 9 medium- and 18 high severity events and in this study 2 medium- and 3 high severity events. Note that the three high severity events, used in this study, were already incorporated in the GDE database, thus also part of the 18 counts from Schilder's (2019) report. Average costs of drilling wells (in euros per meter) that experienced a medium-high event is two and a halve times as much, compared to no or low-event drilled wells (Schilder, 2019).

5.4 Increasing Drilling Safety by Targeting Thickened Zones

Statistics presented in chapter 5.3 show that thickened zones in the stringer have a lower chance of gain events than steep faulted and folded parts of the stringer (Schilder, 2019). Here these statistics will be linked together with the proposed geological history, to produce a coherent story on why these zones produce less gain events and propose an explanation for the wells that did have a gain event. This will result in a view on what seismic features are expected to be less likely over pressured and which features or zones to avoid while drilling.

A possible explanation for the absence of overpressures in the carbonates, around thickened zones, as observed in the data, relates to the dewatering of the gypsum domes. Free water, from the conversion of gypsum to anhydrite, cannot escape the stringer under normal circumstances, e.g. thick sealing salt cover above it. This water must therefore flow into the Zechstein III carbonate and will build up the pressure significantly.

Zones where gypsum doming occurred have reduced overburden thickness, perhaps some domes pierce all the way to the surface. Furthermore, gypsum-anhydrite conversion will likely start at the bottom (ZEZ3C – ZEZ3A interface) and initially water can escape into the carbonates (Paul, 2014). At certain thickness of anhydrite, further released water from gypsum above is trapped between two sealing layers. The conversion to anhydrite will continue and more water will be released. I suggest that the thinnest sealing layer will at some point fail and water will escape through. Around the gypsum domes the thinnest sealing layer is often the overburden salt and thus water will penetrate to the surface, while also dissolving the salts present. This process of leakage will reduce pore pressures and prevent building up of lithostatically pressured Zechstein III carbonates.

5.4.1 Discussing Wells that Penetrated Flowing Stringers

From the 154 selected wells 8 showed a gain event in the stringer, results shown in chapter 4.7.2. Here these 8 events will be examined and interpreted for their cause. N-S and S-E Cross sections through the well sections at the stringer interval, are shown in appendix C.

Wells E10-03-S2, E16-02-S2 and J06-01-S1 had a low severity gain when drilling through the head of gypsum dome (figure 30A). All three wells closed in the borehole after gains were observed and adjusted the mud weight. Thereafter, drilling continued and only E16-02-S2 observed further minor losses while drilling. The report of E10-03-S2 registered a magnesium brine influx, but only after they pulled the shoe, it is not certain if the gain occurred in the Zechstein III anhydrite.

This study proposes that these low severity events happened due to drilling in an enclosed pocket of brine inside the anhydrite. When drilled into such a pocket, the highly overpressured, small amount of, brine releases into the borehole and the well must be closed in. Well control is regained rather quickly (1-2 days) and drilling can continue without problems.

Medium severity gain events were observed in wells E13-02 and K14-05 at the base of the Zechstein III anhydrite. While E13-02 drilled through a TZ (figure 30B), well K14-05 shows an inverted doubling and reported faults in the stringer, likely reason for the gain. Well E13-02 drilled the edge of a broken TZ, this area experienced brittle deformation and zones around it have a high probability of enhanced permeability, which will increase the likelihood of gains (Schilder, 2019).

Drilling through the Zechstein III carbonate, lead to high severity gain events in wells; D15-04 (figure 31A), E17-02 (figure 31B) and E18-02. Well trajectories for E17-02 and E18-02 show that both drilled the edge of a broken TZ. Therefore, it is assumed the same process of well E13-02 lead to the gain here. Difference between them is the severity of the event, which can possibly be explained by the high porosity in the carbonates, thus more water is expected to be connected to the wellbore and therefore more time is needed to regain well control.

Well D15-04 seems to drill through an exemplary anhydrite dome and suffered a high severity gain in the Zechstein III carbonate. Although when observed more carefully the ZEZ3C reflection has an irregular appearance and suggests it is faulted at a certain area, but not convincing. Suggested is that here the gain occurred, because after the gypsum dome formed the released water could not find a way to the surface, but rather escaped into the carbonates. There is no distinct depression above the thickened zone, which would have evolved by the escaping water dissolving the salt on its way to the surface.

5.4.2 Proposed Safer Well Trajectories

From the above-mentioned processes and the seismic features expected to be produced from them, it is possible to better predict overpressured zones. With this in mind and results produced by the report of P. Schilder (2019), some suggestions on safer well trajectories are made. Proposing alternatives well trajectories for studied wells, that encountered a high severity gain event in the stringer.

Schilder (2019) produced a probability of kick while drilling through the stringer at certain locations, based on an "lowest" average kick percentage of 3%. Figure 41 shows the increased likelihood of gain events in the stringer at; isolated blocks, anticlinal structures and edge zones (in red). Moderately increased risk zones (in orange) are in very steep and sunken stringers. Low probability of kicks of the stringers are in; synclinal structures, horizontal parts and areas where pressures could have been bled off to overlaying porous rocks (in green).

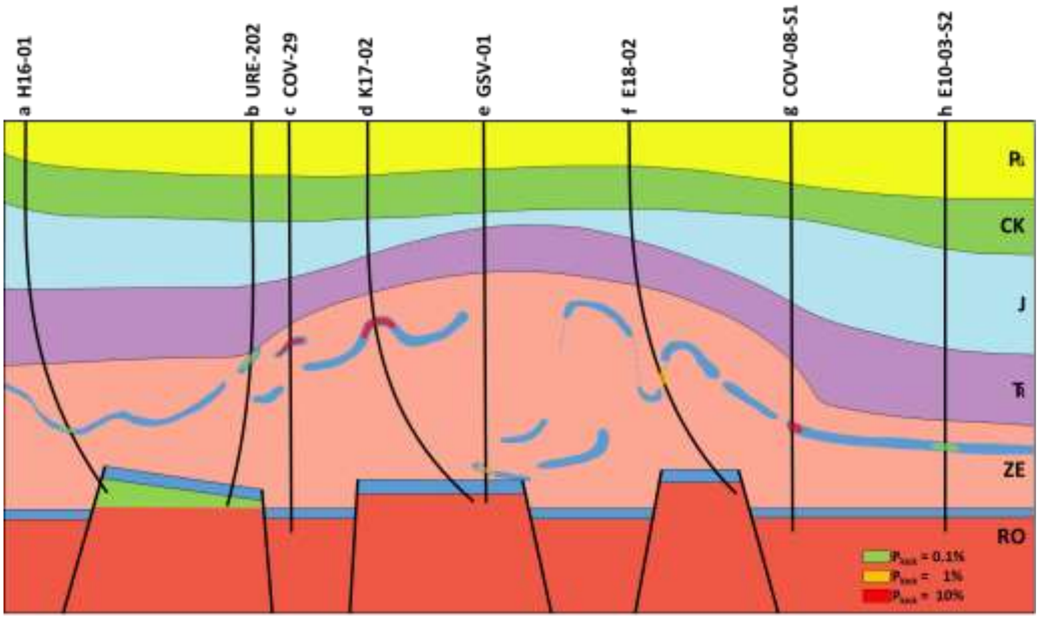

Fig. 41. Schematic illustration of well penetrations of stringers at different locations. Colour codes represent the likelihood of hard overpressures (>1.8 s.g.), based on a "lowest" average probability of 3%. In this figure it is assumed $P_{hit} = 100\%$ and therefore, only P_{kick} must be considered. Wells represent examples of drilled stringer configurations. Taken from Schilder (2019).

Combining the above-mentioned findings with results from this study, more low probability zones can be added. Here it is suggested that anhydrite domes are lower probability zones, due to the combination of their position in synclines and the high possibility of early pressure leak off. Although it must be noted that drilling through and extra ~100 meter of anhydrite instead of halite brings extra costs with it, roughly estimated to be in the order of 100.000 euros for an offshore well (personal communication, Gert Lammers, 2019). In addition to that a slight increase in low severity gains, inside the anhydrite dome, must be considered. When TZs are present in low to moderately deformed stringer setting, recommendation will be to drill near these structures, but not directly through then. Figure 42 shows an alternative, expected to be more cost efficient, drilling trajectory (in orange) for well H16-01.

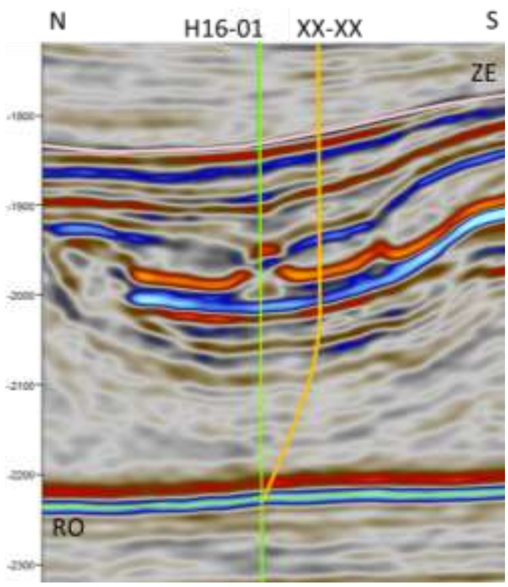

Fig. 42. N-S cross section through well H16-01 (in green). Well trajectory XX-XX (in orange) is an alternatively proposed, more cost efficient, trajectory to the target of H16-01.

Zijp et al. (2018) propose to avoid drilling through the Zechstein in tilted and folded stringers, areas below flanks of folded top Zechstein and areas where the base Zechstein is faulted. This excludes large parts of the Dutch subsurface of drilling the Zechstein, because a highly deformed (internal and external) Zechstein Group is common. This study proposes that in areas where the Zechstein stringer is heavily deformed, anhydrite domes are lower risk zones to penetrate through the stringer. Figure 43 shows a few wells where alternative well trajectories (in orange) have been proposed to avoid high severity gain events in the Zechstein III carbonates. Before deciding to drill through a TZ as seen in wells; E13-02, E18-02 and F16-A-06-S1 (figure 43), an important feature must be present directly above it. That is the depression or V-shaped reflections in the ZEZ3H.

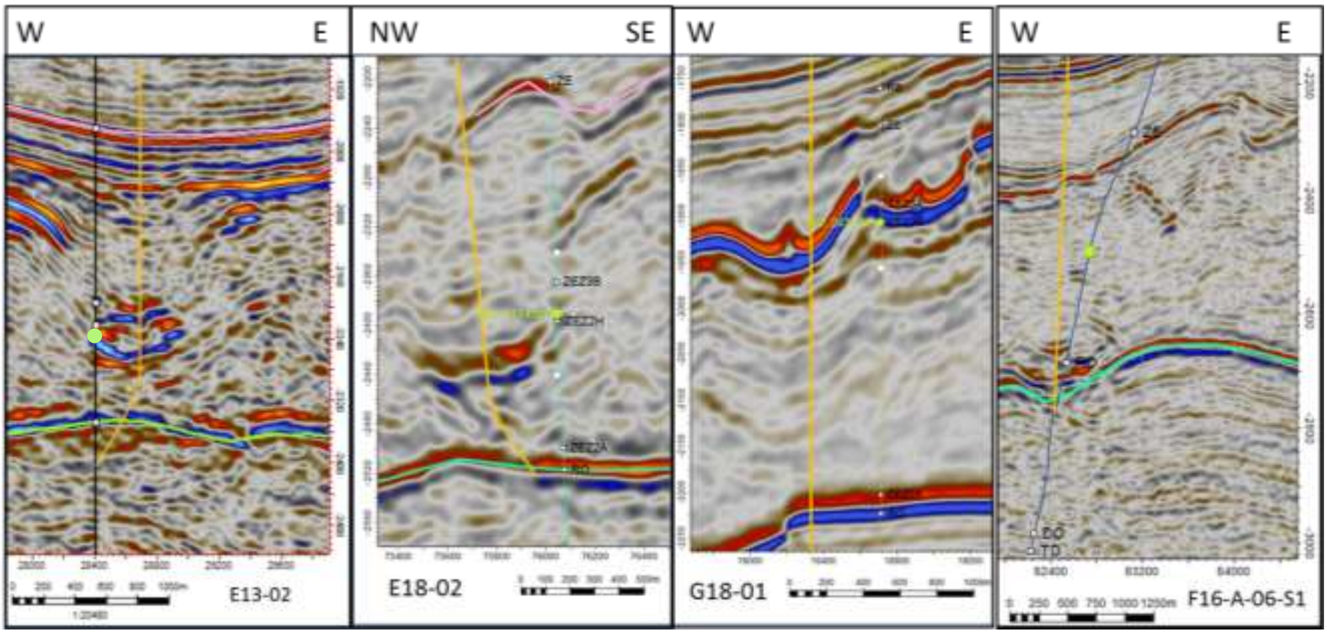

Fig. 43. Cross sections through four wells that encountered a gain event when drilling through the stringer interval. With well tops annotated and a green dot presenting gain location, are the existing well trajectories. In Orange are the proposed safer well trajectories through the middle of thickened zones. RO = Top Rotliegendes and ZE = Top Zechstein.

Well N05-01 and its side-tracks (figure 44), are examples that show the viability of the above proposed safer well trajectories. N05-01-S1 drilled through 140 meters of anhydrite and had no problems penetrating the stringer. Later side-track N05-01-S2 was drilled towards the west of S1 in and edge (broken part) of the stringer, when it hit the Zechstein III carbonates it suffered a high severity gain and the well had to be plugged and side-tracked again. Decision was made to penetrate the stringer at the same location where N05-01-S1 penetrated the stringer, and this side tracked had no issues drilling through.

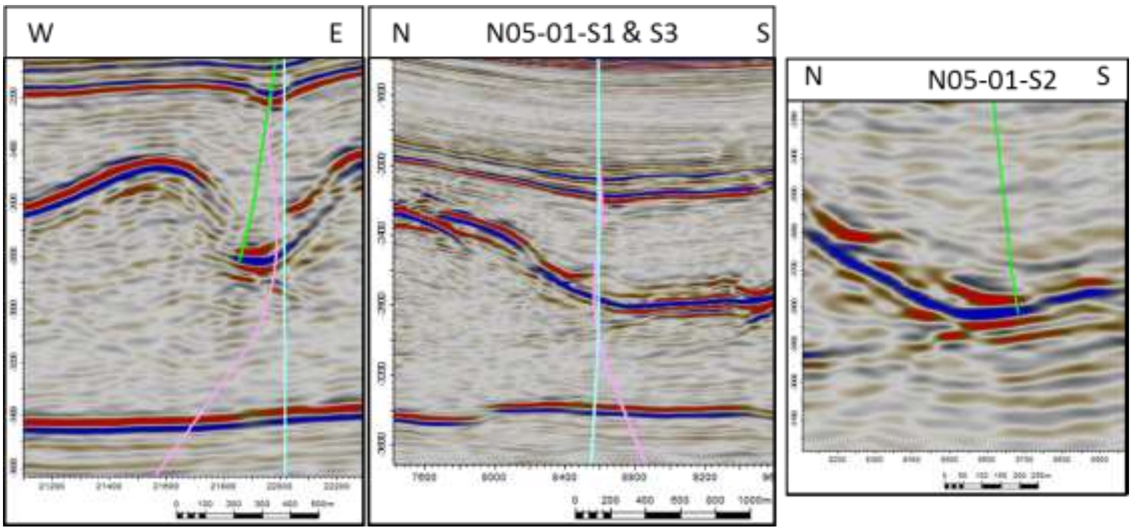

Fig. 44. Cross sections of well N05-01 and its side-tracks. N05-01-S2 (green) suffered a high severity gain event in the ZEZ3C when trying to penetrate the stringer at a broken edge of a TZ. Side-tracks 1 and 3 had no drilling issues.

6. Conclusions

- Thickened zones in the ZEZ3 stringer as found by Van Gent (2011) are also present in many other areas in the Dutch offshore, in particular where the basinal and slope facies of the Zechstein III carbonate member have been identified. Furthermore, thickened zones are also observed in the Silverpit Basin (UK), showing that they appear in a large part of the Zechstein Basin. In the high quality Hansa 4Quad and Hansa GEms seismic surveys, these thickened zones can be mapped in high detail thus giving clues on their possible origin.

- A thickened zone drilled by well H16-01 in the Hansa 4Quad area shows that it consists of thickened ZEZ3A (180 meter versus 50 meters average). Comparable anomalous ZEZ3A thicknesses have been observed in around 80 wells out of 1320 conclusive wells in the Dutch subsurface.

- The Hansa seismic data shows that thickened zones are strongly correlated to synclines in the stringer. Also a strong correlation with depressions in the overlaying K-Mg salts in the upper Zechstein can be observed.
  Mapping thickened zones in 3D reveals them as linear, branching and closing features (pseudo polygonal shapes) throughout the studied area. Linear features are orientated mostly normal or parallel to the large scale domal salt structures (ZEZ2H). Geometries look like salt domes/salt withdrawal, as seen in the Gulf of Mexico evaporates and in the Dutch offshore Zechstein. However thickened zone geometries are a factor of 10 smaller horizontally and vertically.

- Thickened zones can be explained by redistribution of gypsum with withdrawal and doming comparable to halite halokinesis. Publications from outcrop data, Harz mountains in Germany (Paul, 2014), describe a comparable model and refers to anhydrite domes. No seismic data was used to constrain the Harz model by Paul (2014). In this study high quality seismic data was available allowing a much more detailed analyses of these features. Doming started after burial of some 100+ m in the lower parts of the undulated Zechstein III halite member, possibly due to the Tubantian II tectonic pulse (Geluk, 2000). After gypsum doming the conversion to anhydrite releases water, which is able to escape vertically upward and thereby dissolving parts of the overburden evaporites. Volume reduction inherent to the gypsum to anhydrite transition created locally depressions and accommodation space immediately above the domes.
  According to the new model following from this study, thickened zones have a structural origin comparable to halokinesis and can be referred to as *anhydrite domes.*

- Geo-drilling event research based on 154 wells, where ZEZ3A is anomalously thick (>60 meter), show a significantly lower probability of gain events in the Zechstein stringer, compared to an EBN study of P. Schilder (2019). Furthermore, gain events found in selected wells are all situated in the western part of the Dutch offshore. The Northeastern part of the Dutch onshore (Groningen, Friesland and Drenthe) showed no gains from stringers.

- This study suggests that anhydrite domes are relatively safe to drill through, because of early dewatering to the surface that prevented high pressure build ups in the ZEZ3C. Only one example out of the investigated wells showed a gain event in an anhydrite dome (well D15-04), however this example lacks evidence of sufficient dewatering to surface, because no overburden depression can be observed.

- Planning new well trajectories, which require Zechstein drilling can benefit from observations from this report. The improved understanding of the intra-Zechstein geometries, in particular anhydrite domes, can help towards drilling more cost effectively and safer.

Recommendations

- Expanding the EBN GDE database to create a better understanding of the distribution of intra-Zechstein overpressures. This study revealed a difference in the member origin of gain events between the east and the western part of the Dutch territory. Future research should investigate this difference.

- Investigate timing of gypsum doming and subsequent dewatering. This can be done by careful mapping of Zechstein reflectors and determining the exact (stratigraphic) position of the accommodation space growth.

- The dimensional differences in the thickened zones patterns and the halite domes by a factor of 10 is intriguing. It would be interesting to investigate which factors do control these dimensional differences. Does the initial thickness of the ductile layer control the pattern dimensions or rather the rheologies? Halokinetic modeling might provide further insights.

- Little information about geo-drilling events in the northern part of the Dutch offshore is available currently. Further investigating this area can be useful for future exploration in this region.

- More research can be conducted on the distribution of the K-Mg salt layers. Mapping these layers can possibly provide additional insights on the origin of the anhydrite domes.

- This study found examples of anhydrite domes in the Southern Permian Basin (Netherlands, Germany and UK). Have such features been found in other basins around the world?

- Seismic response modeling of (conceptual) anhydrite domes. This could assist more detailed mapping of anhydrite dome features.

References

Al-Habsi, H., 2016. The kinematics of intra-salt layers during salt tectonics, PhD Thesis. Cardiff University.

Baud, A., 2018. Analyses and seismic integration of the Geo-Drilling Events Database: Predicting losses of drilling fluids using a statistical approach. Internship report, EBN and Utrecht University (not published).

Biehl, B. C., Reuning, L., Strozyk, F., and Kukla, P. A, 2014.: Origin and deformation of intra-salt sulphate layers: an example from the Dutch Zechstein (Late Permian), Int. J. Earth Sci. 103, 697–712.

Cameron, T.D.J., Crosby, A., Balson, P.S., Jeffery, D.H., Lott, G.K., Bulat, J. & Harrison, D.H. 1992. United Kingdom Offshore Regional Reports: The geology of the southern North Sea. HMSO for British Geological Survey: 152 pp.

Coelewij, P.A.J., Haug, G.M.W. & Van Kuijk, H., 1978. Magnesium-salt exploration in the northeastern Netherlands. Geologie en Mijnbouw 57: 487–502.

Fossen, H., 2010. Structural geology, Cambridge, Cambridge University Press.

Geluk, M.C., 1999. Late Permian (Zechstein) rifting in the Netherlands: models and implications for petroleum geology. Petrol Geoscience 5:189–199.

Geluk, M.C., 2000. Late Permian (Zechstein) carbonate-facies maps, the Netherlands. Netherlands Journal of Geosciences/Geologie en Mijnbouw 79(1), 17–27.

Geluk, M.C., 2005. Stratigraphy and tectonics of Permo-Triassic basins in the Netherlands and surrounding areas. 171 pp., Dissertation Universiteit Utrecht.

Geluk, M.C., 2007. Permian. In: Wong, T.E., Batjes, D.A.J., De Jager, J. (Eds.), Geology of the Netherlands. Royal Netherlands Academy of Arts and Sciences, Amsterdam, 63–84.

Hardie, L.A., 1967, The gypsum-anhydrite equilibrium at one atmosphere pressure: American Mineralogist, v. 52, p. 1107-1122.

Hemmann, M., 1968. Zechsteinzeitliche Gips/Anhydrit Umwandlung, Anhydritklippenbildung und zugehörige Erscheinungen in der subherzynen Leine-Serie. Mineralogie. Deut sche Akademie der Wissenschaften, 10: 454–462.

Hemmann, M., 1972. Ausbildung und Genese des Leinesteinsalzes und des Hauptanhydrits (Zechstein 3) im Ostteil des Subherzynen Beckens. Berichte der Deutschen Gesellschaft für geologische Wissenschaften, B16: 307–411.

Hsü, K.J., Cita, M.B., and Ryan, W.B.F. (1973) Late Miocene desiccation of the Mediterranean: Nature, v. 242, 240-244.

Hsü, K.J., Montadert, L., Bernoulli, D., et al. (1977) History of the Mediterranean salinity crisis: Nature, v. 267, 399-403.
M. P. A. Jackson and M. R. Hudec, 2007. Book: Salt Tectonics: Principles and Practices. Chapter 3.

Jackson, M. P., and M. R. Hudec, 2017, Salt tectonics: Principles and practice: Cambridge University Press.

Jowett, E.C., Cathles, L.M. & Davis, B.W. (1993) Predicting the depths of gypsum dehydration in evaporitic sedimentary basins. American Association of Petroleum Geologists Bulletin, 77, 402–413.

Klimchouk A., 1996. The dissolution and conversion of gypsum and anhydrite. International Journal Speleology. 25:2.

Kombrink H., J.C. Doornenbal, E.J.T. Duin, M. den Dulk, J.H. ten Veen and N. Witmans, 2012. New insights into the geological structure of the Netherlands; results of a detailed mapping project. Netherlands Journal of Geoscience, Volume 91, Issue 4 pp. 419-446.

Kosmahl, W., 1969. Zur Stratigraphie, Petrographie, Genese und Sedimentation des gebänderten Anhydrits (Zechstein 2), Grauen Salztones und Hauptanhydrits (Zechstein 3) in Nordwest - deutschland. Geologisches Jahrbuch, Beiheft, 71: 1–129.

Kuiper, M.E., 2017. Analysis and inventory of Geo-Drilling Events in the Dutch subsurface; a TIBCO Spotfire interface application. Internship report, EBN and Utrecht University (not published).

Langbein, R., 1987. The Zechstein sulphates: the state of the art. Lecture Notes in Earth Sciences, 10: 143–188.

Li, S., Abe, S., Reuning, L., Becker, S., Urai, J.L., and Kukla, P., 2012. Numerical modelling of the displacement and deformation of embedded rock bodies during salt tectonics: A case study from the South Oman Salt Basin. Salt tectonics, sediments and prospectivity (pp. 503–520). London: Geological Society of London.

Ligtenberg, J.H., 2007. Indications for Pressure Release from Zechstein Rafts during Late Kimmerian – Implications for Reducing Drilling Risks. EAGE 69th Conference & Exhibition – London, UK, 11–14.

Marsal, D., 1952. Der Einfluß des Druckes auf das System CaSO4–H2O. Heidelberger Beiträge zur Mineralogie und Petrographie, 3: 289–296.

Paul, J, 2014. “Gypsum domes and diapirs: Common features in the Zechstein (Upper Permian) of Germany”, Geological Quarterly, vol. 58, no. 3, pp. 521–530,2014.

Ramsay, J. G., 1967, Folding and fracturing of rocks: McGraw-Hill Book Company.

Ramsay, J. G., and M. I. Huber, 1987, The techniques of modern structural geology: Folds and fractures: Academic Press 2.

Rowan, M. G., and B. C. Vendeville, 2006. Foldbelts with early salt withdrawal and diapirism: Physical model and examples from the northern Gulf of Mexico and the Flinders Ranges, Australia, Mar. Pet. Geol., 23(9–10), 871–891.

Raith, A.F., Strozyk, F., Visser, J. & Urai, J.L., 2016. Evolution of rheologically heterogeneous salt structures: a case study from the NE Netherlands. Solid Earth 7(1): 67–82.

A. F. Raith & J. L. Urai & J. Visser, 2017. Structural and microstructural analysis of K–Mg salt layers in the Zechstein 3 of the Veendam Pillow, NE Netherlands: development of a tectonic mélange during salt flow. Netherlands Journal of Geosciences — Geologie en Mijnbouw |96 – 4 | 331–351 |.

Richter-Bernburg, G., 1955. Der Zechstein zwischen Harz und Rheinischen Schiefergebirge. Zeitschr. Deutsch. Geol., Gese 1-1., 105/4, 876-899.

Schilder, P. 2019. Predicting Overpressures in Zechstein Stringers Based on Their Seismic Expression. Internship report, EBN and Vrije Universiteit Amsterdam (not published).

Sonnenfeld, P., 1984. Brines and evaporates. London, Academic Press.

Stanley, M.S., 1986. Earth and life through time: W.H Freeman and company, New York, 690 p.

Strozyk, F., Urai, J.L., Van Gent, H., De Keijzer, M. & Kukla, P.A., 2014. The internal structure of salt: insights from a regional 3D seismic study of the Permian Zechstein 3 intra-salt stringer in the Northern Netherlands and its implications for salt tectonics. Interpretation 2(4): 101–117.

Strozyk, F., 2017. The Internal Structure of the Zechstein Salt and Related Drilling Risks in the Northern Netherlands. In: J. I. Soto, J. F. Flinch, G. Tari (Eds.), Permo-Triassic Salt Provinces of Europe, North Africa and the Atlantic Margins -Tectonics and Hydrocarbon Potential. Elsevier, Amsterdam, 115–126.

Urai, J.L., Schléder, Z., Spiers, C.J., Kukla, P.A., Lange, J.-M. & Röhling, H.-G., 2008. Flow and transport properties of salt rocks. In: Dynamics of Complex Intracontinental Basins: The Central European Basin System. Springer Science & Business Media (Dordrecht): 277–290.

Volozh, Y.A., Antipov, M.P., Brunet, M.-., Garagash, I.A., Lobkovskii, L.I., and Cadet, J.-., 2003. Pre-Mesozoic geodynamics of the Precaspian Basin (Kazakhstan): Sedimentary Geology, v. 156, 35-58.

Van den Belt, F.J.G., 2007. Sedimentary cycles in coal and evaporite basins and the reconstruction of Palaeozoic climate. PhD. Utrecht University.

Van Gent, H., Urai, J.L., de Keijzer, M., 2011. The internal geometry of salt structures – A first look using 3D seismic data from the Zechstein of the Netherlands. Journal of Structural Geology, vol. 33(3), 292–311.

Van Wees, J.-D., Stephenson, R. A., Ziegler, P. A., Bayer, U., McCann, T., Dadlez, R., et al., 2000. On the origin of the Southern Permian Basin, Central Europe. Marine and Petroleum Geology, 17, 43–59.

Williams-Stroud, S.C., Paul, J., 1997. Initiation and growth of gypsum piercement structures in the Zechstein basin. Journal of Structural Geology 19 (7), 897.

Zen. E-an., 1965. Solubility measurements in the system $CaSO_4$·NaCL·H_2O at 35°, 50° and 70°C and one atmosphere pressure: Journal of Petrology. v. 6. p. 124-164.

Ziegler, P.A., 1982. Geological Atlas of Central and Western Europe. Shell International Petroleum, Maatschappij B.V., Amsterdam. 130 pp.

Ziegler, W. H., Doery, R. & Scott, J., 1986. Tectonic habitat of Norwegian oil and gas. - In: A. M. Spencer et al. (eds.): Habitat of Hydrocarbons on the Norwegian continental Shelf. - Norwegian Petrol. Soc., 3-19, 12 figs., 11 Plates, Graham & Trotman, London.

Ziegler, M.A., 1989. North German Zechstein facies patterns in relation to their substrate. Geologische Rundschau 78: 105-127.

Zijp, M.H.A.A., Huijgen, M.A., Wilpshaar, M., Bouroullec, R. & ter Heege, J.H., 2018. Stringers in Salt as a Drilling Risk. TNO report carried out at the request of State Supervisory of Mines (SodM).

Appendix A

Figure of the general European, and for EBN, seismic convention that has been used for this study.

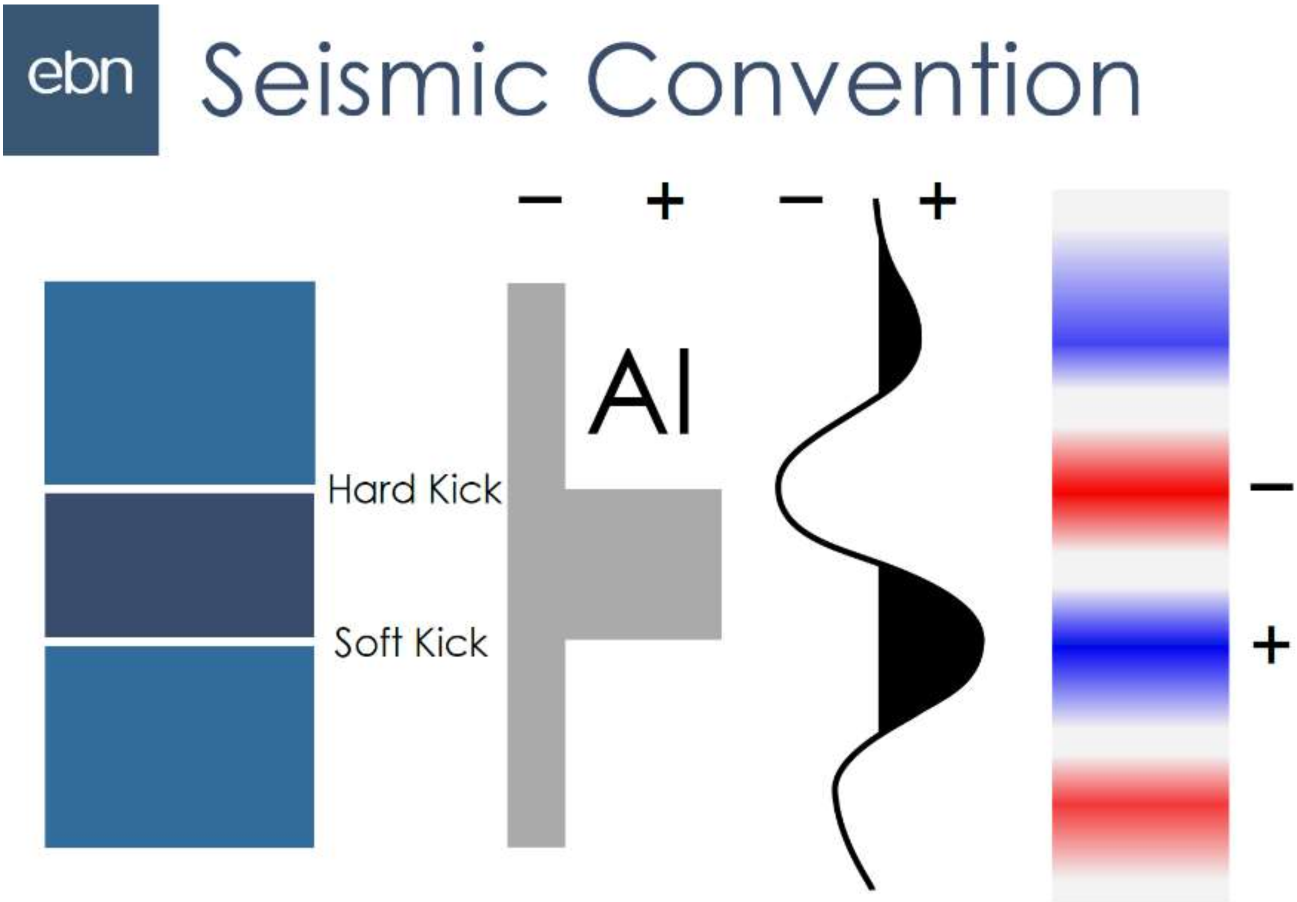

Appendix B

General Info			Event Data	Event Classification		Event Severity	Hazard Classification	Intepretations
Well Name	ZEZ3A TVT (m)	ZEZ3C TVT (m)	Event	GDE Type	Member	Level	HAZ Type	
ZEZ3A >75m								
ALO-01-S1	113.44	9.43	No					
AME-103-S1	138.48	2.95	No					
AME-104	87.6	2.27	No					
AME-106	81.03	2.33	Yes	Stuck Tubular/Tool	ZEZ2H	Low	Squeezing Salt	
AME-203	180		Yes	Gain	ZEZ2C	Med	Anomalous Pressure	"Broken" TZ
AML-01	185	5	No data					
ANV-02	100.63	5.56	No					
ANV-02-S1	80.03	4.82	Yes	Stuck Tubular/Tool	ZEZ3H	Low	Squeezing Salt	
APS-01	104.97	4	No					
AWG-01	139	4	Yes	ROP	ZEZ3A	Low	Rock Properties	
AWG-103-S2	126.6	2.15	Yes	Stuck Tubular/Tool	ZEZ3H	Low	Squeezing Salt	
AWG-104-S2	127.96	4.39	No					
AWG-106	234.52	3.1	No					
AWG-106-S1	234.52	3.1	No					
BHM-05-S2	84.45	1.69	Yes	Stuck Tubular/Tool	ZEZ2H	Low	Squeezing Salt	
BHM-05-S3	94.58	0.87	Yes	Stuck Tubular/Tool	ZEZ3H	Low	Squeezing Salt	
			Yes	Stuck Tubular/Tool	ZEZ2H	Low	Squeezing Salt	
BHM-07-S1	177	0	Yes	Stuck Tubular/Tool	ZEZ3H	Low	Squeezing Salt	Low qaulity seismic, seems like TZ.
			Yes	ROP	ZEZ3A	Med	Rock Properties	
BLF-106	94.67	2.25	No					
BLH-01	79.93	3.91	No					
COV-04	99.32	21.96	No					
COV-19	202.5	7.48	Yes	Losses	ZEZ2C	Low	Anomalous Pressure	
			Yes	Stuck Tubular/Tool	ZEZ2C	Low	Rock Properties	
COV-49	86.55	4.3	Yes	Stuck Tubular/Tool	ZEZ2H	Med	Squeezing Salt	
			Yes	Losses	ZEZ2C	Med	Anomalous Pressure	
D12-05	87.58	7.96	No					
D15-04			Yes	Gain	ZEZ3C	High	Anomalous Pressure	Penetrated TZ.
DAL-01	95.12	1	Yes	H2S	ZEZ2C	Low	H2S	
			Yes	Losses	ZEZ2C	Low	Fault	
DAL-06	100.26	4.06	No					
DAL-09	115.15	4.73	Yes	Stuck Tubular/Tool	ZEZ4H	Med	Squeezing Salt	Fault intepreted.
			Yes	Stuck Tubular/Tool	ZEZ4H	Low	Squeezing Salt	
DAL-09-S2	131.31	5.88	No					
DAL-11-S1	75.73	10.32	No					Fault intepreted.
DAL-12	94.37	3.68	Yes	Stuck Tubular/Tool	ZEZ4H	Low	Squeezing Salt	
			Yes	Stuck Tubular/Tool	ZEZ2H	Low	Squeezing Salt	
DIV-01	76.99	9	Yes	Losses	ZEZ3A	Low	Anomalous Pressure	
DKK-03	100.1	1.72	Yes	ROP	ZEZ3A	Low	Rock Properties	
E10-03-S2			Yes	Gain	ZEZ3A	Low	Anomalous Pressure	Penetrated TZ. Gain in top part ZEZ3A.
			Yes	Stuck Tubular/Tool	ZE	High	Squeezing Salt	
			Yes	Stuck Tubular/Tool	ZEZ4R	Low	Rock Properties	
E16-02-S2	195	0	Yes	Losses	ZEZ3H	Low	Anomalous Pressure	

			Yes	Gain	ZEZ3A	Low	Anomalous Pressure	“Broken” TZ. 4 m carbonate interval at depth of gain.
E17-01	98	0	Yes	Gain	ZEZ2H	Low	Anomalous Pressure	Fault or very steep stringer.
E17-02	30	2	Yes	Gain	ZEZ3C	High	Anomalous Pressure	“Broken” TZ. Well hit the edge.
EKR-108	114.98	27.05	No					
EKR-201	123.76	54.94	No					
EKR-202	86.87	34.95	No					
EKR-203	136.54	22.97	No					
EKR-206	75.8	19.96	Yes	Gain	ZEZ1C	Low	Anomalous Pressure	
EKR-208	161.3	34.56	No					
EKR-210	77.33	25.33	Yes	Gain	ZEZ2A	Low	Anomalous Pressure	
EMM-08-S1	143	2.24	Yes	Stuck Tubular/Tool	ZEZ2H	Low	Squeezing Salt	
EMM-14	106.87	1	Yes	Stuck Tubular/Tool	ZEZ3H	Med	Squeezing Salt	
			Yes	Stuck Tubular/Tool	ZEZ2H	Low	Squeezing Salt	
			Yes	Losses	ZEZ1A	Low	Anomalous Pressure	
EMM-15	97.53	7.41	Yes	Stuck Tubular/Tool	ZEZ3H	Low	Squeezing Salt	
			Yes	Stuck Tubular/Tool	ZEZ2H	Low	Squeezing Salt	
ESV-01	83	0	No					
EWM-01	103.87	3.52	Yes	Stuck Tubular/Tool	ZEZ2H	Low	Squeezing Salt	
FAN-01	108.66	5.67	No					
G16-01	112.02	8	No					
GGT-101-S2	95.94	7.92	Yes	Stuck Tubular/Tool	ZEZ2H	Low	Squeezing Salt	
			Yes	Stuck Tubular/Tool	ZEZ2H	Low	Squeezing Salt	
GGT-102	190.89	3.29	Yes	Stuck Tubular/Tool	ZEUC	Med	Swelling clay	
GGT-103	104.76	2.71	Yes	Gain	ZEZ2C	Low	Anomalous Pressure	
GTV-01	125.65	1.66	Yes	Stuck Tubular/Tool	ZEZ2H	Low	Squeezing Salt	
			Yes	Lithology	ZEZ3A	Low	Mapping Uncertainty	
H16-01	180	3	Yes	ROP	ZEZ3A	Low	Squeezing Salt	Penetrated TZ.
HBG-02-S1	87.71	7.99	Yes	Stuck Tubular/Tool	ZEZ2H	Low	Squeezing Salt	
HND-01	90	17	Yes	Stuck Tubular/Tool	ZEZ2H	Low	Squeezing Salt	
J06-A-03	133.71	3.18	Yes	Losses	ZEZ1W	Low	Fault	
K04-02-S1	80.39	8.67	No					Low qaulity seismic, seems like double stringer.
K07-04	163.7	3.98	Yes	Losses	ZEZ1C	Medium	Other / Unknown	
K07-FA-103	220.31	1.46	Yes	Gain	ZEZ3H	Low	Anomalous Pressure	
			Yes	Stuck Tubular/Tool	ZEZ3G	Low	Swelling clay	
K07-FA-103-S1	227.2	1.3	No data					
K07-FA-103-S2	222.91	1.7	No data					
K08-07	91.88	2.5	No					
K08-FA-103-S1	88	2	No data					
K08-FA-201	134.38	18.98	No					Low quality seismic, seems like TZ.
K08-FA-201-S1	142.81	8.37	No data					
K08-FA-201-S3	147.66	9.92	No data					
K08-FA-202	122.62	12.46	Yes	Stuck Tubular/Tool	ZEZ2H	Med	Squeezing Salt	Low quality seismic, seems like TZ.
K08-FA-301-S3	83.39	1.11	Yes	ROP	ZEZ3A	Low	Swelling clay	
K08-FA-302	80		No					
K08-FA-304	151		Yes	Stuck Tubular/Tool	ZEZ4H	Low	Squeezing Salt	
K08-FA-306	143.97	37.14	No					
K10-07	83.31	3.65	No					
K11-01	200.94	2.95	No					
K11-15	187.93	2.46	No					Low quality seismic.
K14-05	126.18	2.49	Yes	Stuck Tubular/Tool	ZEZ3H	Low	Squeezing Salt	Low quality seismic, seems like TZ.

			Yes	Gain	ZEZ3A	Med	Anomalous Pressure	Doubling mentioned at Nlog.
K15-13	197.34	5.61	Yes	Losses	ZEZ3C	Low	Anomalous Pressure	Fault intepreted and visible on seismic. No Tz.
			Yes	Losses	ZEZ3A	High	Fault	
			Yes	Lithology	ZEZ1C	Low	Mapping Uncertainty	
L08-14-S1	88.15	17.92	No					
L12-05	76.39	2.67	Yes	Stuck Tubular/Tool	ZEZ3H	Low	Squeezing Salt	Low quality seismic, seems like inclined hit.
L13-14	123.74	34.96	No					
L13-FC-101-S1	95.71	4.64	Yes	Stuck Tubular/Tool	ZEZ2H	Low	Squeezing Salt	Log data shows 50 m of ZEZ3A.
			Yes	ROP	ZEZ1A	Low	Rock Properties	
L09-09	88	2.75	Yes	Stuck Tubular/Tool	ZEZ3H	Low	Squeezing Salt	
L13-FC-104-S1	124	5.33	Yes	Stuck Tubular/Tool	ZEZ3A	Low	Rock Properties	
			Yes	Stuck Tubular/Tool	ZEZ2H	Low	Squeezing Salt	
			Yes	Stuck Tubular/Tool	ZEZ2C	Low	Rock Properties	
L13-FC-105	96	5.36	No data					
L13-FC-105-S1	130.95	5.36	Yes	Stuck Tubular/Tool	ZEZ2H	Low	Squeezing Salt	
L13-FE-103	75.87	2.47	No					
L13-FE-104-S3	123.74	3.62	No					
L13-FE-104-S4	95.71	3.62	No					
L15-FA-103-S5	83.73	3.43	No data					
L15-FA-104	93.93	4.8	No					
L13-FE-102-S2	131	2.76	No					
L16-03	84	18.94	No					
L16-04	114.93	35.47	Yes	Stuck Tubular/Tool	ZEZ3H	Low	Squeezing Salt	Penetrated TZ.
L16-16A	115	16.99	No					
L17-03	139	23.46	No					
NOR-05	80.74	17.76	No					
NSN-01	230.97	3	No					
ODP-01	81.95	18.1	Yes	Stuck Tubular/Tool	ZEZ2H	Low	Squeezing Salt	
SAU-01	84.21	1.92	No					
SDB-09	85.6	19.65	Yes	Stuck Tubular/Tool	ZEZ3H	Low	Squeezing Salt	
			Yes	Stuck Tubular/Tool	ZEZ2H	Low	Squeezing Salt	
			Yes	Gain	ZEZ2C	High	Anomalous Pressure	
SDB-11	112.26	17.98	No					
SEB-02	182	0	No					
TID-102	170.72	5.77	No					
TID-103	124.95	7.58	No					
VHN-02	97.46	10.68	No					
VLW-02	112.6	0.95	No					
WRF-01	87.77	2.87	No					
ZRP-01	75.89	21.97	No					

ZEZ3B > 60m

B10-02-S1	75.99	0	Yes	ROP	ZEZ3A	Low	Rock Properties	
E18-02	72.8	2	Yes	Gain	ZEZ3C	High	Anomalous Pressure	Hit isolated steep stringer. TZ nearby.
K15-FA-109	110	60	Yes	Lithology	ZEZ1A	Low	Mapping uncertainty	Dolomite intervals at top.
L08-P-03-S1	93.97	4	Yes	ROP	ZESA	Low	Rock Properties	
			Yes	Steering	ZESA	Low	Other / Unknown	
			Yes	Stuck Tubular/Tool	ZESA	Med	Squeezing Salt	

ZEZ3A 60-75m

AME-101	73.41	4.03	Yes	ROP	ZEZ3A	Low	Rock Properties	
			Yes	ROP	ZEZ2C	Low	Rock Properties	
AME-102-S3	70.09	2.48	Yes	ROP	ZEZ2H	Low	Rock Properties	
ANS-01	71.79	20.45	No					
COV-07-S3	65.97	15.03	Yes	Stuck Tubular/Tool	ZEZ2C	Low	Other / Unknown	
COV-13	71.68	3.26	Yes	Gain	ZEZ1C	Med	Anomalous Pressure	
COV-25	60.24	2.84	Yes	Stuck Tubular/Tool	ZEZ3H	Low	Squeezing Salt	
			Yes	Stuck Tubular/Tool	ZEZ2H	Low	Squeezing Salt	
			Yes	Losses	ZEZ2C	Low	Anomalous Pressure	
COV-26-S1	64.63	3.2	Yes	Stuck Tubular/Tool	ZEZ2H	Low	Squeezing Salt	
			Yes	Stuck Tubular/Tool	ZEZ2H	Low	Squeezing Salt	
			Yes	Losses	ZEZ2C	Low	Anomalous Pressure	
COV-26-S2	62.21	1.78	Yes	Stuck Tubular/Tool	ZEZ2H	Low	Squeezing Salt	
D15-02	67	3	No					
D15-FA-103	74.58	4.71	No					
E12-02	66.49	5	No					
E13-02	66.98	3	Yes	Gain	ZEZ3A	Med	Anomalous Pressure	Penetrated edge of "broken" TZ. Gain at base ZEZ3A.
EKR-110-S1	62.61	24.4	No					Faults intepreted.
G13-01	60.58	1.5	Yes	Stuck Tubular/Tool	ZEZ3H	Low	Squeezing Salt	
			Yes	Stuck Tubular/Tool	ZEZ3H	Low	Squeezing Salt	
GSV-01-S2	63.71	0	Yes	Losses	ZEZ2C	Med	Anomalous Pressure	Fault intepreted.
HOA-01-S6	69.48	2	No					
J06-01-S1	61.48	2.5	Yes	Gain	ZEZ3A	Low	Anomalous Pressure	Looks like TZ, low quality seismic. Gain in top of TZ.
K04-08-S3	67.36	8.67	No data					
K05-A-02	69.95	3.21	No					
K06-08	67.93	3	Yes	Stuck Tubular/Tool	ZEZ2H	Low	Squeezing Salt	Hit inclined stringer, no TZ.
			Yes	Losses	ZEZ2A	Low	Anomalous Pressure	
K06-DN-01	64.2	2.73	No					Hit inclined stringer, no TZ.
K10-01-S1	68.15	0.96	Yes	Gain	ZEZ3H	Med	Anomalous Pressure	Hit fault zone, low quality seismic.
K17-04	65.87	17.52	No					
KPD-05	62.29	24.42	No					
KPD-09	70.84	22.69	No					
L10-M-01	70.08	19.89	No					Drilled through salt diapir.
L13-04	62.43	3	Yes	Losses	ZECP	Med	Anomalous Pressure	Fault intepreted Nlog. Low quality seismic.
			Yes	Stuck Tubular/Tool	ZEZ2H	Low	Squeezing Salt	
L13-FC-103-S3	65.06	4.77	No					
L16-09	70.94	7.99	Yes	Losses	ZEZ3A	Low	Anomalous Pressure	Log data shows 40 m of ZEZ3A.
LEW-05	60	11	No					
MAL-01	60.26	3.52	No					
NOR-35	72.19	34	No					
OSH-06-S1	73.08	10	No data					

PSP-03	60.33	24.79	No					
RDW-01	70.46	6.19	No					
SCH-463	74.72	11.95	Yes	Stuck Tubular/Tool	ZEZ4H	Low	Squeezing Salt	
			Yes	Losses	ZEZ2C	High	Anomalous Pressure	
SWO-01	70.37	2.6	Yes	Gain	ZEZ2C	Low	Anomalous Pressure	
TER-01-S2	62.94	3.18	Yes	Gain	ZEZ1A	Med	Anomalous Pressure	
VLR-01	71.85	3.16	No					
WAV-08	71.39	5	Yes	Losses	ZEZ2A	Low	Anomalous Pressure	
ZLV-02	63.8	2.56	Yes	Gain	ZEZ2C	Low	Anomalous Pressure	
			Yes	Losses	ZEZ1C	Med	Anomalous Pressure	

- Thicknesses marked in red are faulty
- Event Data column; events marked in green are already in the EBN GDE database, events marked in yellow not yet in the EBN GDE database and marked in grey are wells with very minimal or no data available.

Appendix C

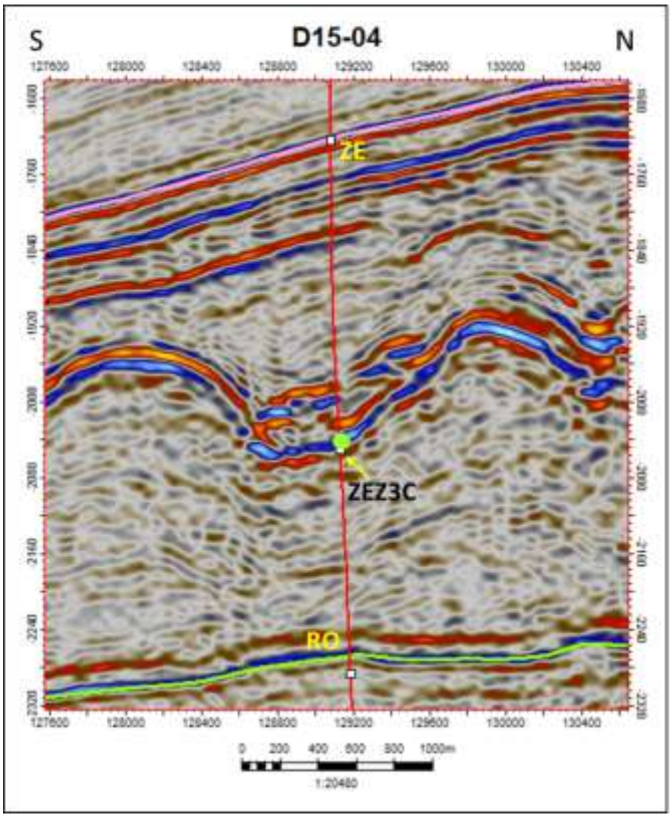
S
D15-04
N
ZE
ZEZ3C
RO
0 200 400 600 800 1000m
1:20480

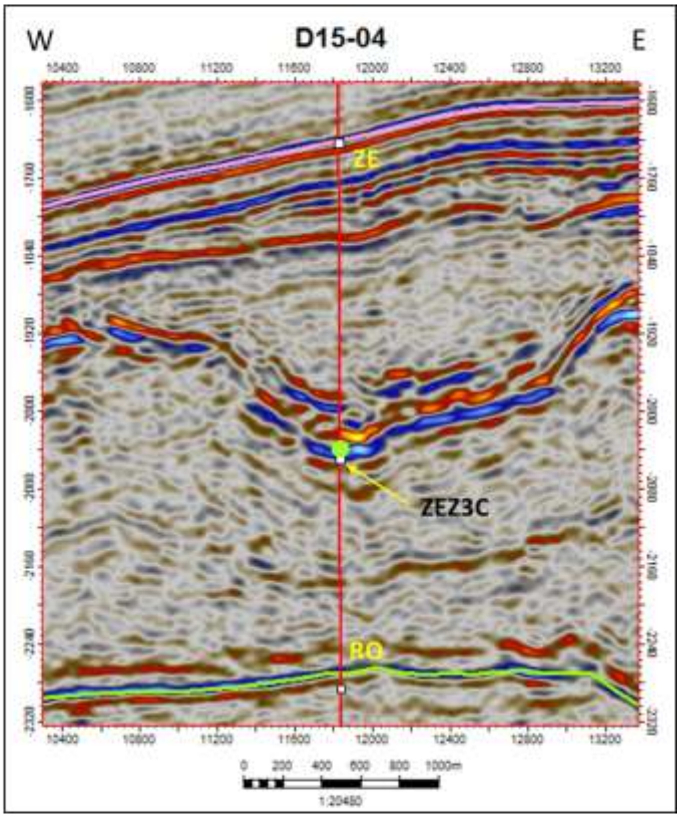
W
D15-04
E
ZE
ZEZ3C
RO
0 200 400 600 800 1000m
1:20480

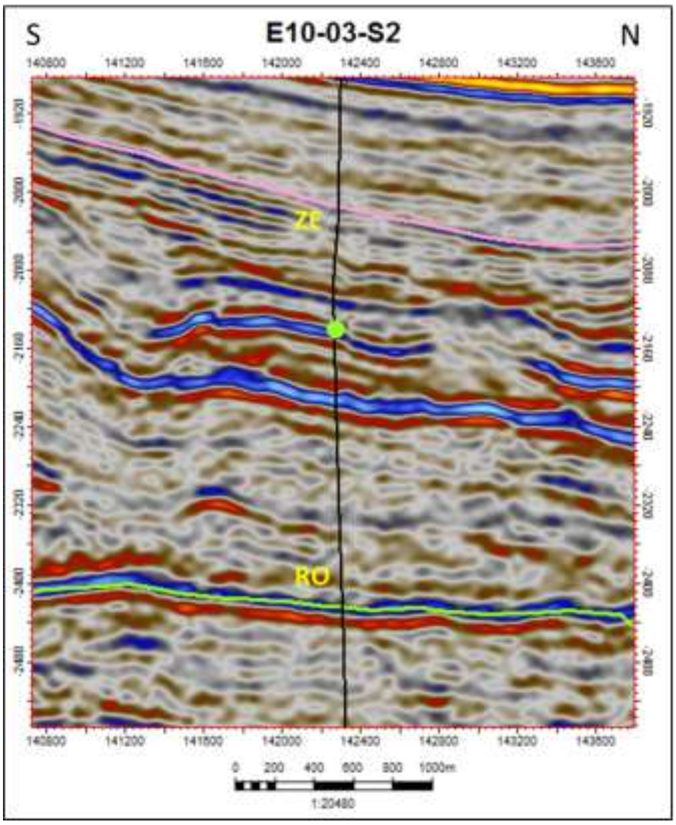
S
E10-03-S2
N
ZE
RO
0 200 400 600 800 1000m
1:20480

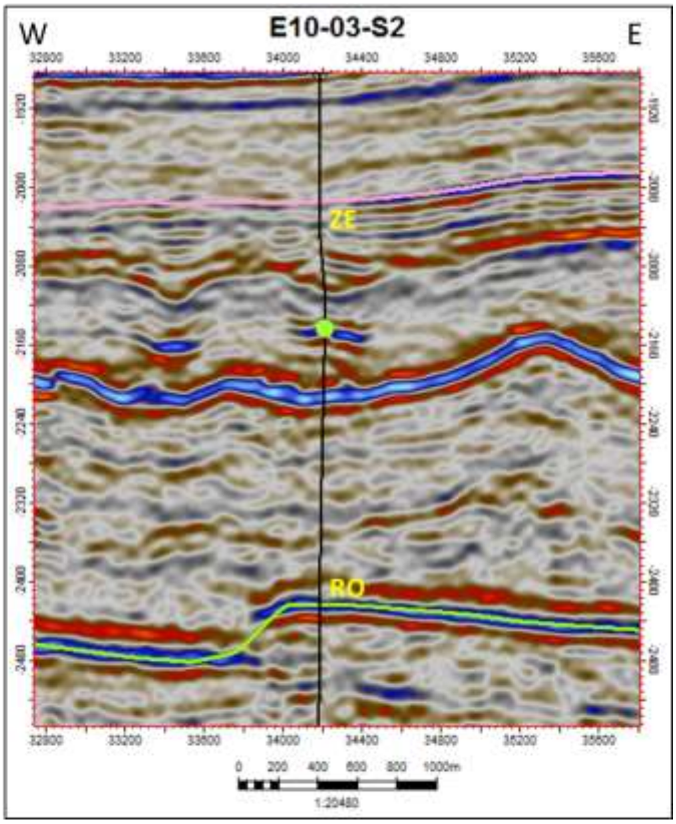
W
E10-03-S2
E
ZE
RO
0 200 400 600 800 1000m
1:20480

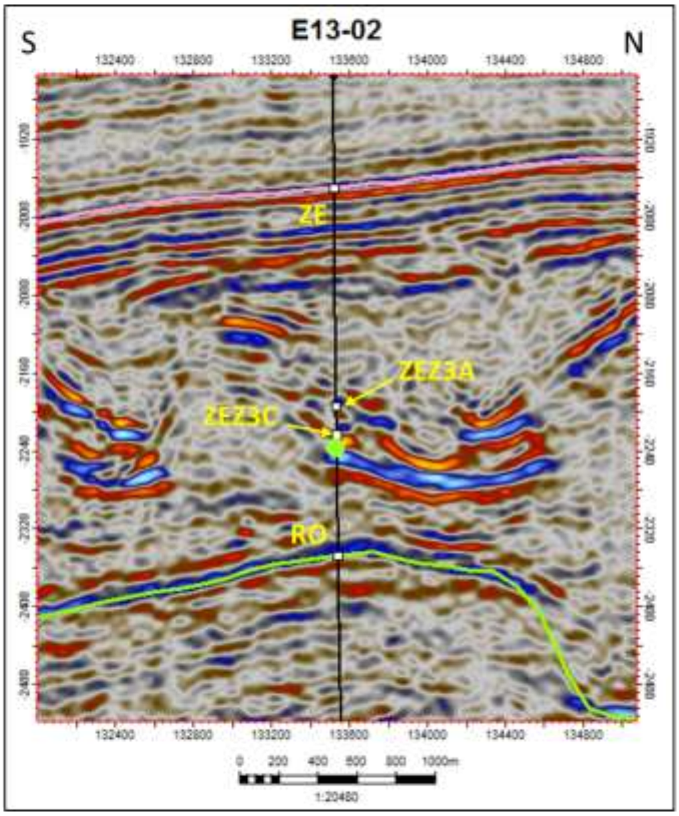
S
E13-02
N
ZE
ZEZ3A
ZEZ3C
RO
0 200 400 600 800 1000m
1:20480

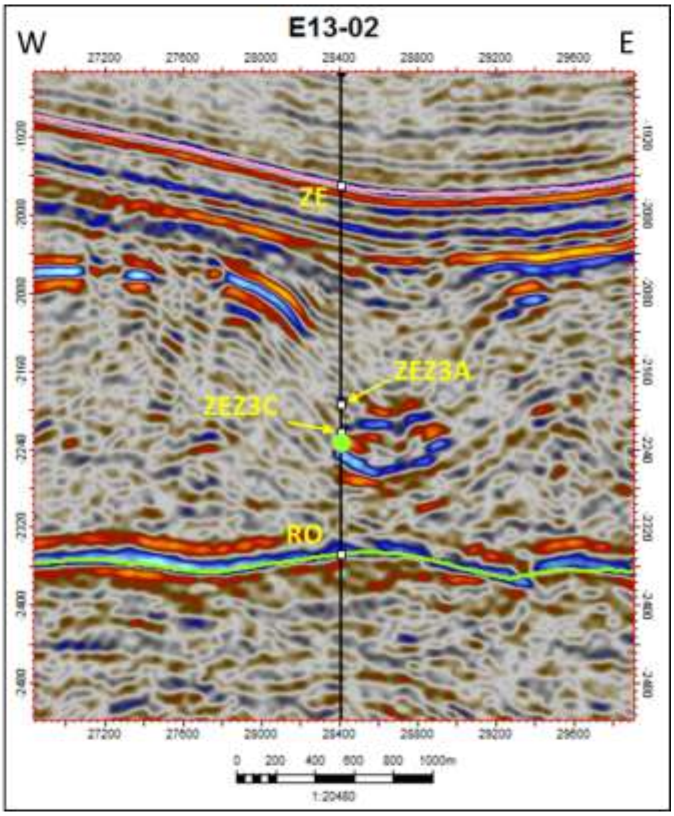
W
E13-02
E
ZE
ZEZ3A
ZEZ3C
RO
0 200 400 600 800 1000m
1:20480

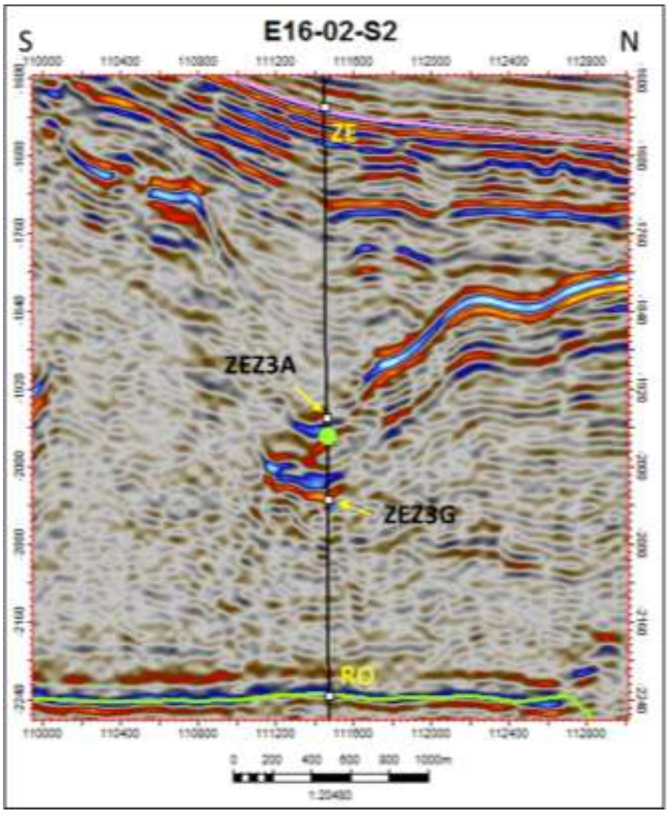
S
E16-02-S2
N
ZE
ZEZ3A
ZEZ3G
RO
0 200 400 600 800 1000m
1:20480

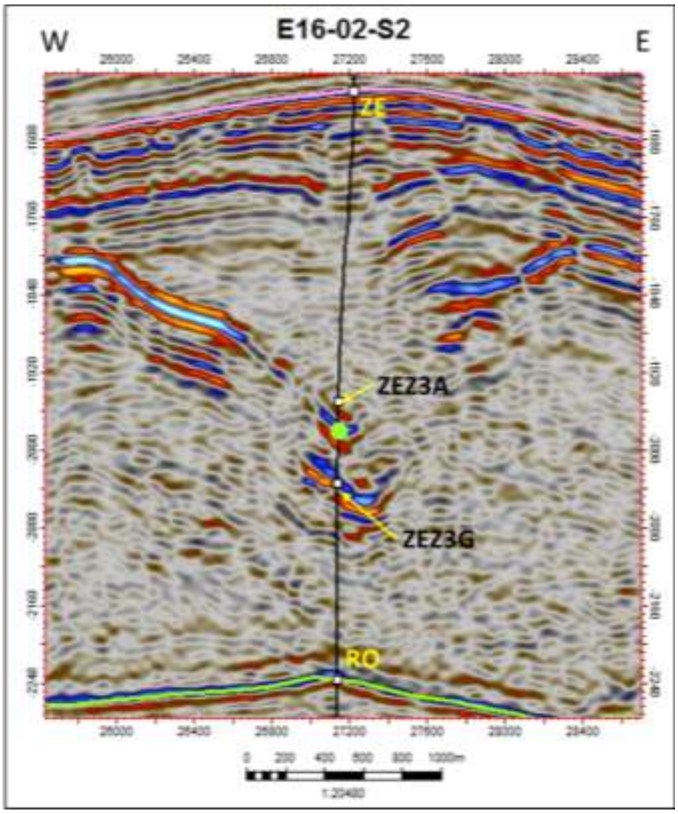
W
E16-02-S2
E
ZE
ZEZ3A
ZEZ3G
RO
0 200 400 600 800 1000m
1:20480

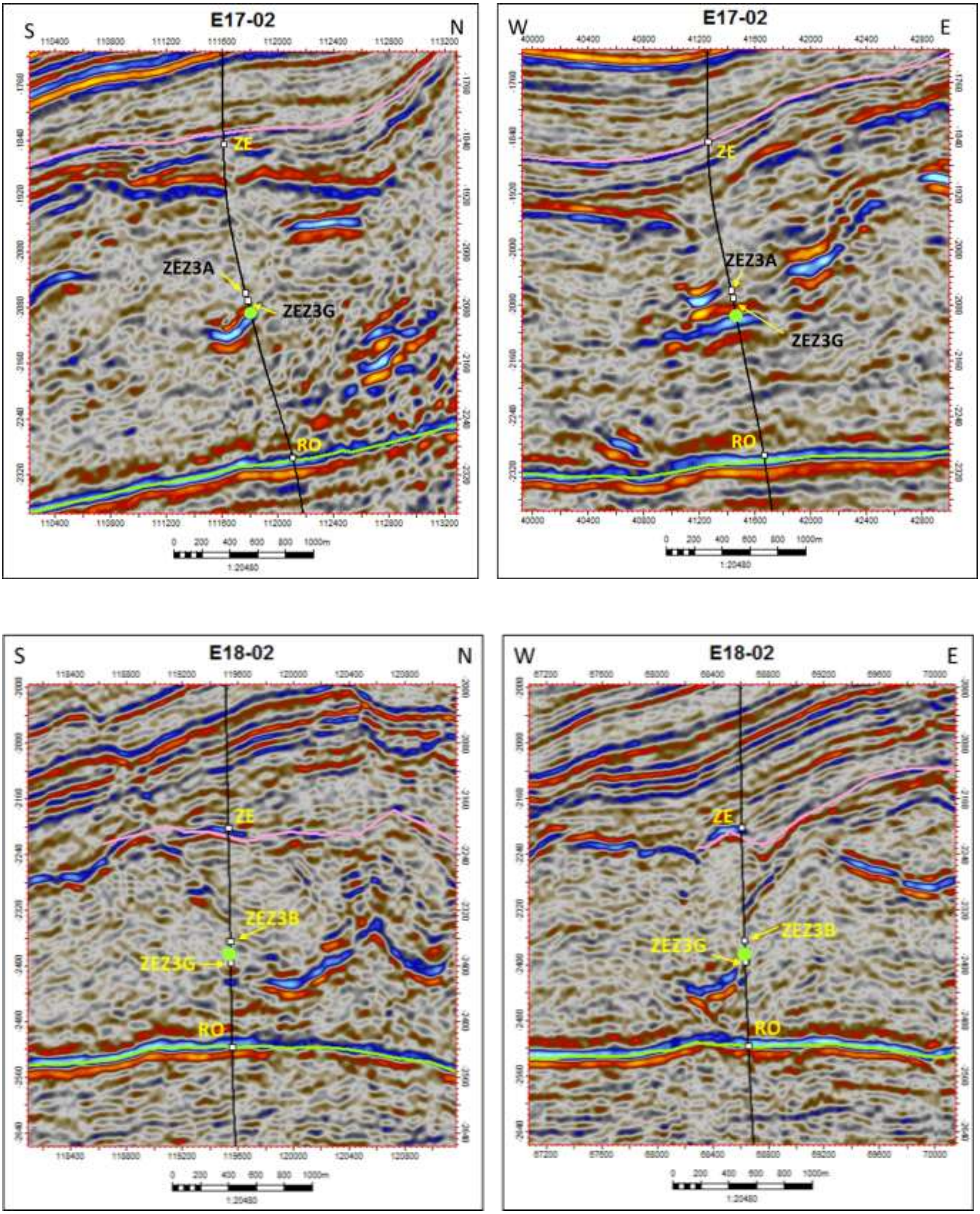
S
E17-02
N
ZE
ZEZ3A
ZEZ3G
RO
W
E17-02
E
ZE
ZEZ3A
ZEZ3G
RO
S
E18-02
N
ZE
ZEZ3B
ZEZ3G
RO
W
E18-02
E
ZE
ZEZ3G
ZEZ3B
RO

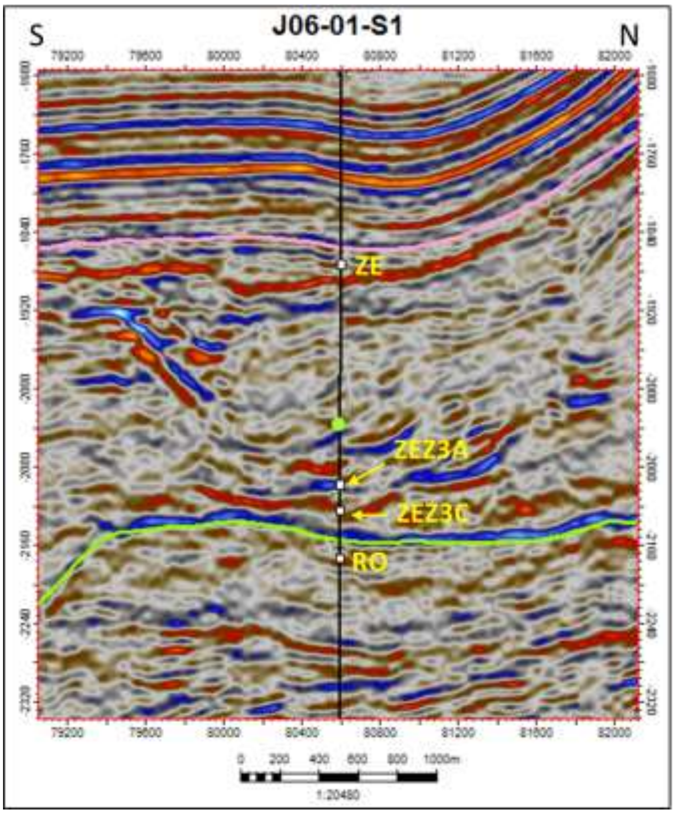
S
J06-01-S1
N
ZE
ZEZ3A
ZEZ3C
RO
1:20480

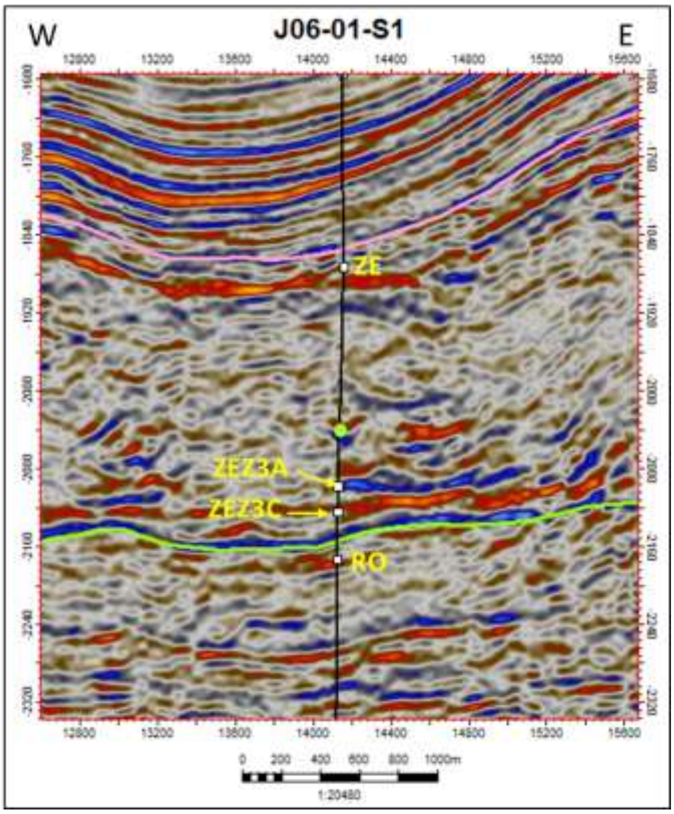
W
J06-01-S1
E
ZE
ZEZ3A
ZEZ3C
RO
1:20480

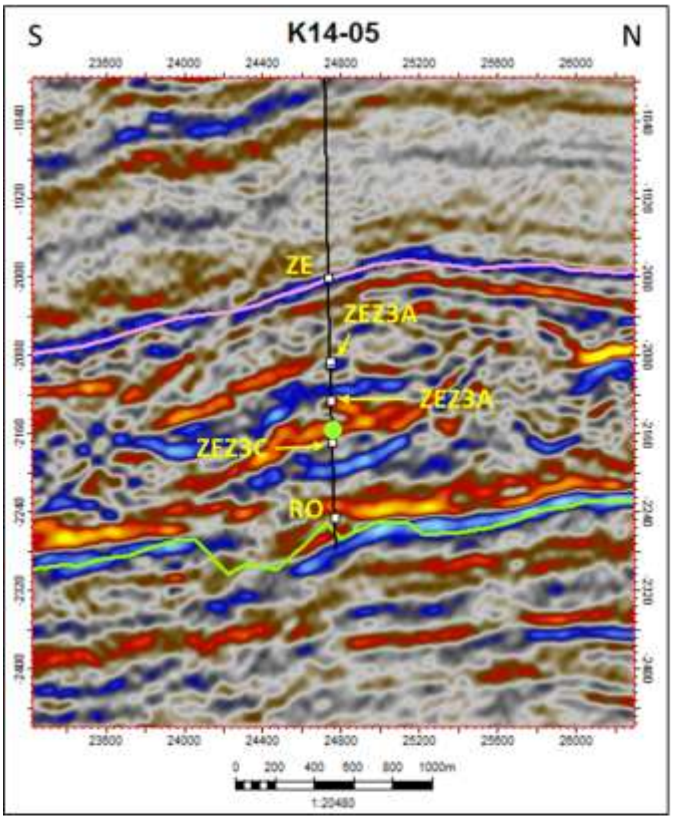
S
K14-05
N
ZE
ZEZ3A
ZEZ3A
ZEZ3C
RO
1:20480

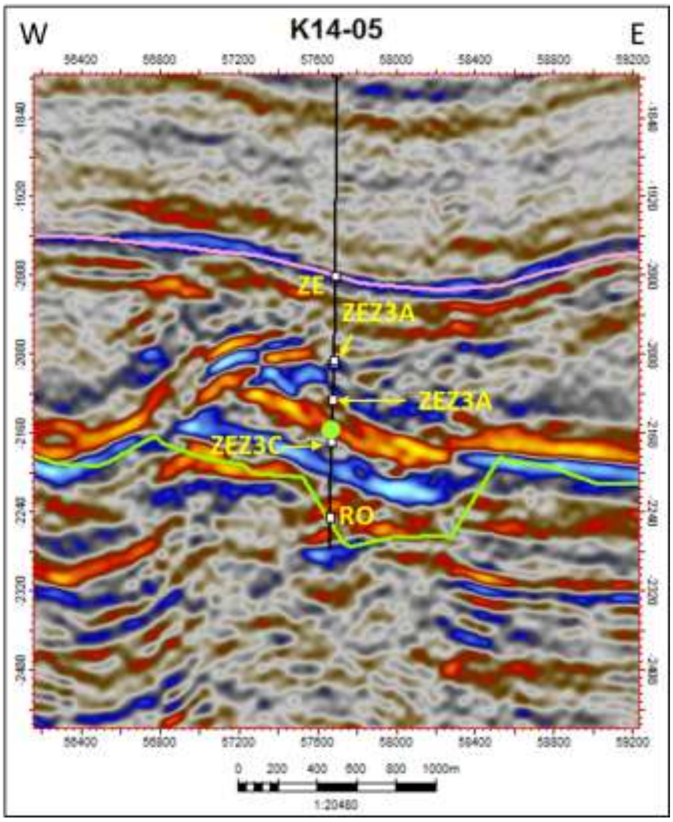
W
K14-05
E
ZE
ZEZ3A
ZEZ3A
ZEZ3C
RO
1:20480

Appendix D